NASA CR-1302

# SUMMARY OF RANDOM VIBRATION PREDICTION PROCEDURES

By R. L. Barnoski, A. G. Piersol, W. F. Van Der Laan,
P. H. White, and E. F. Winter

Distribution of this report is provided in the interest of information exchange. Responsibility for the contents resides in the author or organization that prepared it.

APRIL 1969

Prepared under Contract No. NAS 8-20020 by
MEASUREMENT ANALYSIS CORPORATION
Los Angeles, Calif.

for George C. Marshall Space Flight Center

NATIONAL AERONAUTICS AND SPACE ADMINISTRATION

For sale by the Clearinghouse for Federal Scientific and Technical Information
Springfield, Virginia 22151 – CFSTI price $3.00

# FOREWORD

This report was prepared by the Measurement Analysis Corporation, Los Angeles, California, for the NASA Marshall Space Flight Center, Huntsville, Alabama, under Contract NAS 8-20020, "Improvement of Techniques for the Derivation of Vibration Test Specifications. The work was administered under the direction of the Structures Division of the Propulsion and Vehicle Engineering Laboratory by Mr. Claude Green. The study producing the report was initiated in January 1967. The first draft of the report was submitted in May 1967, and the final draft was submitted in October 1967.

The material presented in this report was derived not only from the available literature, but also from personal discussions with many individuals concerned with flight vehicle vibration problems. Of particular value were the contributions and reviews by Mr. Franz Biehl of McDonnell-Douglas Corp., Dr. Allen Curtis of Hughes Aircraft Co., Mr. Harry Himelblau of North American Aviation, and Mr. Harold Klein of Mechanics Research Inc. Further assistance was provided by Bolt Beranek and Newman, Inc., who permitted review of the monograph "Random Noise and Vibration in Flight Vehicles," SVM-1, by Richard Lyon prior to its publication by the Shock and Vibration Information Center, USDOD, Washington, D. C. The assistance of these and all other individuals who contributed to this document is gratefully acknowledged.

## ABSTRACT

Various procedures suggested in recent years for the prediction of random vibration environments in modern flight vehicles are summarized and discussed. A total of fifteen individual techniques are included. The basic principles of the procedures are outlined, and known experience in their use are reviewed. Special attention is given to the assumptions inherent in their use as well as the information required for their application. The relative advantages and limitations of the procedures are detailed.

## CONTENTS

CONTENTS (Continued)

# LIST OF FIGURES

LIST OF FIGURES (continued)

LIST OF FIGURES (continued)

# INTRODUCTION

The random vibration environments for modern aerospace vehicles are continually increasing in severity while, simultaneously, mission requirements are becoming more stringent. These facts are producing a demand by structural and equipment designers for more accurate vibration predictions needed to establish design criteria and test specifications. Many vibration prediction procedures of various types have been proposed over the years by individuals in both private companies and government agencies. The documentation for these procedures is scattered throughout the literature. As a first step towards the development of improved vibration prediction procedures, it appears appropriate to review and catalog all previous approaches to the problem which are believed to have merit. Such is the purpose of this document. To facilitate comparisons of the relative merits of previous procedures, each is summarized in the following way.

1. Description
2. Assumptions
3. Information required to apply
4. Advantages
5. Limitations

This information will hopefully form a proper basis for selecting an appropriate prediction procedure for specific current applications, and for developing improved procedures for future applications.

## 2. GENERAL RANDOM VIBRATION PREDICTION PROCEDURES

In this document, the various procedures for predicting random vibration levels are grouped and discussed according to the type of approach as follows:

1. Classical Approach
2. Multiple Input Approach
3. General Extrapolation Approach
4. Specific Extrapolation Approach
5. Statistical Energy Approach
6. Model Study Approach

The classical approach refers to the direct calculation of vibration levels by solving an equation which relates the response of a distributed elastic structure to a distributed stochastic excitation. The multiple input approach consists of quantizing a continuous structure into a finite number of constant parameter linear systems, and the distributed excitation into a finite number of point forces which may or may not be coherent. The response at specific structural locations can then be calculated directly for any set of assumed excitation forces. The extrapolation approach is the most common technique for predicting vibration levels for launch vehicles. The approach consists of extrapolating vibration data measured on previous structures to some new structure of interest. This may be accomplished using pooled data from one or more general vehicles (general extrapolation), or specific data from a selected similar vehicle (specific extrapolation). In either case, the extrapolation

rules may be arrived at either analytically or empirically. The statistical energy approach utilizes a statistical description of a structure as a vibrating system. Motion of the structure is assumed to be dominated by resonant response rather than forced nonresonant response. The response is predicted on the basis of the average vibration energy contained within a band of frequencies. The model study approach to vibration prediction utilizes dynamically equivalent physical models, and generally requires extensive testing and/or laboratory facilities. Such models may be either scaled replicas of the prototype or other analogous systems such as electrical networks. By simulating both the prototype and the excitation, appropriate data may be obtained which will describe the vibration environment of the prototype.

In the sections which follow, these approaches are discussed separately in detail.

# 3. CLASSICAL APPROACH

## 3.1 DESCRIPTION

Classical techniques of prediction evolve directly from conventional structural analysis methods, as given in References 1 through 4. Specifically, it is assumed that the motion of a vibrating structure can be represented as the sum of the motions of individual normal modes. That is,

$$y(\underline{x}, t) = \Sigma \phi_i(\underline{x})\, q_i(t) \tag{1}$$

where

$y(\underline{x}, t)$ = response displacement at vector point $\underline{x}$ and time $t$

$\phi_i(\underline{x})$ = mode shape for ith normal mode

$q_i(t)$ = response displacement of ith normal mode

It is further assumed that the excitation of the structure can be described by a random pressure field with a spatial cross spectral density function given by

$$G_p(\underline{\xi}, \underline{\xi}', f) = \left\langle \lim_{T \to \infty} \frac{2}{T} P_T^*(\underline{\xi}, f)\, P_T(\underline{\xi}', f) \right\rangle \quad ; \quad f \geq 0$$

$$= 0 \quad ; \quad f < 0 \tag{2}$$

where

$$P_T(\underline{\xi}, f) = \int_0^T p(\underline{\xi}, t)\, e^{-j2\pi ft}\, dt \quad ; \quad f \geq 0$$

$$= 0 \quad ; \quad f < 0$$

$p(\underline{\xi}, t)$ = excitation pressure at vector point $\underline{\xi}$ and time $t$

$P_T^*(\underline{\xi}, f)$ = complex conjugate of $P_T(\underline{\xi}, t)$

$\langle\ \rangle$ = stochastic average

From References 1 through 4, the power spectral density function for the structural response is then given by

$$G_y(\underline{x}, f) = \sum_{i=1}^{\infty} \sum_{k=1}^{\infty} \phi_i(\underline{x})\, \phi_k(\underline{x})\, L_{ik}(f)\, H_i^*(f)\, H_k(f) \qquad (3)$$

where

$$L_{ik}(f) = \frac{1}{16\pi^4 f_i^2 f_k^2 \overline{M}_i \overline{M}_k} \int_0^{\underline{\ell}} \int_0^{\underline{\ell}} G_p(\underline{\xi}, \underline{\xi}', f)\, \phi_i(\underline{\xi})\, \phi_k(\underline{\xi}')\, d\underline{\xi}\, d\underline{\xi}'$$

$$\overline{M}_i = \int_0^{\underline{\ell}} \phi_i^2(\underline{x})\, m(\underline{x})\, dx \quad ; \quad \text{(generalized mass for ith mode)}$$

$m(\underline{x})$ = mass density at vector point $\underline{x}$

$$H_i(f) = \frac{1}{1 - \left(f/f_i\right)^2 + j2\zeta_i\, f/f_i} \quad ; \quad \text{(frequency response function for ith mode)}$$

$f_i$ = undamped natural frequency for ith mode

$\zeta_i$ = viscous damping ratio for ith mode

A slightly different way of writing the relationship in Eq. (3) which is more convenient for discussions in later sections is as follows.

$$G_y(\underline{x}, f) = \sum_{i=1}^{\infty} \sum_{k=1}^{\infty} \frac{\phi_i(\underline{x})\, \phi_k(\underline{x})}{4\pi^2 f^2 Z_i^*(f)\, Z_k(f)} \int_0^{\underline{\ell}} \int_0^{\underline{\ell}} G_p(\underline{\xi}, \underline{\xi}', f)\, \phi_i(\underline{\xi})\, \phi_k(\underline{\xi}')\, d\underline{\xi}\, d\underline{\xi}' \tag{4}$$

where

$$Z_i(f) = \frac{2\pi f_i^2 \overline{M}_i}{f H_i(f)} \quad ; \quad \text{modal impedance}$$

Equation (4) may be further reduced to the form

$$G_y(\underline{x}, f) = \sum_{i=1}^{\infty} \sum_{k=1}^{\infty} \frac{\phi_i(\underline{x})\, \phi_k(\underline{x})\, A^2\, G_{\xi_0}(f)\, j_{ik}^2(f)}{4\pi^2 f^2 Z_i^*(f)\, Z_k(f)} \tag{5}$$

where

$$j_{ik}^2(f) = \frac{1}{A^2\, G_{\xi_0}(f)} \int_0^{\underline{\ell}} \int_0^{\underline{\ell}} G_p(\underline{\xi}, \underline{\xi}', f)\, \phi_i(\underline{\xi})\, \phi_k(\underline{\xi}')\, d\underline{\xi}\, d\underline{\xi}'$$

is called the "cross joint acceptance function." In Eq. (5), A is the area of the structure and $G_{\xi_0}(f)$ is the power spectral density for the excitation at some reference point $\xi_0$.

Equations (3) through (5) are mathematical analogs, and their solutions describe the physical behavior of the system. Methods of solution generally include topics common to Fourier and Laplace Transforms, Matrix Procedures, Partial Differential Equations, Wave Solutions, Statistical Mathematics, Complex Variables and Variational Principles. The specific techniques generally depend upon the personal interest of the analyst.

The prediction of vibration environments by direct application of Eqs. (3), (4) or (5) involves a number of practical problems. Among these problems is the accurate definition of mode shapes and damping. Unless the structure is relatively simple (a uniform beam or rectangular plate), the higher frequency mode shapes may be difficult to define by either analytical or experimental techniques. Analytical expressions (including computer solutions) for the mode shapes become increasingly complicated and inaccurate as the mode number becomes larger and the structure becomes less homogeneous. Experimental procedures require a minimum of about 3 measurements per bending wavelength to describe adequately a mode shape. The accurate calculation or measurement of modal damping is also difficult in practice for similar reasons. A second problem area is the proper definition of the required spatial cross-spectral density function for the excitation. This function varies widely for different types of random pressure fields, and is not well defined for all cases of interest. Considerable research on this subject is currently in progress.

In summary, the classical approach is best suited for problems where the excitation is limited to relatively low frequencies, say, less than the 10th normal mode frequency of the structure of concern. Acceptable results for excitation at higher frequencies, say, up to the

50th normal mode of the structure, are possible if sufficient effort is made. However, the accuracy of the results at these higher frequencies may be no better than those which could be obtained using a less laborious prediction procedure.

## 3.2 SUMMARY

### Assumptions

The structure is a constant parameter linear system.

### Information Required

1. Normal mode shapes, frequencies, and damping ratios for the structure
2. The spatial cross-spectral density function for the excitation

### Advantages

The procedure yields precise results if all required information is available.

### Limitations

1. The required information is difficult to obtain in practice.
2. The required computations are laborious.

# 4. MULTIPLE INPUT APPROACH

## 4.1 DESCRIPTION

The multiple input approach is an extension of the classical approach where the distributed structure is reduced to a finite number of discrete constant parameter linear systems, and the distributed pressure excitation is reduced to a finite number of point forces. Schematically, the structure is reduced to a multiple input system as shown below. From Reference 5, the power spectral density

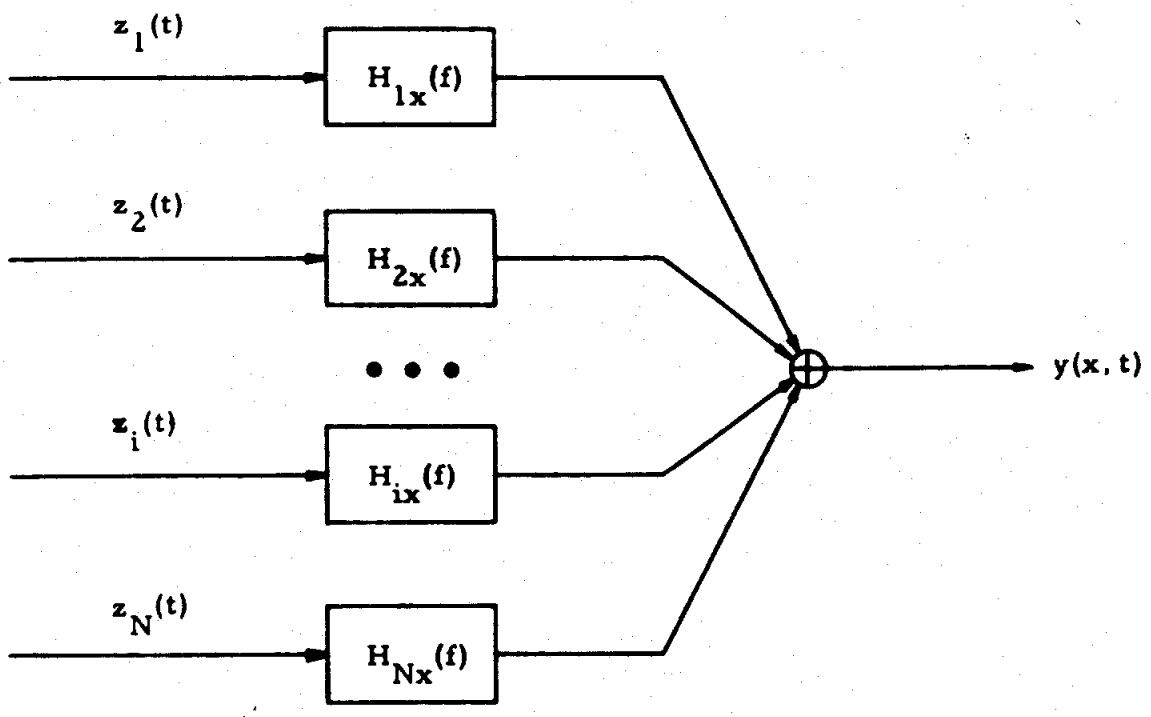


Multiple Input Model

function for the structural response is now given by

$$G_y(x, f) = \sum_{i=1}^{N} \sum_{k=1}^{N} H_{ix}^{*}(f)\, H_{kx}(f)\, G_{ik}(f) \qquad (6)$$

where

$H_{ix}(f)$ = frequency response function for the structure between the ith input and the response point

$G_{ik}(f)$ = cross-spectral density function between the ith and kth input

For the special case where the assumed inputs are incoherent (uncorrelated), Eq. (6) reduces to

$$G_y(x, f) = \sum_{i=1}^{N} \left| H_{ix}(f) \right|^2 G_i(f) \qquad (7)$$

where

$G_i(f)$ = power spectral density function for the ith input

From an analytical viewpoint, the multiple input approach provides little or no advantage over the classical approach discussed in Section 3. The problems involved in calculating point-to-point frequency response functions for a structure are similar to those associated with calculating

structural mode shapes and damping. Likewise, point-to-point cross-spectra for forces are no easier to calculate than continuous spatial cross-spectra for a pressure field. From an experimental viewpoint, however, the multiple input approach does offer an advantage in that the point-to-point quantities are generally easier to measure than the spatial functions required for the classical approach. It is for this reason that the multiple input approach has been most widely applied to problems where experimental techniques are feasible. Examples include studies of aircraft response to atmospheric gust loads and component response to mounting point structure vibration.

For the case of general environmental prediction, the multiple input approach is sometimes used to extend vibration predictions for a mounting point structure to obtain predictions for the response of an attached component. The general approach is to measure the desired frequency response function for a component of interest in the laboratory. Equation (6) or (7) can then be applied using the predicted vibration of the supporting point structure as the input. Beyond this application, however, the multiple input approach has not been widely used as a tool for predicting flight vehicle vibration environments. Details on the measurement of point-to-point frequency response functions and the general theory of the multiple input approach are presented in Reference 5.

## 4.2 SUMMARY

### Assumptions

1. The structure is a constant parameter linear system.
2. The excitation can be described with reasonable accuracy by a collection of point forces or point motions.

### Information Required

1. Frequency response functions for the structure between various input points and response points of interest.
2. Cross-spectral density functions for the excitations at the various input points.

### Advantages

1. The procedure yields reasonably accurate results if all required information is available.
2. The required calculations are straightforward and easy to implement on a computer.

### Disadvantages

1. The required information is sometimes difficult to obtain in practice.
2. Failure to define properly all inputs will produce serious errors.

# 5. GENERAL EXTRAPOLATION APPROACH

The general extrapolation approach includes all those procedures which use empirical relationships developed from regression studies of past data to predict vibration environments in future vehicles. Such procedures are widely used for flight vehicle vibration prediction at the present time. Seven of the best known general extrapolation procedures are presented in this section.

## 5.1 MAHAFFEY AND SMITH METHOD

### 5.1.1 Description

This method, originally proposed in Reference 6, was designed to predict the acoustically induced vibration environment of new jet powered vehicles by use of an acoustic-vibration frequency response function developed from measured data collected on the B-58 airplane. The data consisted of vibration and acoustic measurements at many locations on B-58 primary structure for the condition of maximum thrust on all four engines with afterburners operating during ground runup. The vibration and acoustic data were analyzed in octave bands with the vibration presented in g's peak (g's peak were defined as 3.3 times the rms values), and the acoustic noise presented in decibels (dB). The reduced data were then plotted with vibration as the ordinate and acoustic noise as the abscissa. Statistical methods were used to determine a regression line and appropriate percentage intervals for the data scatter. The statistical analysis indicated that the data in each octave band best fit an equation of the form

$$\log_e g = (M)(SPL) + \log_e A \qquad (8)$$

where

g = peak acceleration level divided by the acceleration due to gravity

M = slope of the empirical regression line

SPL = sound pressure level in decibels re 0.0002 dynes/cm$^2$

A = intercept of the empirical regression line on the g-axis

Figures 1 through 6 show the plots of the empirical equations and various percentage intervals for each octave band from 20 to 2400 cps. Predicting vibration environments in new flight vehicles is easily accomplished with these figures. For each octave band, the vibration level is read from the appropriate figure by using the known sound pressure level and the desired percentage limit. No specific technique is suggested for estimating excitation sound pressure levels for new flight vehicles.

The authors indicate that the empirically derived curves were used to predict vibration levels on other vehicles where both jet engine noise and vibration data were available. The predicted vibration levels for the different octave bands fit the measured data with about the same degree of accuracy as they fit the B-58 data. They therefore conclude that Figures 1 through 6 could be used with reasonable success for predicting the vibration of primary structure on other jet powered vehicles.

In Reference 7, a comparison was made between measured data on the Skybolt missile and the levels predicted by other methods. It is stated in this reference that the B-58 data should not be applied directly to vehicles of small diameter. Most of the B-58 low frequency resonances could be expected in the range of 100-300 cps, whereas vehicles

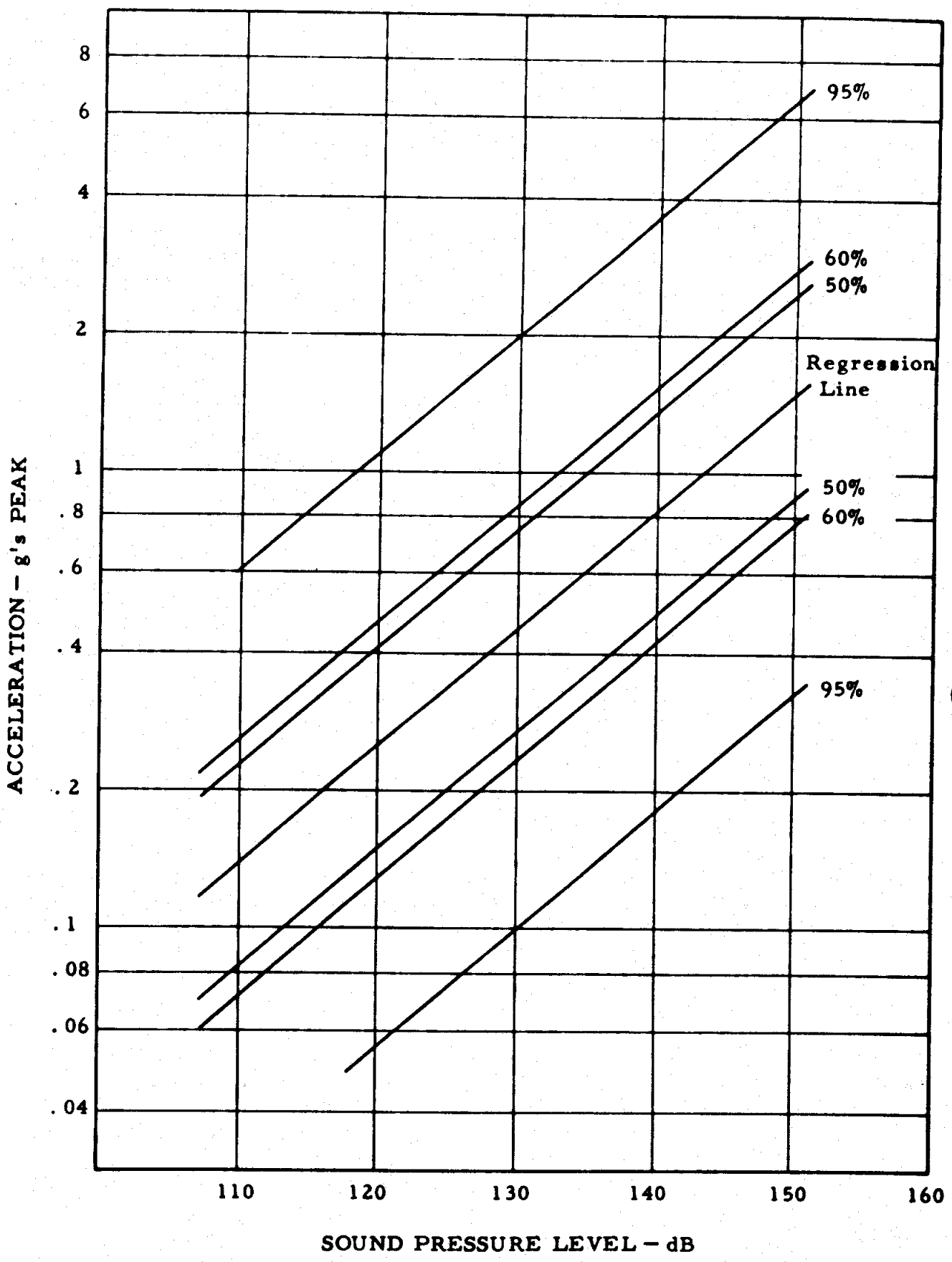


Figure 1. Prediction Curves for Mahaffey-Smith Method, 20-75 cps Octave

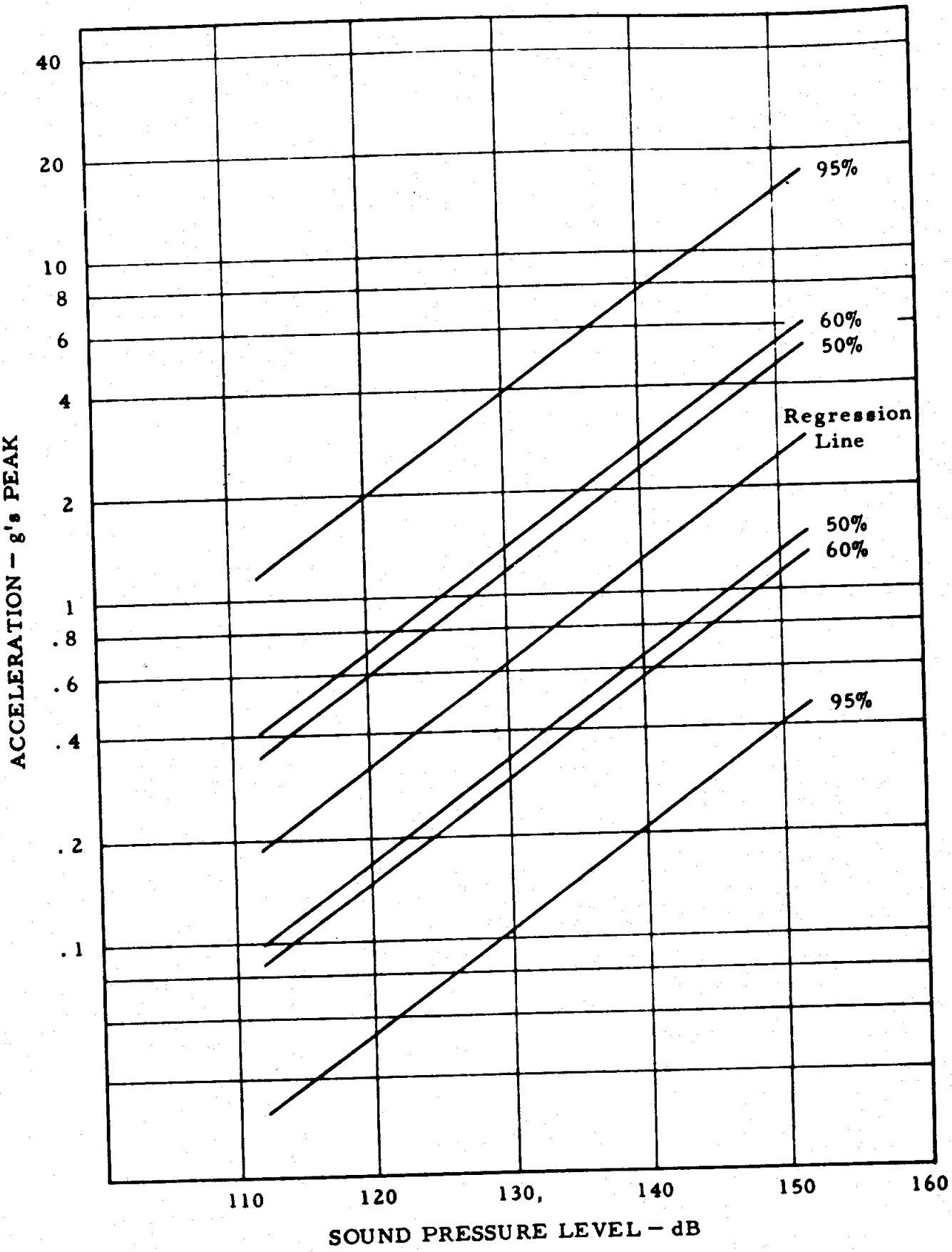


Figure 2. Prediction Curves for Mahaffey-Smith Method, 75-150 cps Octave

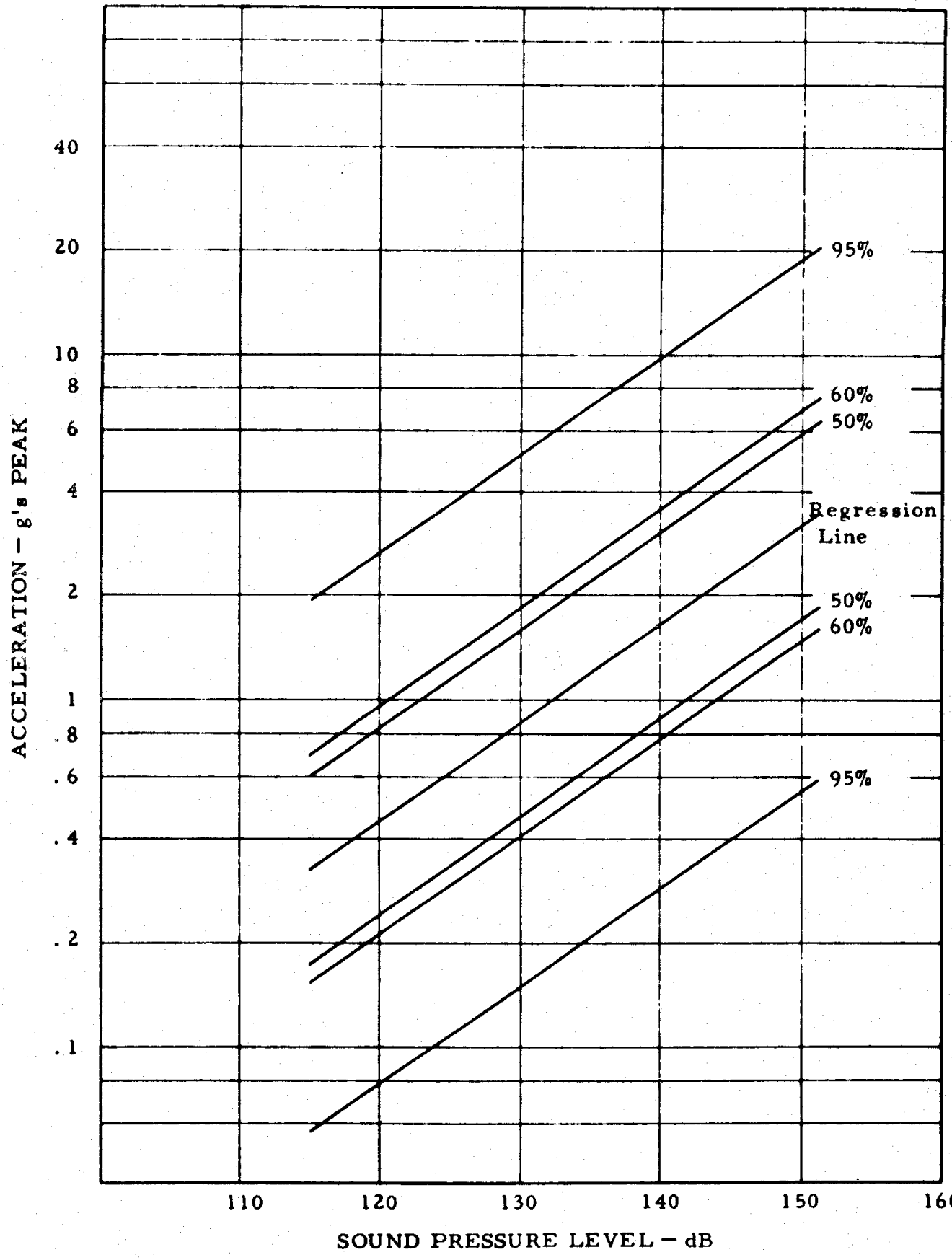


Figure 3. Prediction Curves for Mahaffey-Smith Method, 150-300 cps Octave

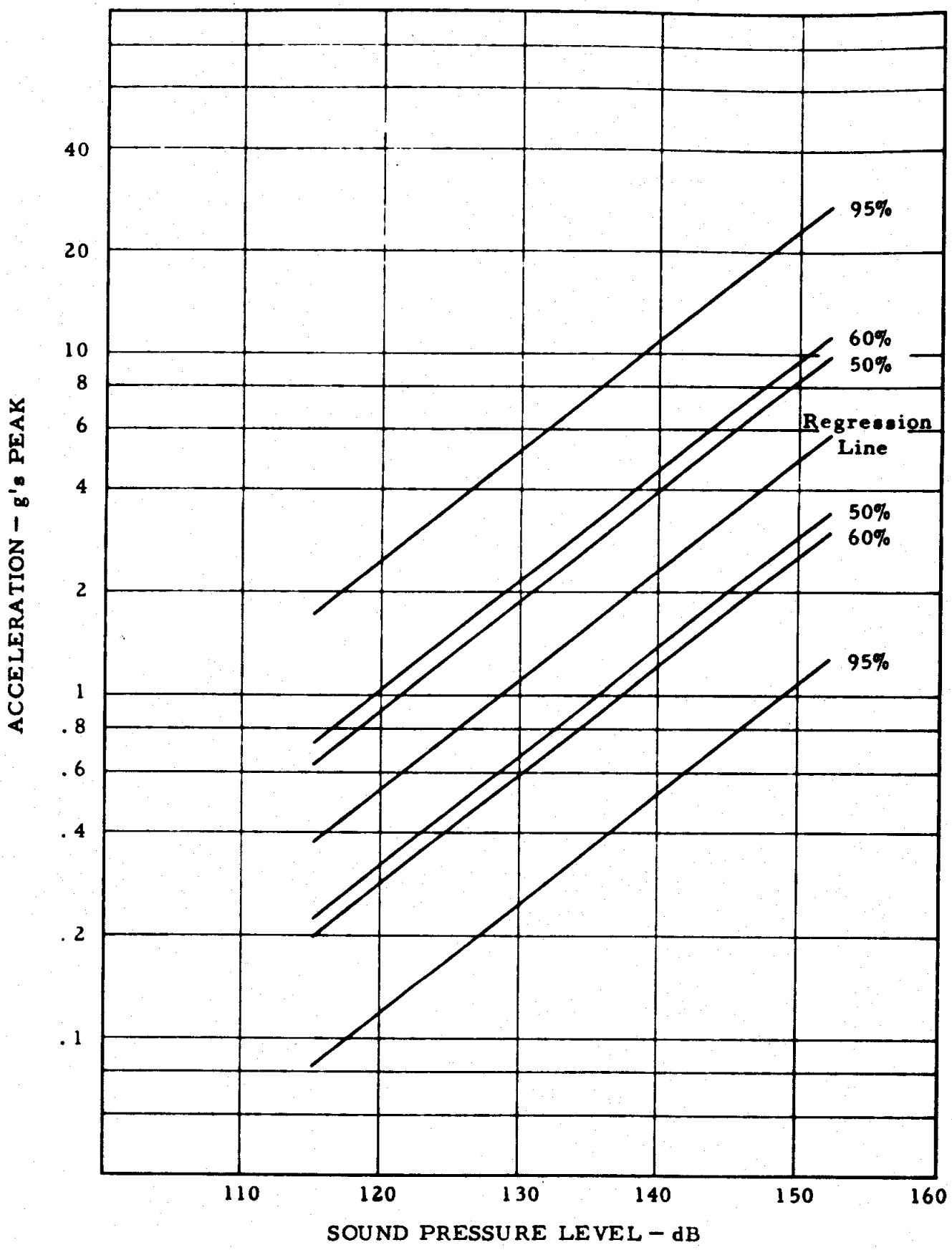


Figure 4. Prediction Curves for Mahaffey-Smith Method, 300-600 cps Octave

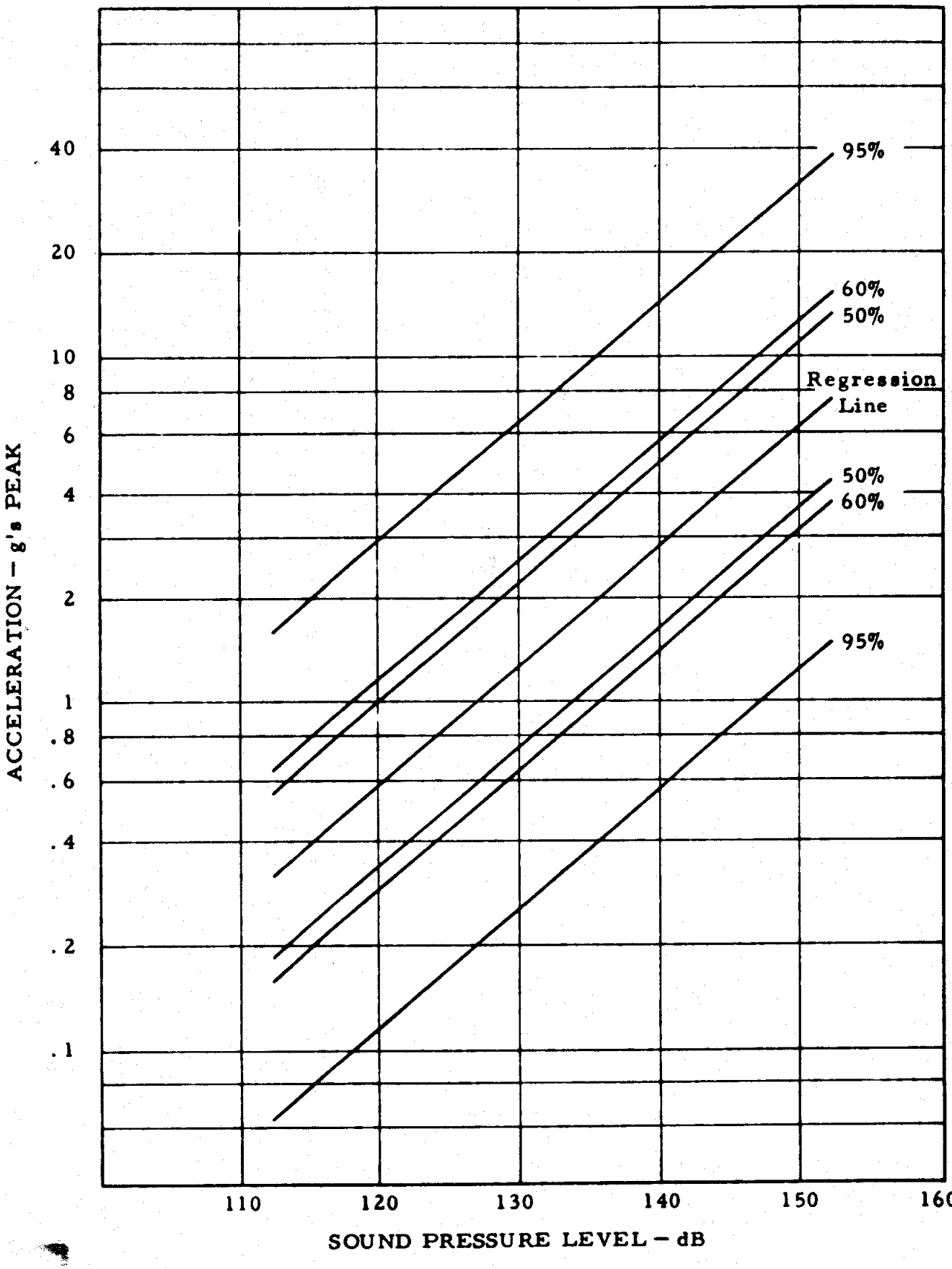


Figure 5. Prediction Curves for Mahaffey-Smith Method, 600-1200 cps Octave

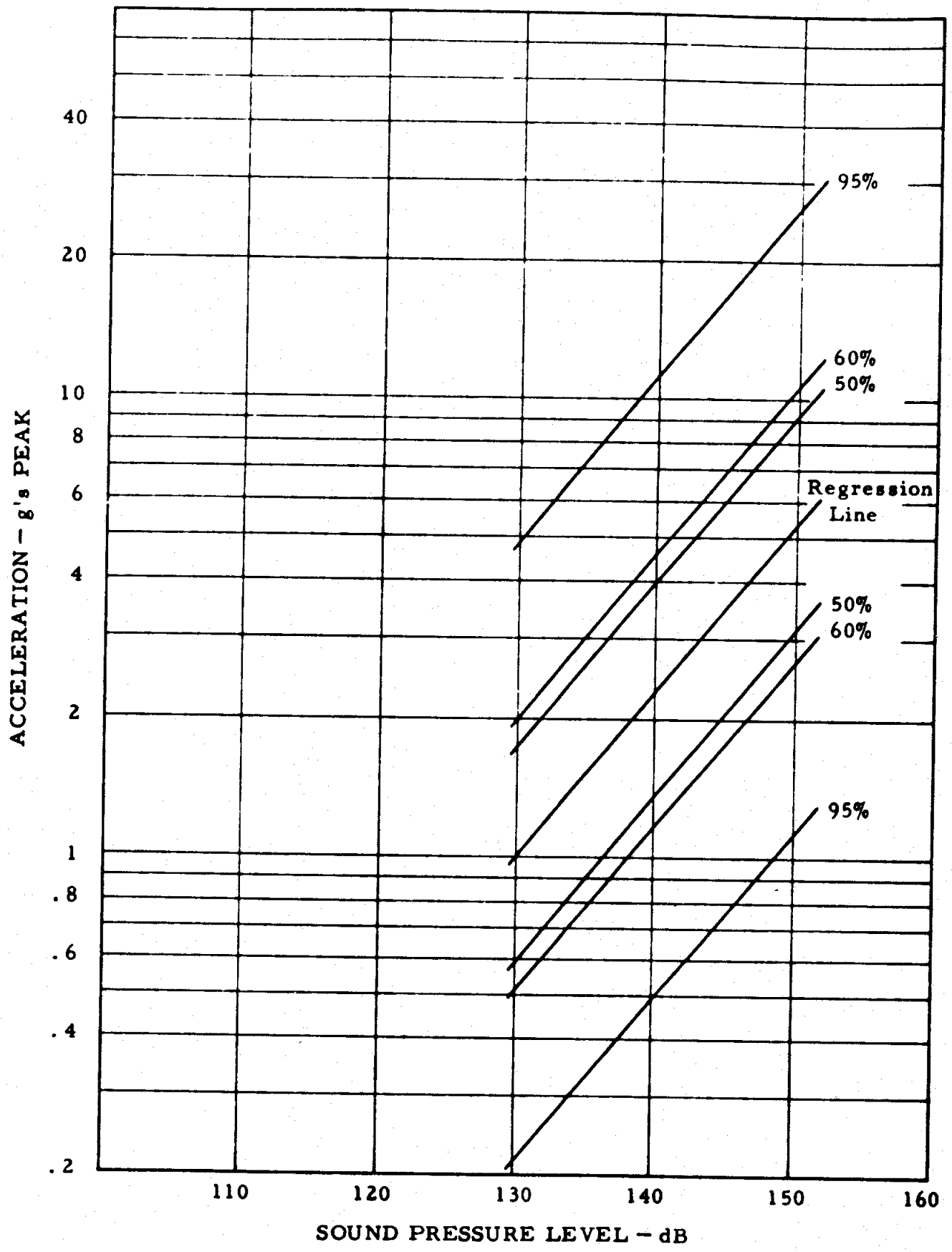


Figure 6. Prediction Curves for Mahaffey-Smith Method, 1200-2400 cps Octave

of small diameter have their low frequency resonances in the 300-1200 cps region. The curves in Reference 7 support this conclusion. In addition, other experience indicates that the Mahaffey-Smith Method gives results which are consistently too low in the high frequencies, and too high in the low frequencies, when applied to aerospace vehicles.

### 5.1.2 Summary

#### Assumptions

1. All flight vehicles to which the procedure will be applied are dynamically similar to the B-58 airplane.
2. Vibration is due principally to acoustic noise excitation during takeoff.
3. Spatial variations in vibration can be considered a random variable.
4. Vibration response is the same in all three orthogonal directions.
5. Peak response is equal to 3.3 times the rms response.

#### Information Required

Measurements or prediction of acoustic noise environment.

#### Advantages

1. The procedure is simple and easy to use.
2. No structural design details are required.

Limitations

1. The procedure is based upon aircraft data only. The applicability of the procedure to spacecraft data is questionable.
2. No excitation factors other than acoustic noise are considered.
3. The prediction of vibration in terms of peak g's is inappropriate for the case of random vibration environments.
4. No distinction is made for different equipment mountings and between different orthogonal directions.

## 5.2 BRUST AND HIMELBLAU METHOD

### 5.2.1 Description

This method, which is presented in Reference 7, extends the Mahaffey-Smith method (Section 5.1) to provide vibration predictions in terms of average acceleration spectral density rather than g's peak. It also includes specific suggestions for estimating the acoustic noise environment for new vehicles, and for converting the predicted vibration levels into test specifications.

The specific acoustic-vibration frequency response function suggested by Brust and Himelblau is presented for each frequency octave in Figures 7 and 8. Only one percentage line is provided for each frequency octave. This line corresponds to the upper 60% scatter limit for individual values. According to Brust and Himelblau, the 60% line was selected because it will envelope nearly all vibration measurements

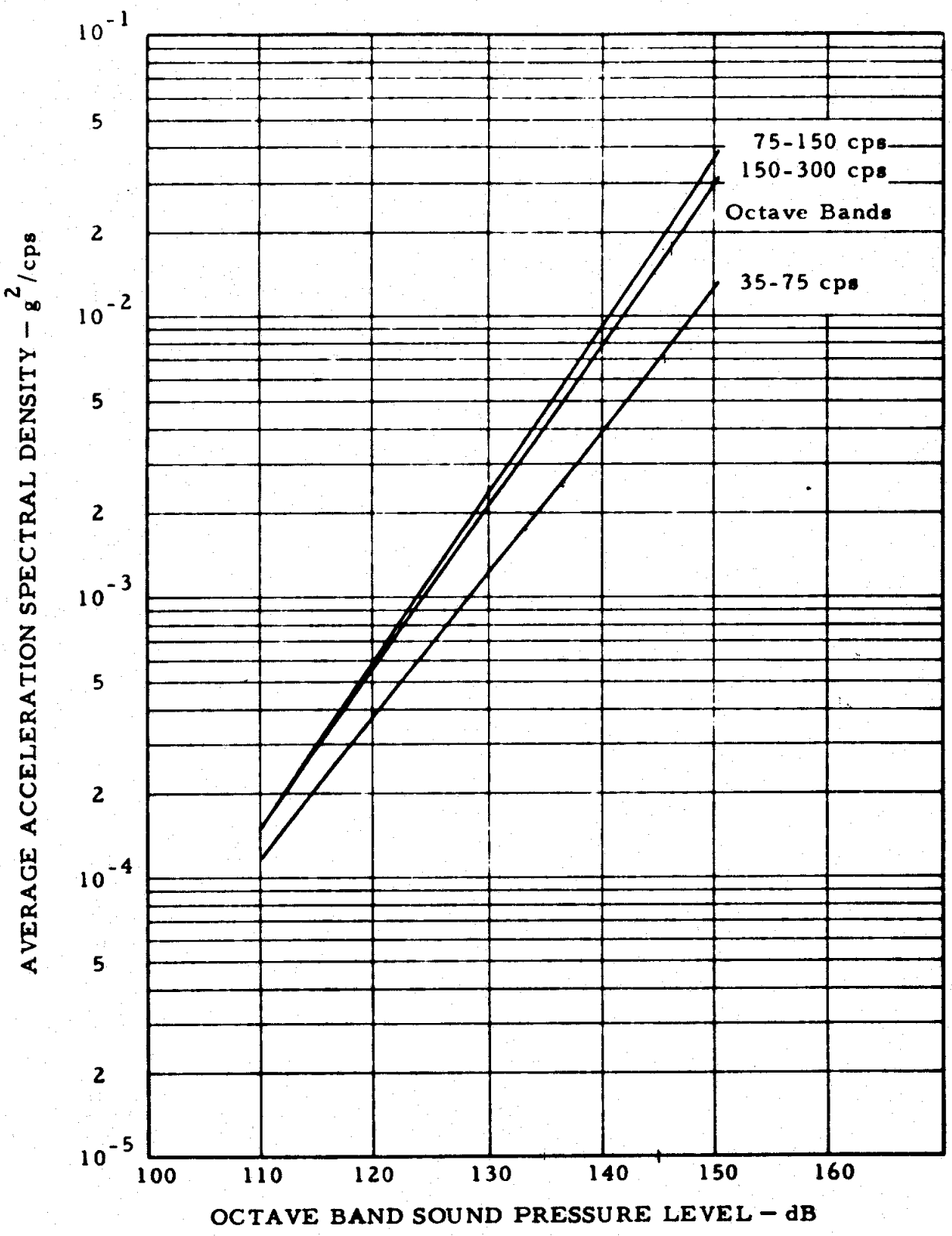


Figure 7. Prediction Curves for Brust-Himelblau Method, 35-300 cps

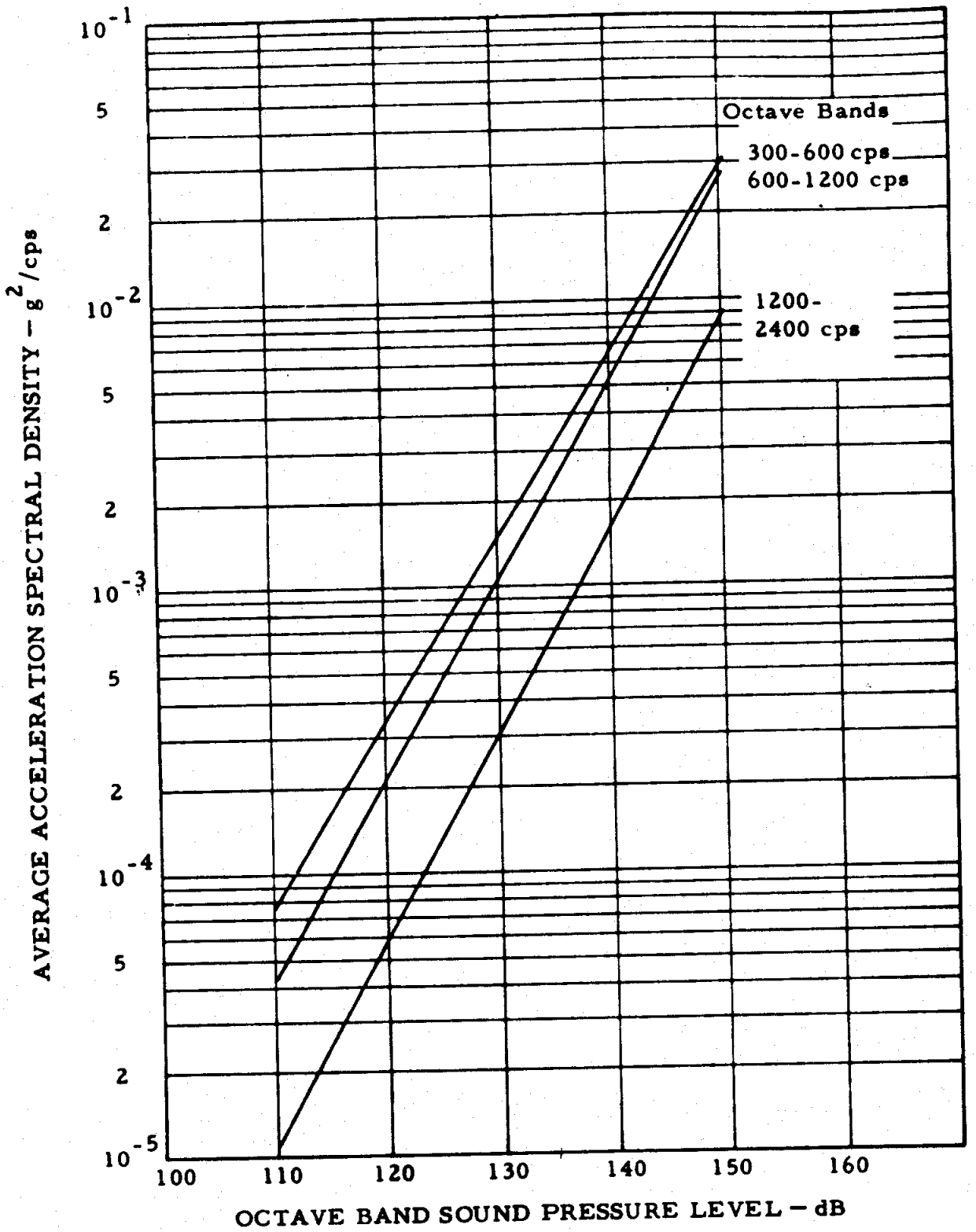


Figure 8. Prediction Curves for Brust-Himelblau Method, 300-2400 cps

which apply to equipment locations. Hence, the curves should provide conservative predictions for the vibration inputs to mounted equipment. However, the vibration of unloaded structure will generally be more severe than indicated by the predictions.

The procedure predicts average acceleration spectral densities in frequency octaves, as opposed to maximum spectral densities which would be observed in a narrow bandwidth analysis of the data. This fact led Brust and Himelblau to recommend that a factor of 7 dB be added to the predictions if an envelope for spectral density peaks is desired. This factor was arrived at by analyzing available TITAN I vibration data with different analysis bandwidths, and comparing the results for narrow band analysis with those for octave band analysis.

The procedure is applied to the Skybolt missile and compared to measured data in Reference 7. The results indicate the procedure tended to overestimate the Skybolt vibration environment in the frequency range below 300 cps by as much as 10 dB, and to sometimes underestimate the environment in the frequency range from 300 to 600 cps by up to 6 dB. The authors attributed this to differences between the structures of the Skybolt missile and the B-58 aircraft (the procedure is based upon B-58 data).

Specific procedures are suggested in Reference 7 for estimating the acoustic input needed to apply the procedure. These suggestions are now summarized.

## Estimation of Acoustic Noise Pressures Produced by Turbojet and Rocket Engines

It is suggested that actual field measurements be used when possible. Examples of acoustic data for various 1955 vintage flight vehicles are presented in Table 1. If acoustic data are not available for the actual

Table 1. External Acoustical Noise Levels for Rocket-Propelled Missiles at Liftoff or Jet-Propelled Aircraft at Takeoff

| Vehicle | Location | OA SPL |
|---|---|---|
| TITAN I | Nose Cone | 139 dB |
| | Interstage | 143 dB |
| | Engine Compartment | 155 dB |
| JUPITER | Nose Cone | 148 dB |
| | Engine Compartment | 153 dB |
| B-52 | Forward Fuselage | 137 dB |
| | Mid Fuselage | 155 dB |
| | Aft Fuselage | 157 dB |
| B-58 | Forward Fuselage | 128 dB |
| | Mid Fuselage | 148 dB |
| | Aft Fuselage | 156 dB |
| | Forward Pod | 145 dB |
| | Aft Pod | 157 dB |
| RB-66 | Forward Fuselage | 124 dB |
| | Mid Fuselage | 133 dB |
| | Aft Fuselage | 148 dB |

vehicle of interest, then measurements for a similar vehicle or configuration should be used. This includes properly scaled models, as pointed out in References 8 and 9. If an entirely new configuration is being proposed, then an acoustical prediction should be made. References 10 through 13 provide information on this subject. The near field overall sound pressure level generated by a typical 1955 vintage turbojet engine at takeoff is shown in Figure 9. Average octave band sound pressure levels are given in Figure 10 (these plots are taken from Reference 14). The overall and octave band sound pressure levels typical at the surface of a large ballistic missile during liftoff are shown in Figure 11 (taken from Reference 15). It may sometimes be possible to estimate an approximate overall sound pressure level, but not the shape of the spectrum. In such cases, the octave band levels should be estimated using an average noise spectrum shape, as given in Figure 12.

## Estimation of Boundary Layer Pressures Produced by Aerodynamic Turbulence

The pressure fluctuations in turbulent aerodynamic boundary layers do not necessarily produce the same amount of structural vibration as acoustic pressures of equivalent magnitude. This is due to the difference in the space-time correlation characteristics of turbulence and acoustic pressure fields (see Reference 16 for further discussions). As a first order of approximation, however, Brust and Himelblau state that the prediction curves in Figures 7 and 8 can be used to predict turbulence induced vibration. As for acoustic environments, actual field measurements provide the best estimate for a boundary layer turbulence environment. If such measurements are not available for the vehicle of interest, a prediction must be used. References 10, 11 and 15 give useful guidance

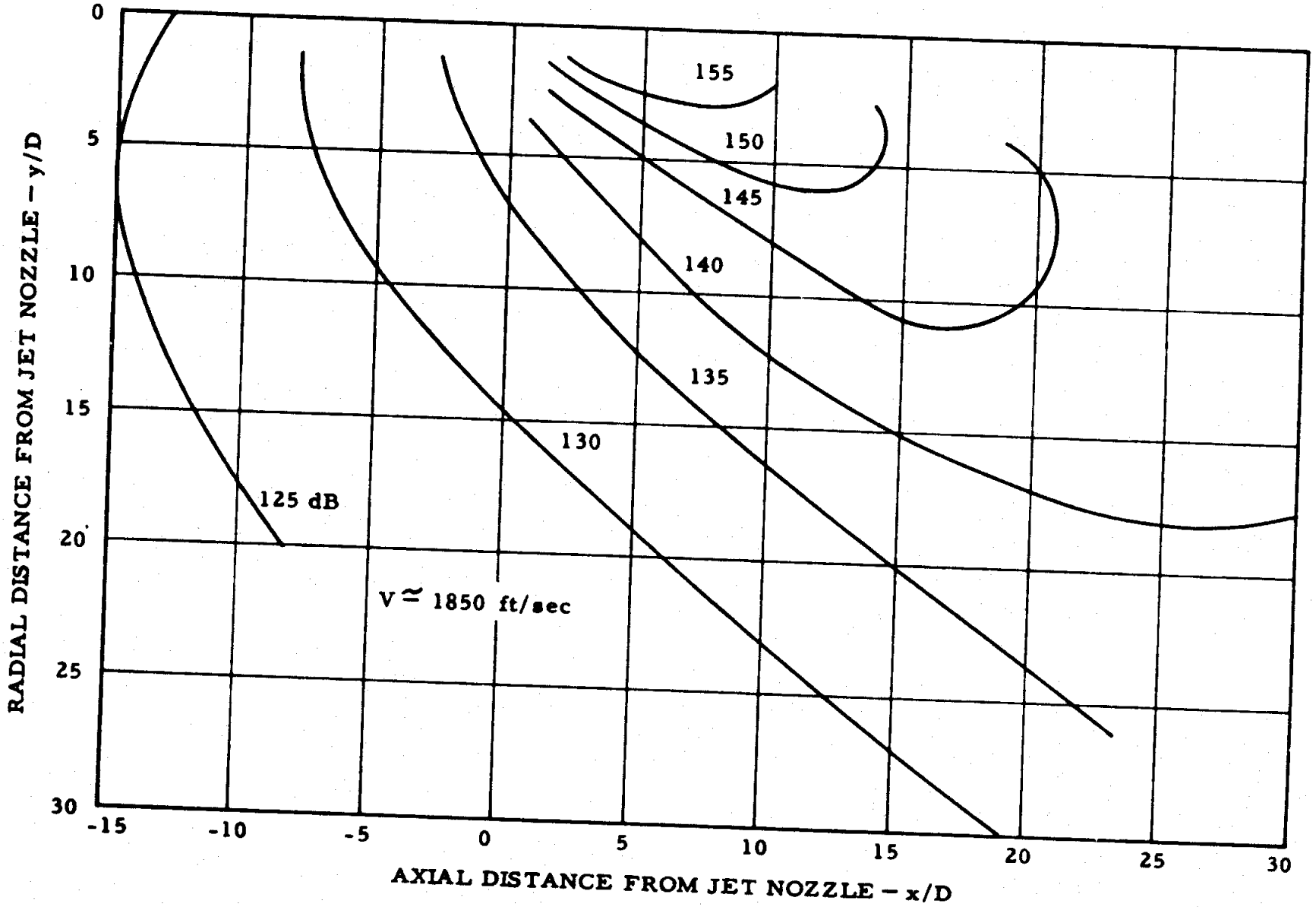


**Figure 9.** Contours of Overall Sound Pressure Level in the Near Field of a Typical 1955-Vintage Turbojet Engine (Reference 14)

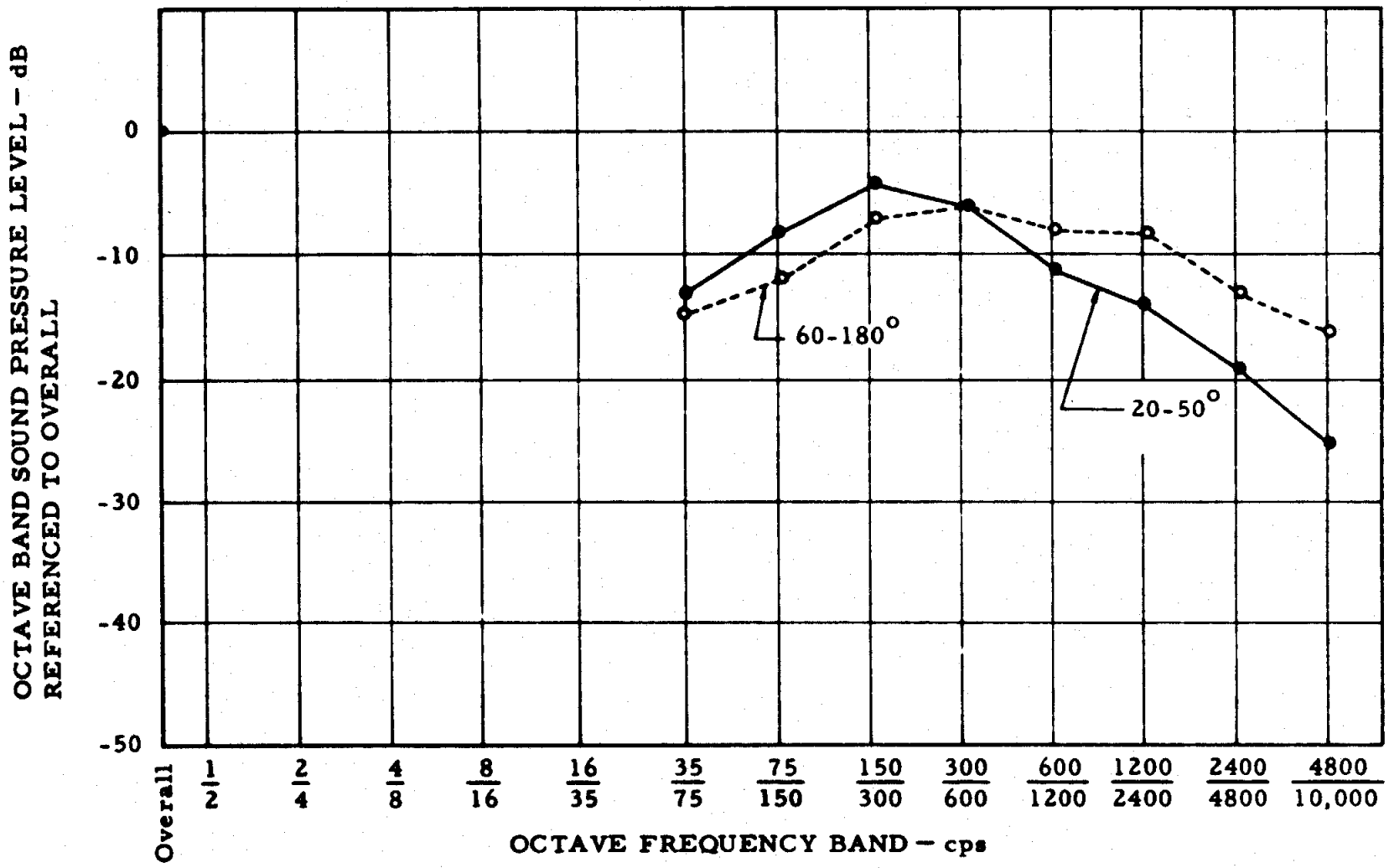


**Figure 10. Typical Acoustic Noise Spectra for a 1955-Vintage Turbojet Engine (Reference 14)**

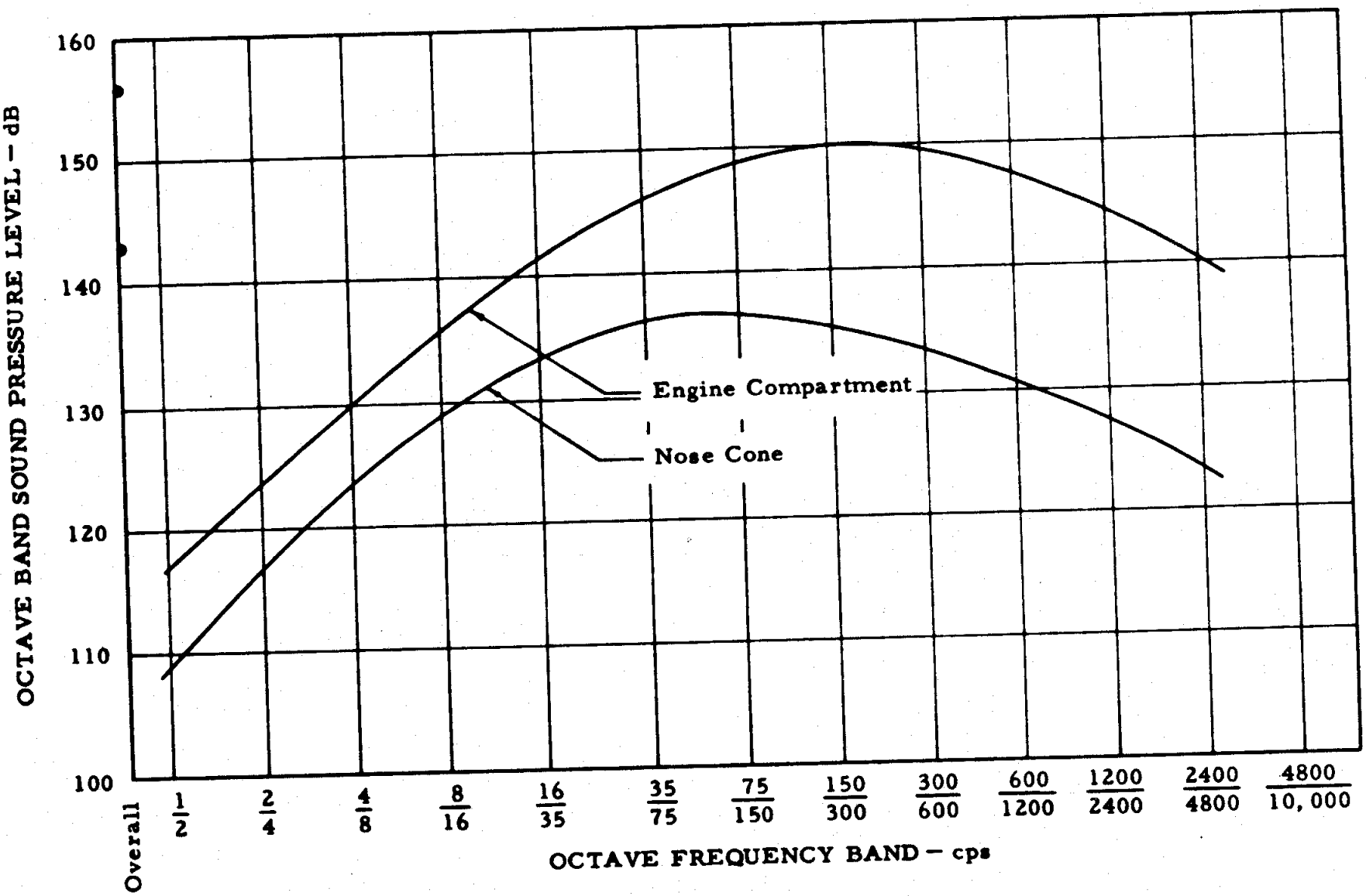


**Figure 11. Typical Acoustic Noise Spectra for the Surface of a Large Liquid-Propelled Ballistic Missile (Reference 15)**

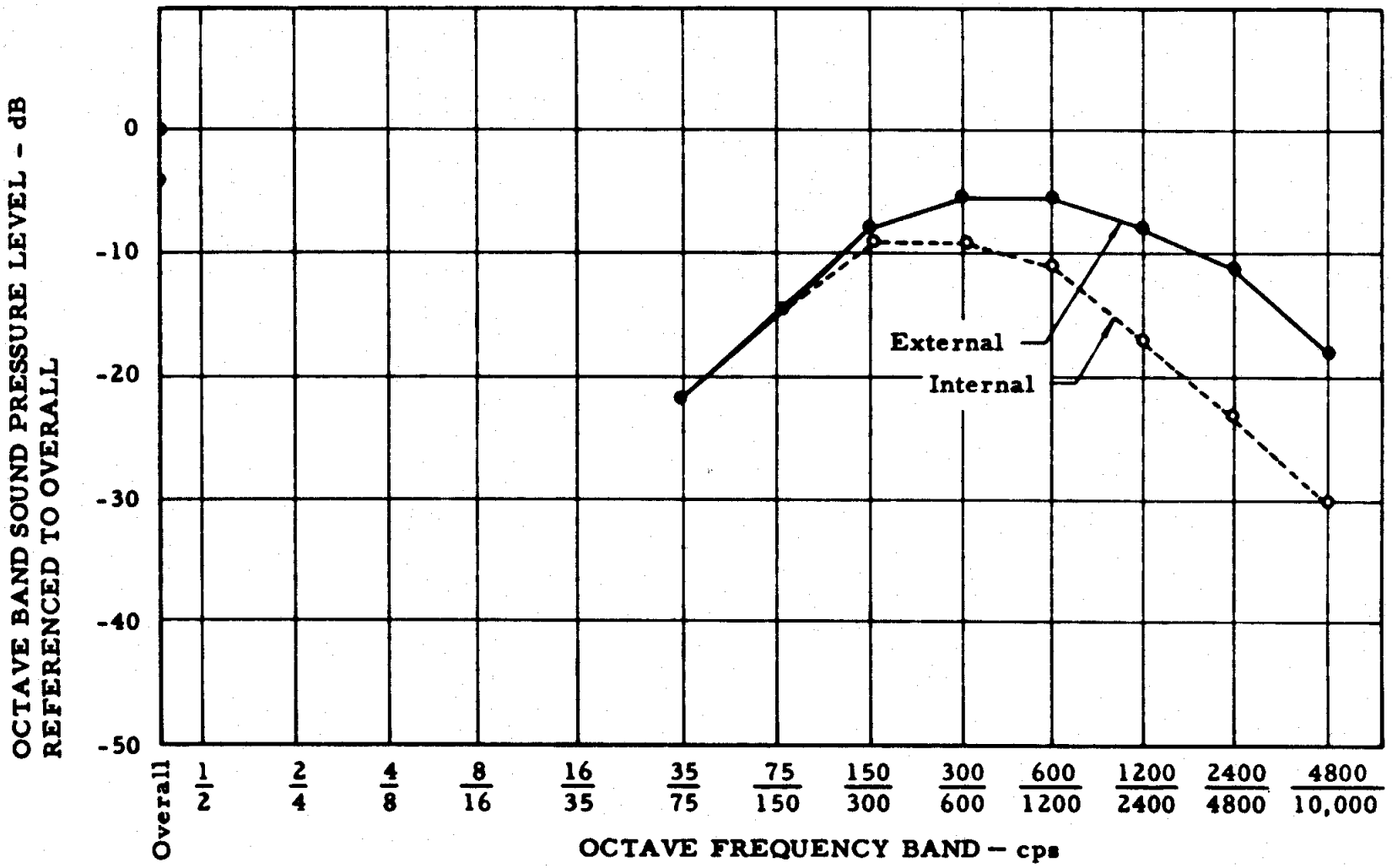


**Figure 12. Typical Acoustic Noise or Turbulence Spectra (Reference 7)**

on this subject. Based on empirical data from References 10 and 17, the rms boundary layer turbulence ($p_r$) is related to the free stream dynamic pressure ($q_\infty$) by

$$p_r = K_t q_\infty \tag{9}$$

where $q_\infty = 0.7\ PM_\infty^2$, p = atmospheric pressure at the altitude of operation, and $M_\infty$ = free stream Mach number of the vehicle. The term $K_t$ is a function of the aerodynamic "cleanliness" of the flight vehicle. Values of $K_t$ for various vehicle contouring are presented in Figure 13. For vehicles that are relatively clean, a value of $K_t = 5 \times 10^{-3}$ is often used, particularly in a preliminary design stage. This value produces boundary layer pressure estimates which coincide with data for plate experiments discussed in Reference 10. Using $K_t = 5 \times 10^{-3}$, it follows that the overall turbulence pressure level in decibels is given by

$$\text{OA TPL} = 20 \log p_r = 20 \log q_\infty + 82 \text{ dB} \tag{10}$$

Table 2 shows the Mach number required to produce various dynamic pressures at several altitudes and the corresponding values for the overall turbulence pressure levels, assuming $K_t = 5 \times 10^{-3}$. Once the overall turbulence pressure level has been determined, the shape of the spectrum can be determined from Figure 14, which is taken from References 10 and 18. The octave band turbulence pressure level (OB TPL) can be calculated from the turbulence spectrum level by

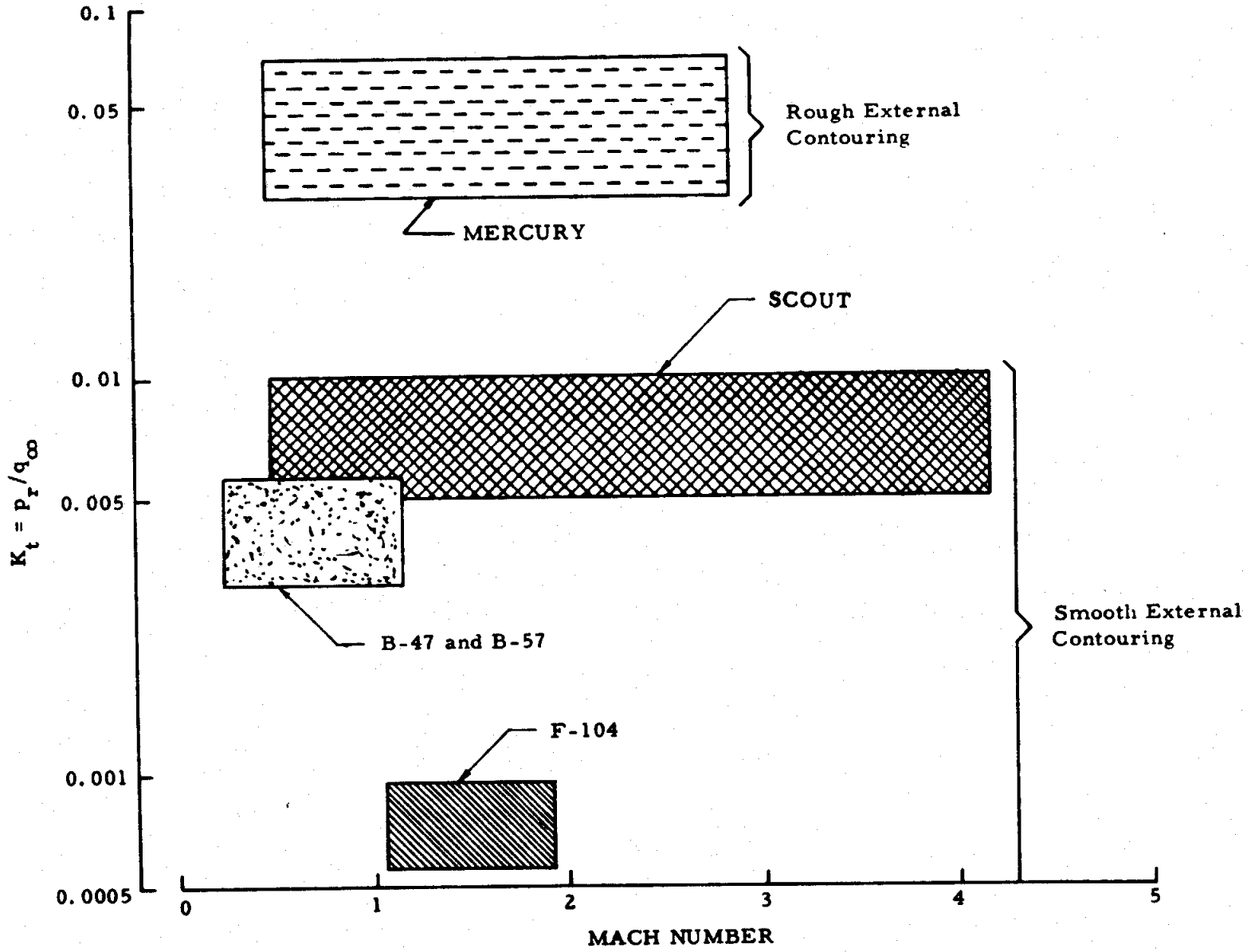


**Figure 13. Ratio of Boundary Layer Turbulence Pressure to Free Stream Dynamic Pressure as a Function of Vehicle Mach Number and Aerodynamic Cleanliness (Reference 16).**

Table 2. Mach Number Required to Produce Certain Free Stream Dynamic Pressures at Various Altitudes of a Vehicle (Overall Turbulent Pressure Levels are shown in parenthesis for $K_t = 5 \times 10^{-3}$)

| Pressure Altitude (ft) | Speed of Sound (ft/sec) | Kinematic Viscosity ($ft^2/sec$) | Free Stream Dynamic Pressure (and OA TPL) | | | | |
|---|---|---|---|---|---|---|---|
| | | | 450 psf (135 dB) | 800 psf (140 dB) | 1400 psf (145 dB) | 2500 psf (150 dB) | 4500 psf (155 dB) |
| Sea Level | 1120 | $1.57 \times 10^{-4}$ | 0.5 | 0.7 | 1.0 | 1.3 | 1.7 |
| 10,000 | 1080 | 2.01 | 0.7 | 0.9 | 1.2 | 1.6 | 2.1 |
| 20,000 | 1040 | 2.62 | 0.8 | 1.1 | 1.4 | 1.9 | 2.6 |
| 30,000 | 990 | 3.49 | 1.0 | 1.3 | 1.8 | 2.4 | 3.2 |
| 40,000 | 970 | 5.06 | 1.3 | 1.7 | 2.3 | 3.0 | |
| 50,000 | 970 | 8.16 | 1.6 | 2.2 | 2.9 | | |
| 60,000 | 970 | 13.16 | 2.1 | 2.8 | 3.6 | | |
| 70,000 | 970 | 21.22 | 2.6 | 3.5 | | | |
| 80,000 | 970 | 34.20 | 3.3 | | | | |

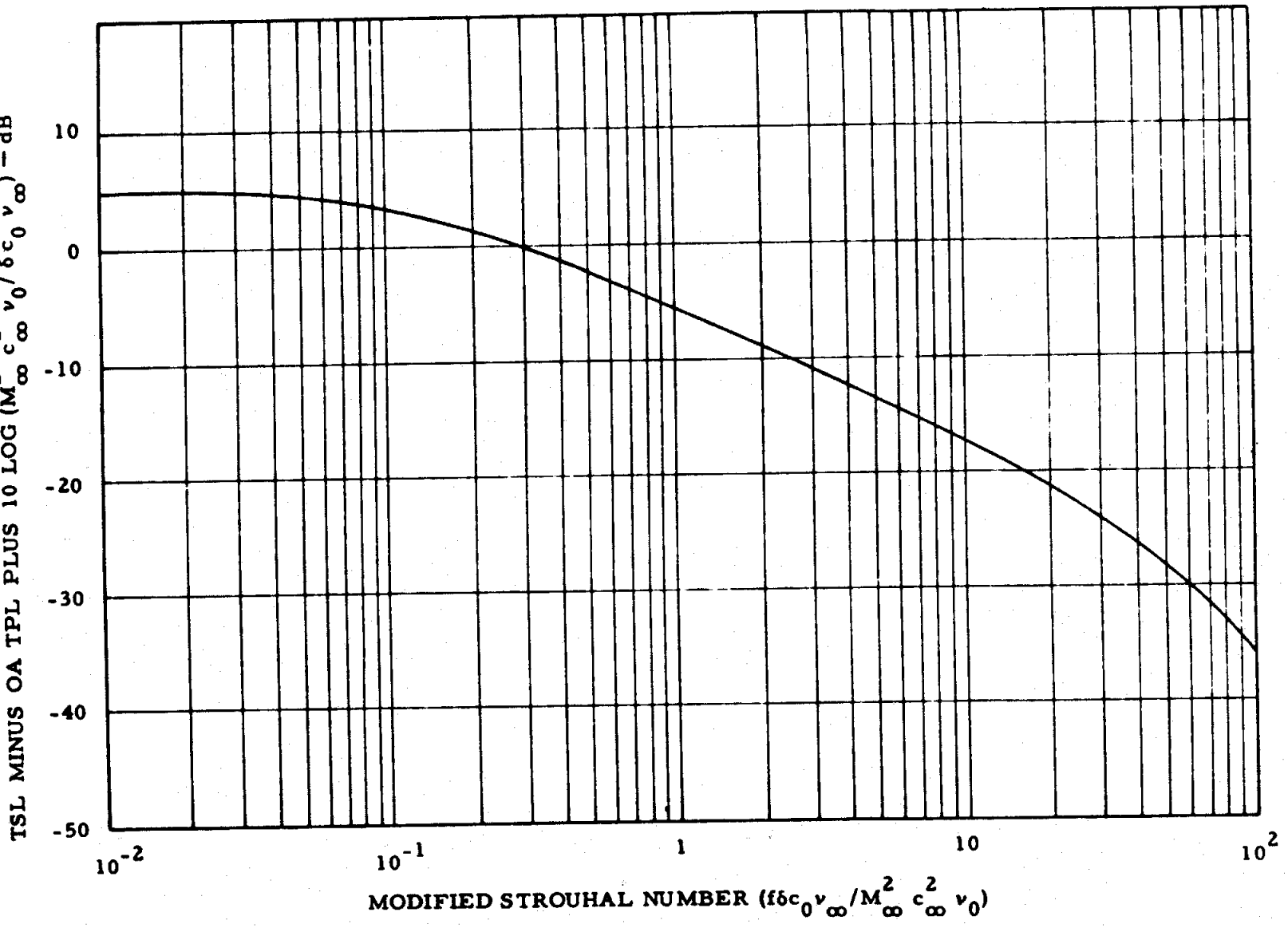


**Figure 14. Normalized Boundary Layer Pressure Spectrum (Reference 10)**

$$OB\ TPL = TSL + 10 \log \Delta f \qquad (11)$$

where the TSL is established at the geometric mean frequency $f_m = (f_\ell f_h)^{1/2}$ of the octave band of interest, and $\Delta f = f_h - f_\ell$ is the bandwidth.

### 5.2.2 Summary

#### Assumptions

1. All flight vehicles to which the procedure will be applied are dynamically similar to the B-58 airplane.
2. Vibration is due principally to acoustic noise during takeoff or liftoff, and boundary layer turbulence during flight at high dynamic pressures.
3. Acoustic noise pressures and boundary layer turbulence pressures of similar magnitude produce similar structural vibration.
4. The vibration to be predicted is on primary structure at equipment mounting points.
5. Spatial variations in vibration can be considered a random variable.
6. Vibration is the same in all three orthogonal directions.

#### Information Required

Measurements or predictions of acoustic noise and boundary layer pressure environments.

Advantages

1. The procedure is simple and easy to use.
2. No structural design details are required.

Limitations

1. The procedure is based upon aircraft data only. The applicability of the procedure to spacecraft data is questionable.
2. No excitation factors other than acoustic noise and boundary layer turbulence are considered.
3. No distinction is made between different equipment mountings and between different orthogonal directions.
4. The procedure is unconservative for unloaded structural vibration predictions.
5. The procedure assumes acoustic noise and boundary layer turbulence of similar magnitudes will produce similar structural vibration, which is not actually true.

## 5.3 ELDRED, ROBERTS, AND WHITE METHOD NO. 1

In Reference 10, Eldred, Roberts, and White summarize the results of two vibration data studies which could be used for vibration prediction. The first is based upon aircraft missile data and the second is based upon ballistic missile data. The first procedure is reviewed in this section. The second is covered in Section 5.4.

### 5.3.1 Description

Method No. 1 consists of an acoustic-vibration frequency response function developed from Snark Missile data. The data consisted of vibration and acoustic measurements at many different locations on the Snark structure for the condition of full engine thrust prior to launch. The data

were analyzed in octave bands with the vibration presented in g's rms and the acoustic noise presented in decibels (dB). The data were plotted with vibration as the ordinate and acoustic noise as the abscissa, and a trend line for the data was estimated. No statistical analysis, however, was performed.

The results are presented for each octave band in Figures 15 through 20. The plots may be used to predict the acoustically induced structural vibration of similar vehicles using a known sound pressure level. Since no statistical descriptions for the data scatter are provided, the user must interpret the plots using his own statistical calculations or engineering judgment. No specific techniques are suggested for estimating excitation sound pressure levels for new flight vehicles. General use of the procedure has not been sufficient to assess its accuracy directly. However, by squaring the ordinate values and dividing by bandwidth, it is seen that the curves in Figures 15 through 20 are quite similar to the Brust and Himelblau prediction curves presented in Section 5. 2. Hence, similar accuracies should be expected in its use as a prediction technique.

### 5. 3. 2 Summary

#### Assumptions

1. All flight vehicles to which the procedure is to be applied are dynamically similar to the Snark Missile.
2. Vibration is due principally to acoustic noise during takeoff.
3. Spatial variations in the vibration can be considered a random variable.
4. Vibration is the same in all three orthogonal directions.

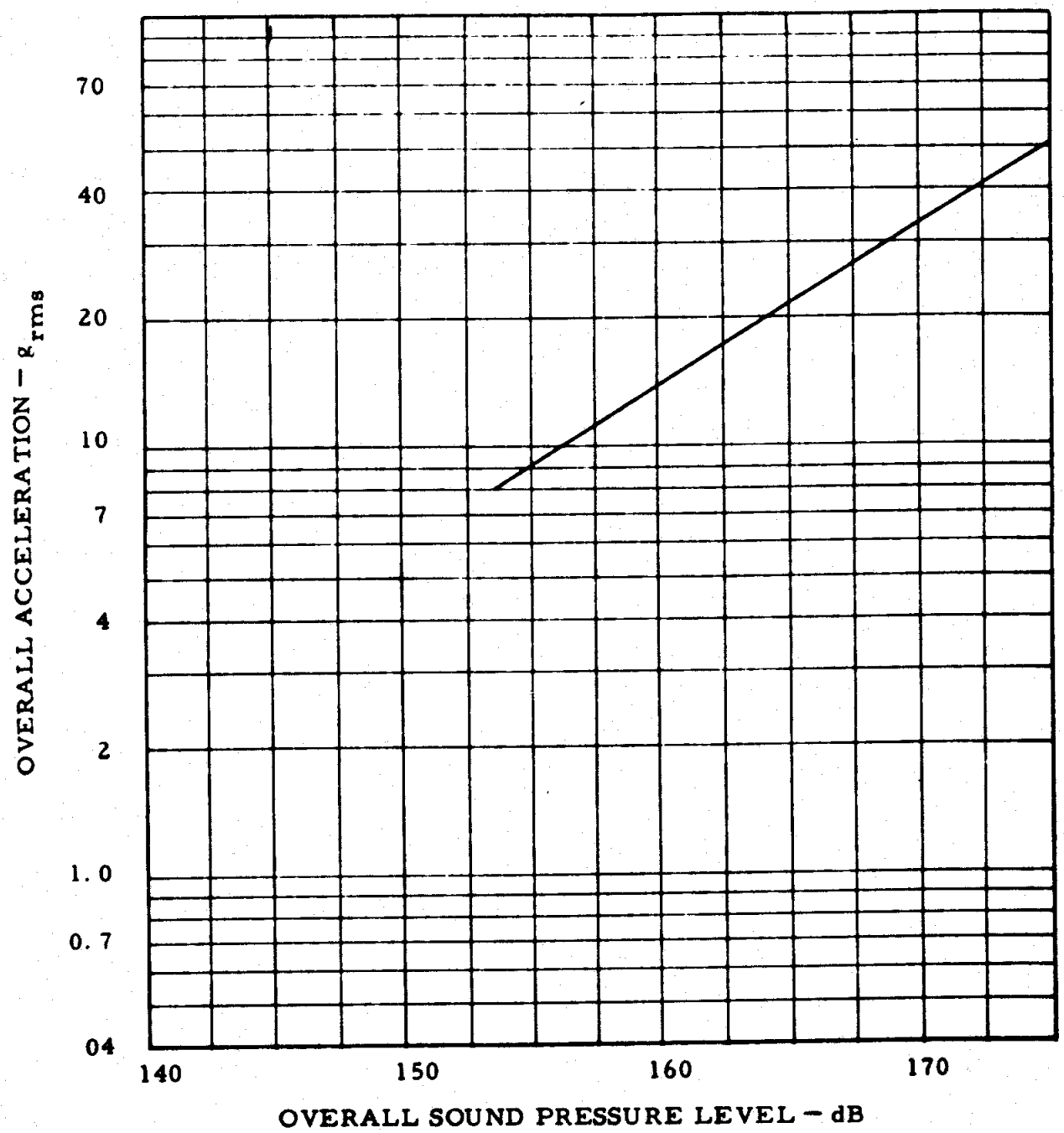


Figure 15. Correlation Between the Vibration Level and the External Acoustic Excitation of the Snark Missile – OAL Levels

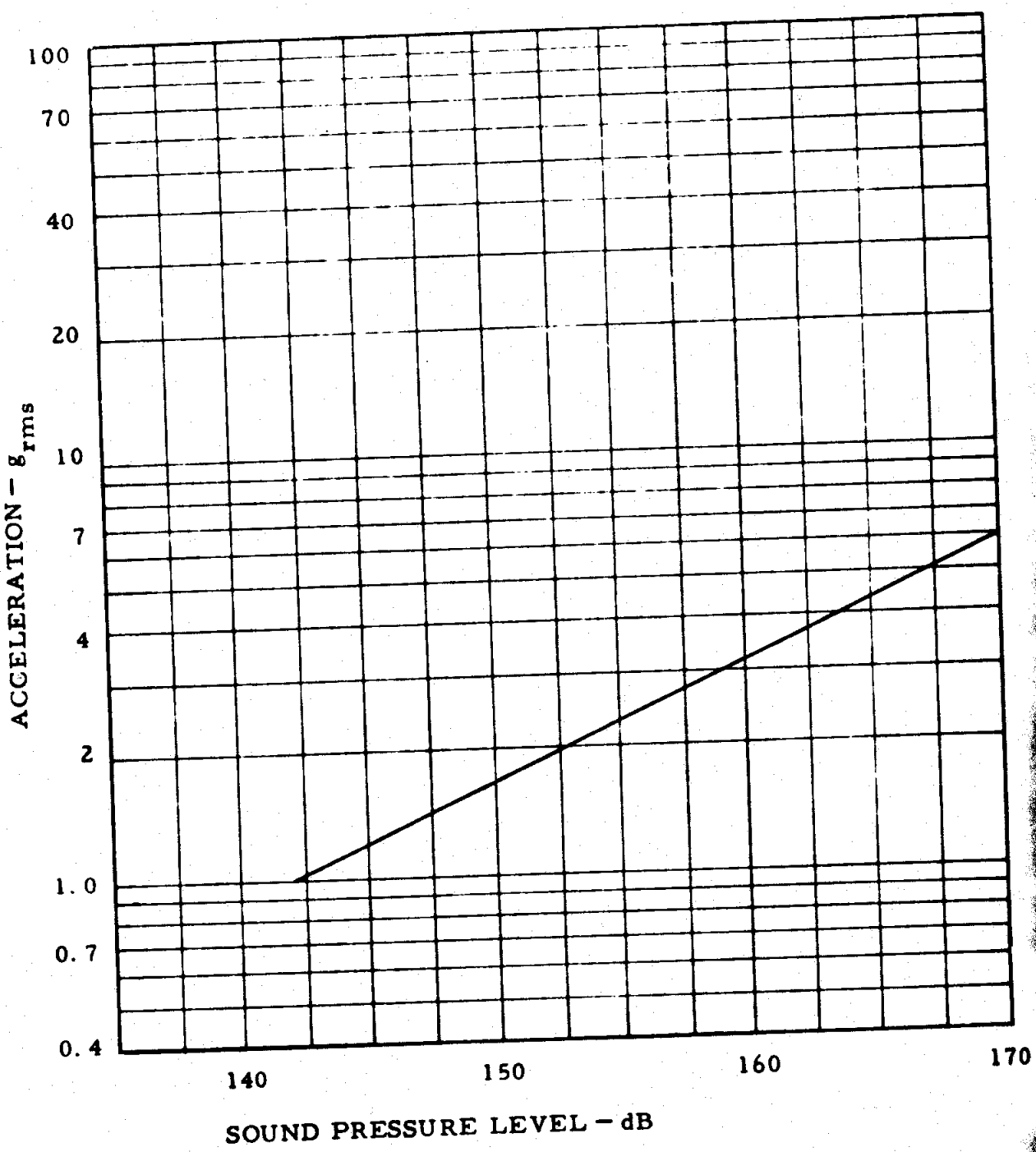


Figure 16. Correlation Between the Vibration Level and the External Acoustic Excitation of the Snark Missile – 20-75 cps Octave Band

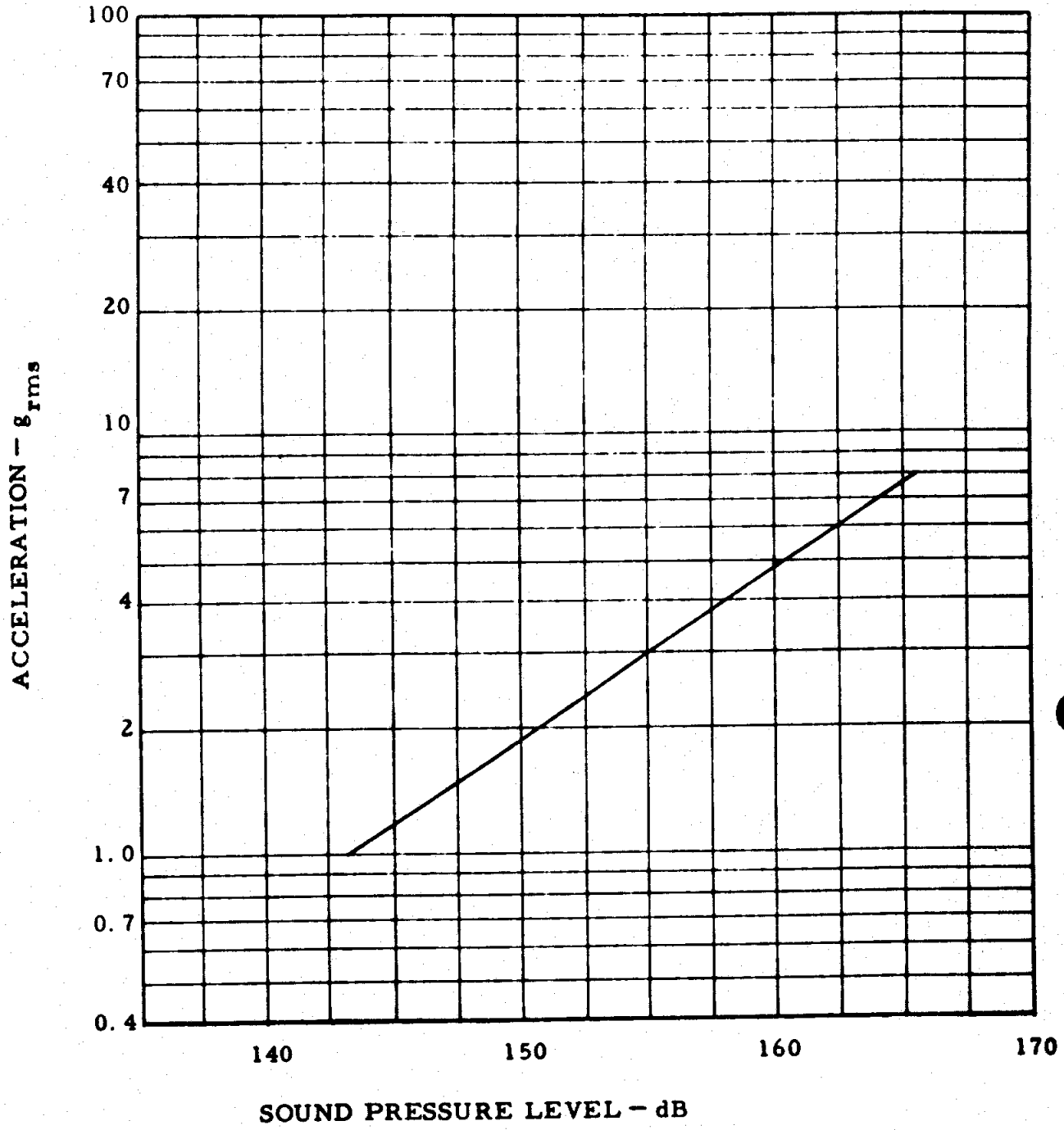


Figure 17. Correlation Between the Vibration Level and the External Acoustic Excitation of the Snark Missile – 75-150 cps Octave Band

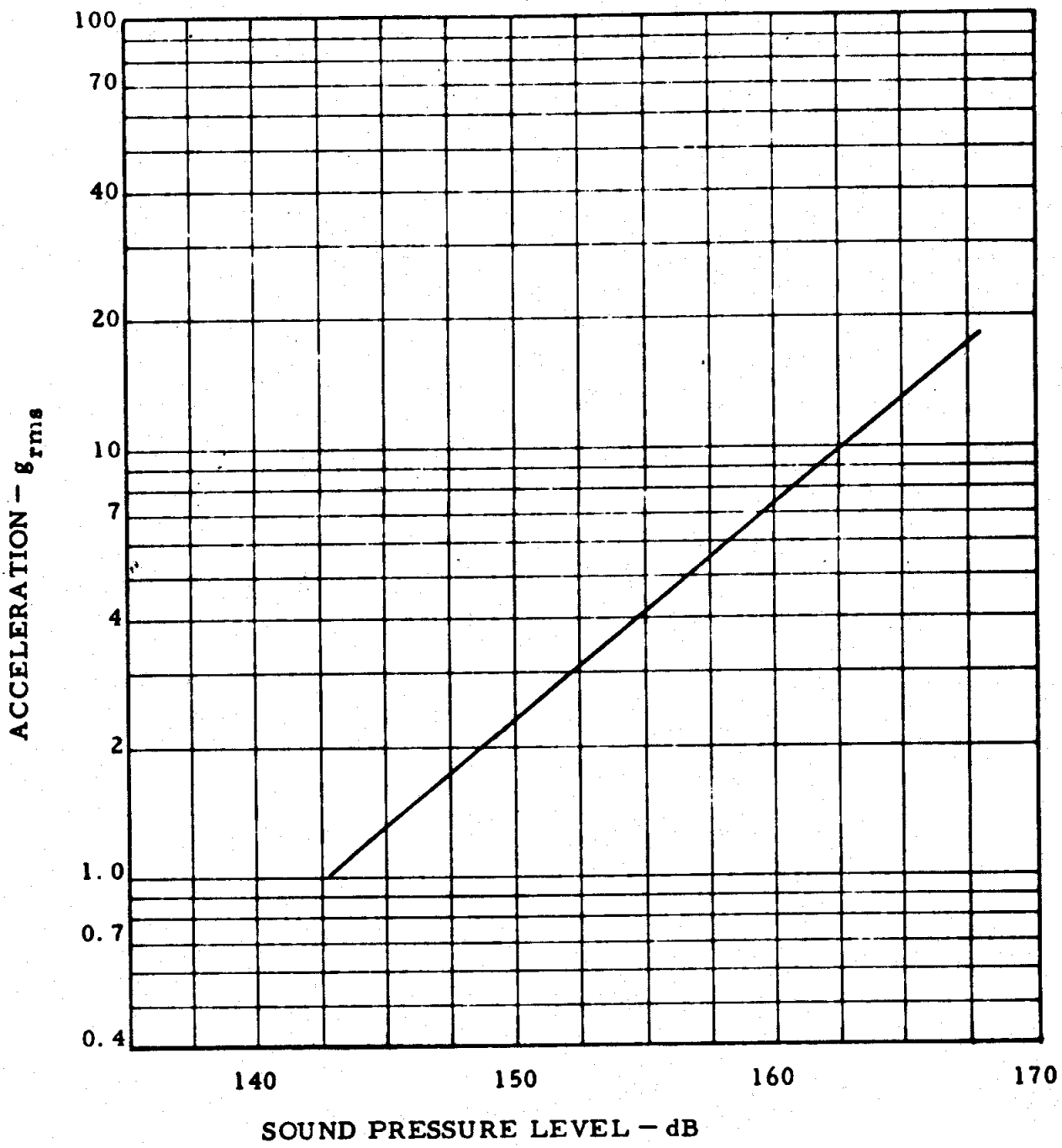


**Figure 18. Correlation Between the Vibration Level and the External Acoustic Excitation of the Snark Missile – 150-300 cps Octave Band**

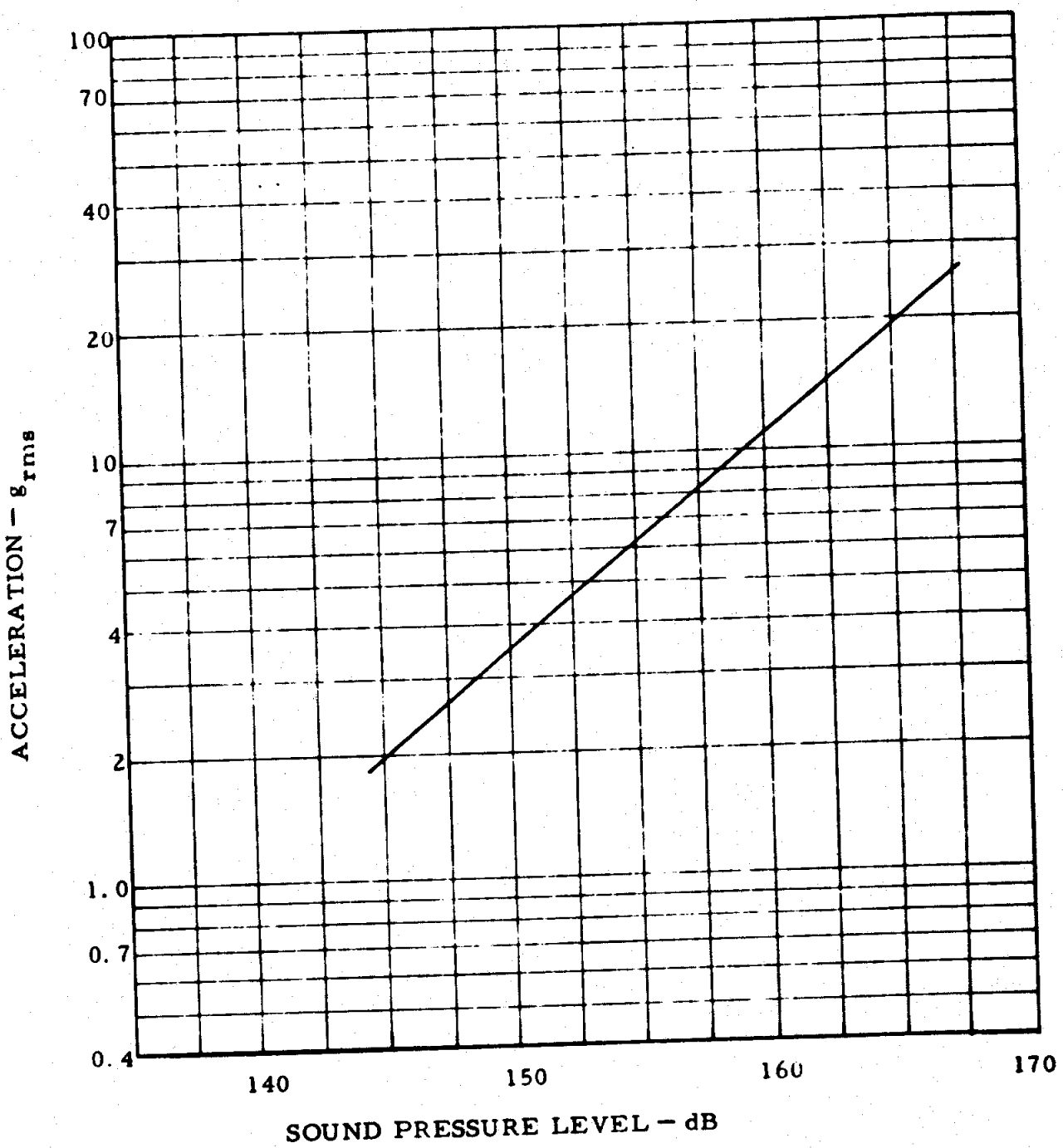


**Figure 19.** Correlation Between the Vibration Level and the External Acoustic Excitation of the Snark Missile – 300-600 cps Octave Band

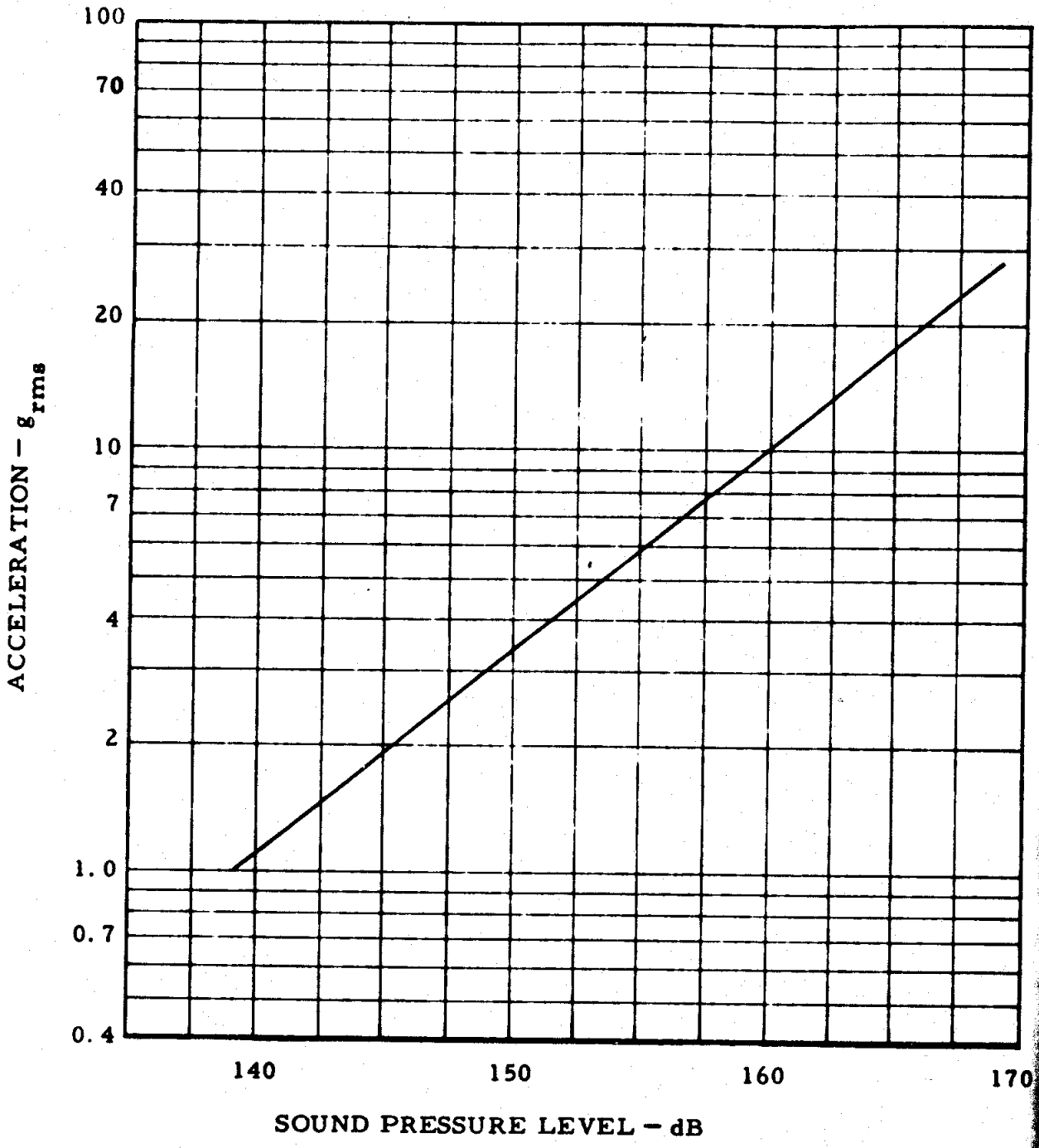


Figure 20. Correlation Between the Vibration Level and the External Acoustic Excitation of the Snark Missile – 600-1200 cps Octave Band

Information Required

Measurements or prediction of acoustic noise environment.

Advantages

1. The procedure is simple and easy to use.
2. No structural design details are required.

Limitations

1. The procedure is based upon a limited amount of aircraft missile data only. The application of the procedure to other types of flight vehicles is questionable.
2. No excitation factors other than acoustic noise are considered.
3. No distinction is made between different equipment mountings and different orthogonal directions.
4. No statistical considerations are directly incorporated in the prediction curves.

## 5.4 ELDRED, ROBERTS, AND WHITE METHOD NO. 2

### 5.4.1 Description

Method No. 2 evolves from a study of the acoustically induced vibration response of missile structures during liftoff based upon rudimentary structural properties and empirical correlations. The development starts with the assumption that each normal mode of vibration in a complex structure is not coupled to any other mode.

Thus, the vibration characteristics of a structure can be found by considering each mode individually. The response in any mode is obtained using single degree-of-freedom relations. The total response for any location is the sum of the responses from each of the modes.

The response of a single degree-of-freedom system to a random forcing function is approximated by

$$\psi_y^2 \approx \frac{\pi Q f_n G_f(f_n)}{2k^2} \tag{12}$$

where

$\psi_y^2$ = mean square displacement response

$Q = \frac{1}{2\zeta}$

$\zeta$ = damping ratio

$f_n$ = natural frequency

$G_f(f_n)$ = power spectral density of the applied force at frequency $f_n$

$k$ = stiffness

Reference 10 uses Eq. (12) as a basis to state that the acceleration response in $g^2$ will be given by

$$\psi_g^2 = \left(\frac{\psi_a}{g}\right)^2 = \frac{\pi f_n Q G_f(f_n)}{2W^2} \tag{13}$$

where

W = weight of the structure of interest

It should be noted that the validity of the result in Eq. (13) is questionable.

To apply the one degree-of-freedom relation to a complex structure, some comparison must be made between the single mass, single force system and the generalized mass, generalized force system. The resulting equation for a complex structure is assumed to be

$$\psi_g^2 = \frac{\beta^2 \pi f_n Q G_f(f_n)}{2W^2} \tag{14}$$

where

$\beta$ = proportionality constant assumed to be a function of the wave number

The application of Eq. (14) requires five pieces of information: the total structural weight (W), the power spectrum for the total applied force $[G_f(f_n)]$, the structural damping (Q), the structural natural frequency $(f_n)$, and the value of the parameter $\beta$.

The total weight of the structure in question is usually easy to estimate. Reference 10 suggests that the power spectrum for the total applied force can be estimated by multiplying the predicted power spectrum for surface pressure by the square of the surface area. Specifically,

$$G_f(f) = A_t \int_{A_t} G_p(f, A)\, dA \tag{15}$$

where

$G_p(f, A)$ = power spectral density for applied pressure over incremental area A

$A_t$ = total surface area of structure

For the damping term, Reference 10 suggests that a value of Q = 15 be assumed. No suggestions are provided for the estimation of the natural frequency, $f_n$. Appropriate values for $\beta$ were determined empirically by examining data collected from several unidentified ballistic missiles. These data are summarized in Figure 21. Note that the average value for $\beta$ is near unity, and that the value decreases only slightly with wave number.

The predictions provided by Eq. (14) are for the mean square vibration of individual modes. Overall vibration predictions can be obtained by summing the mean square values for the individual modal vibrations. General use of the procedure has not been sufficient to assess its accuracy accuracy.

5.4.2 Summary

Assumptions

1. All flight vehicles to which the procedure is to be applied have dynamic characteristics similar to conventional ballistic missiles.
2. Vibration is due principally to acoustic noise during liftoff.
3. Vibration is proportional to the total integrated pressure over the surface of the structure of interest, divided by the structural weight.
4. The normal modes of the vehicle structure are uncoupled.

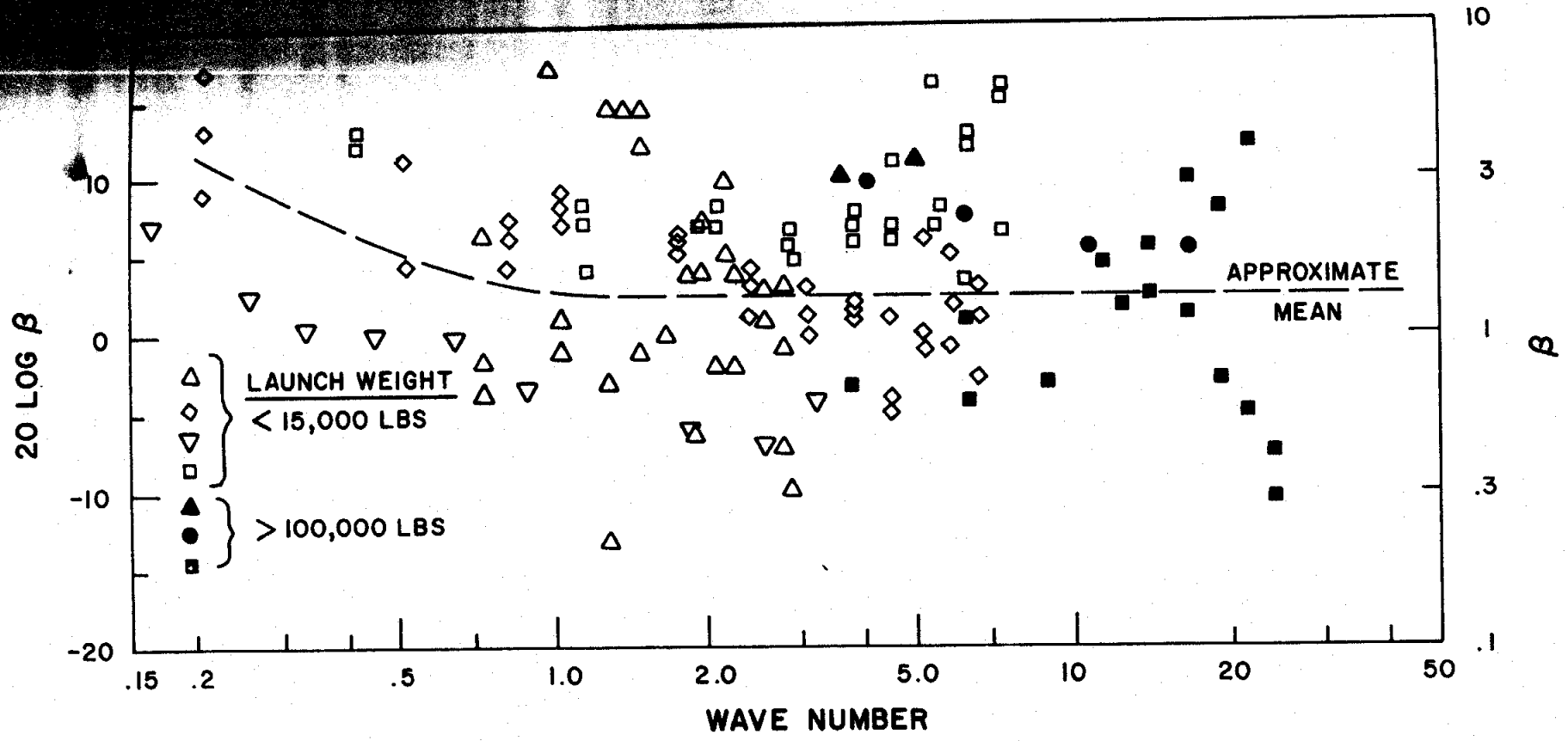


Figure 21. Variation of the Parameter β with Wave Number (Reference 10)

$$\beta^{*} = \left[ \frac{2 \psi_g^2 \omega^2}{\pi f_n Q G_f(f_n)} \right]^{1/2}$$

* NOTE THAT THE VALUE OF $\beta$ SHOULD THEORETICALLY BE GREATER THAN UNITY. THE EMPIRICAL VALUES OF LESS THAN UNITY ARE DUE TO TO IMPRECISIONS I THE VALUES FOR THE PARAMETERS USED TO CALCULATE $\beta$.

Information Required

1. Measurements or predictions of the acoustic noise environment.
2. Estimates for the weight of each structure of interest.
3. Estimates for the damping ratio of structural modes of vibration (the authors suggest using an assumed Q of 15).
4. Estimates for the natural frequency of the structural modes of vibration.

Advantages

1. The procedure is relatively simple.
2. Only rudimentary structural details are required.

Limitations

1. The procedure is based upon ballistic missile data only. The application of the procedure to other types of flight vehicles is questionable.
2. No excitation factors other than acoustic noise are considered.
3. The procedure provides no suggestions for estimating the required structural natural frequencies.

## 5. CURTIS METHOD

### 5.5.1 Description

This method, which is presented in Reference 19, was designed to predict the vibration inputs to internally mounted and externally exposed equipment in aircraft during high-speed flight. The method was developed based upon the assumption that the random vibration environment for aircraft can be described by a broadband vibration background, plus several superimposed narrowband vibration spikes representing resonance structural response modes. The only significant difference between aircraft, or between specific locations in different aircraft for equivalent flight conditions will be in the center frequency of the spikes (representing the resonant frequencies of the structures).

The development of the prediction rules for both the broadband vibration background and narrowband vibration spikes was based upon data measured on various equipments installed in the F-8U, B-59, F-101, and F-106 aircraft. The data were obtained during flight at dynamic pressures over a range from 90 psf to 1760 psf. It was concluded from this data that, for equipment mounted inside a typical aircraft, the broadband vibration background can be described by a power spectral density in $g^2$/cps of

$$G_b(f) = 0.006\,(q/2130)^2 \quad ; \quad 10 \leq f \leq 2650 \text{ cps} \tag{16a}$$

where q is free stream dynamic pressure in psf. Furthermore, about 98% of the narrowband spikes (assuming a Rayleigh distribution) are bounded by a peak spectral density in $g^2$/cps of

$$G_s(f) = 0.11\,(q/2130)^2 \quad ; \quad 10 \leq f \leq 2650 \text{ cps} \tag{16b}$$

where again q is free stream dynamic pressure in psf. For external exposed equipment, the broadband vibration background is given by

$$G_b(f) = \begin{cases} 0.011\,(q/2130)^2 & ; \quad 20 \leq f \leq 150 \text{ cps} \\ 0.020\,(q/2130)^2 & ; \quad 150 \leq f \leq 2000 \text{ cps} \end{cases} \tag{17a}$$

and the bound for about 98% of the narrowband spikes is

$$G_s(f) = \begin{cases} 0.13\,(q/2130)^2 & ; \quad 20 \leq f \leq 150 \text{ cps} \\ 0.23\,(q/2130)^2 & ; \quad 150 \leq f \leq 2000 \text{ cps} \end{cases} \tag{17b}$$

Additional studies of the available data indicated that the use of a single prediction for all three orthogonal directions appeared reasonable. It is stated, however, that vibration in the longitudinal direction might be less severe than vibration in the vertical and lateral directions for frequencies below 500 cps.

Reference 19 is somewhat vague as to how the above vibration predictions should be used as design or test criteria. Specifically, the reference does not specify how many narrowband spikes should be used or how their center frequencies should be selected for, say, a vibration test of aircraft equipment. An optimum approach would be to use spikes with center frequencies corresponding to the predominate resonant response modes of the equipment mounting structure. The prediction of

such resonant frequencies, however, is not always feasible. An alternate procedure would be to use a few spikes (perhaps three) which are assumed to occur sequentially at all possible frequency combinations. For example, a vibration test would be performed by slowly sweeping the three vibration spikes through all possible combinations of frequencies in the range of interest while the broadband vibration background is continuously applied. This should provide a conservative test of the equipment, no matter what resonant frequencies may be present in the mounting structure. Note that this approach would generally require less testing facility capacity than that required to simulate the broadband predictions produced by other procedures discussed in Sections 5.1 through 5.3. General use of the procedure has not been sufficient to assess its accuracy.

### 5.5.2 Summary

#### Assumptions

1. All flight vehicles to which the procedure will be applied are dynamically similar to the four aircraft used to develop the procedure.
2. Vibration is due principally to aerodynamic boundary layer turbulence during flight at high dynamic pressures.
3. The vibration environment can be described by a broadband vibration background with almost constant spectral density plus one or more superimposed narrowband vibration spikes.
4. For equivalent flight conditions, differences in the vibration environment between different aircraft or different specific locations in the same aircraft can be accounted for by variations in the center frequencies of the narrowband vibration spikes.

5. The magnitude of the narrowband vibration spikes is proportional to dynamic pressure.

6. The vibration to be predicted is that of internal or external exposed equipment.

7. Spatial variations in the vibration can be considered a random variable.

8. Vibration is the same in all three orthogonal directions.

## Information Required

1. Estimate for maximum dynamic pressure.

2. Estimates for first few natural frequencies of structure in question (desired but not necessary).

## Advantages

1. The procedure is simple and easy to apply.

2. No structural details are required although estimates for the first few natural frequencies are desirable.

3. The resulting predictions can be implemented as vibration tests using testing equipment with limited capacity.

## Limitations

1. The procedure is based upon aircraft data only. The application of the procedure to spacecraft data is questionable.

2. No excitation factor other than boundary layer turbulence is considered.

3. No distinction is made between different equipment mountings and different orthogonal directions.

4. The procedure is unconservative for unloaded structural vibration predictions.

## 5.6 FRANKEN METHOD

### 5.6.1 Description

This method, which is presented in Reference 20, was designed to predict acoustically induced skin vibration levels for cylindrical structures based upon external sound pressure levels, vehicle diameter, and average surface weight density for the vehicle skin. The method employs a generalized acoustic-vibration frequency response function developed empirically from studies of JUPITER and TITAN 1 acoustic and radial skin vibration data collected during static firings. The generalized frequency response function, which is presented in Figure 22, predicts skin vibration levels in g's from the input acoustic pressures in dB, vehicle diameter in feet, and surface weight density in pounds per square foot. The bandwidth for the predicted vibration levels is the same as the bandwidth for the acoustic input levels. For example, if the acoustic environment is defined in terms of octave band pressure levels, then the vibration predictions will be in terms of octave band acceleration levels. Note that Figure 22 predicts vibration levels in terms of a 6 dB wide range. No details are given in Reference 20 as to the statistical considerations used to arrive at this range for predicted levels.

The specific procedure for using Figure 22 is as follows.

1. Divide the abscissa of Figure 22 by the average vehicle diameter, measured in feet. This converts the abscissa to a frequency scale in cps.
2. Add the quantity "external sound pressure level (dB) minus 20 $\log_{10} w$" to the ordinate of Figure 22. w is the average surface weight density of the vehicle skin, measured in psf. This converts the ordinate to a vibration level in dB referenced to 1 g.

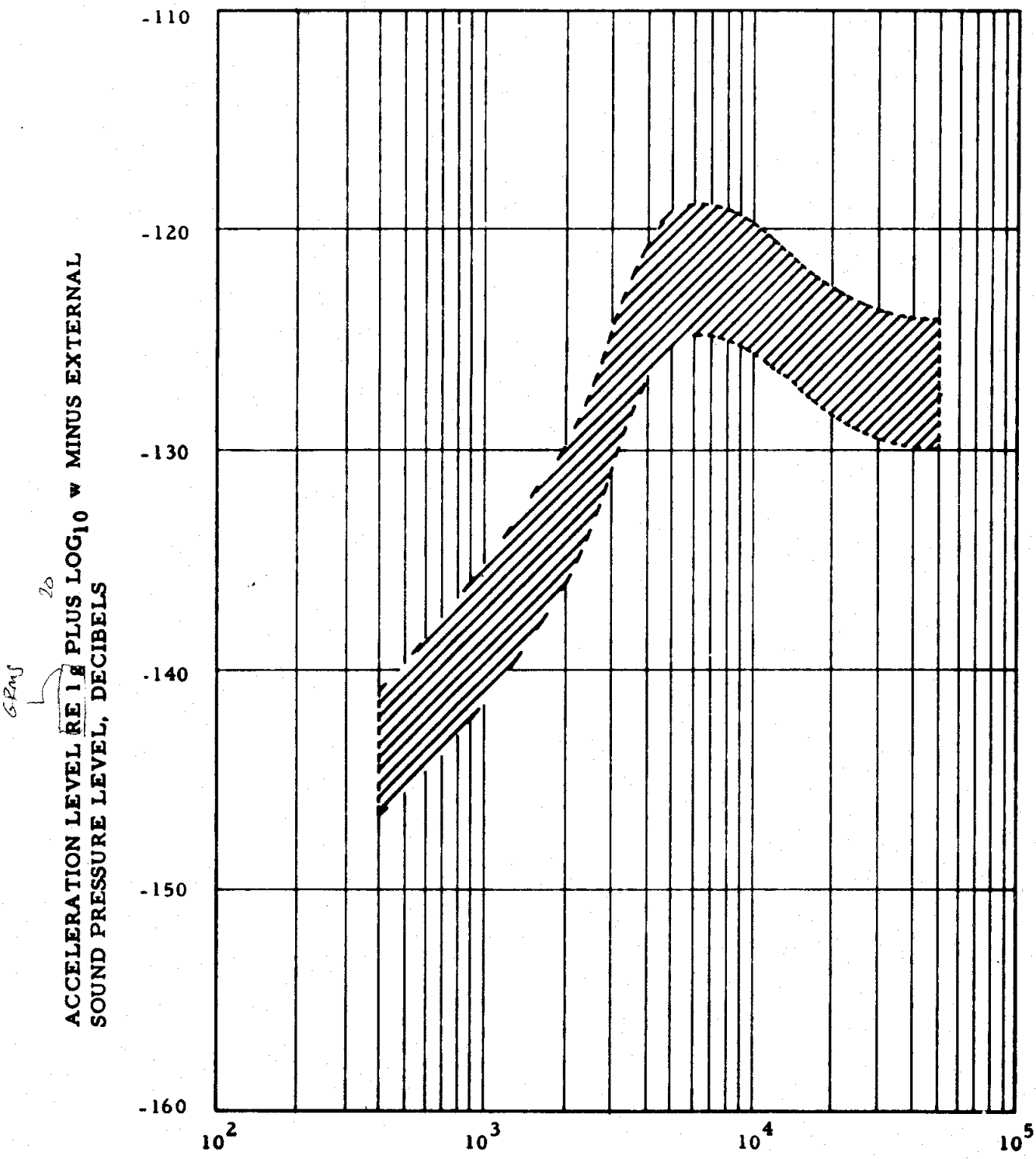


Figure 22. Frequency Response Function for Franken Method

Reference 20 evaluated the method by comparing predictions for the vibration in the MINUTEMAN Instrumentation Section to actual vibration measurements. The agreement between predicted and measured levels was reasonably good (most measurements fell within the 6 dB prediction range). The method was also evaluated in Reference 7 where predicted vibration levels for the SKYBOLT missile were compared to measured data. In general, the method produced predictions which were somewhat higher than the measured vibration levels at the higher frequencies (above 1000 cps). This is not surprising, however, since the Franken method estimates skin vibration levels, while the SKYBOLT measurements represented equipment levels. Skin vibration levels would be expected to be more intense at the higher frequencies than loaded structural vibration levels. A third comparison using measured data is presented in Reference 21. The data used for the comparison were vibration levels measured on the transition section between the RANGER spacecraft and the AGENA vehicle during transonic flight for six different launches (RANGER 1 through 6). The data were compared to predictions using the Franken method, where the input pressure levels during transonic flight were estimated from experimental studies of a 1/10 scale ATLAS-AGENA-RANGER model. Favorable agreement (within 3 dB in most cases) was observed between the measured and predicted octave band vibration levels on RANGER 1 through 5. The agreement was poor for RANGER 6, but the accelerometer had been repositioned for this flight.

## 5.6.2 Summary

### Assumption

1. All flight vehicles to which the procedure is to be applied have similar dynamic characteristics to the JUPITER and TITAN 1 vehicles.
2. Vibration is due principally to acoustic noise during liftoff or other pressure fields during flight which can be estimated.
3. Vibration magnitude is directly proportional to the pressure level of the excitation and inversely proportional to the surface weight density of the structure.
4. Predominant vibration frequencies are inversely proportional to the diameter of the vehicle.
5. Spatial variations in the vibration can be considered a random variable.

### Information Required

1. Predictions for the acoustic noise environment (or the aerodynamic pressure field if applied to predict flight vibration).
2. Average surface weight density of the structure.
3. Diameter of the vehicle.

### Advantages

1. The procedure is simple and easy to use.
2. Only rudimentary structural details are required.

### Limitations

1. The procedure predicts only radial skin vibration levels.

2. The procedure is based upon a limited amount of space vehicle data only. Its application to other types of flight vehicles is questionable.

3. No excitation factors other than acoustic noise are considered, although the procedure can be applied to flight predictions if appropriate pressure field estimates are available.

4. Statistical considerations are not clearly defined.

## 5.7 WINTER METHOD NO. 1

Winter has proposed two procedures for predicting flight vehicle vibration environments which have not been previously published. The first method is a generalized extrapolation technique which is suggested for use when predicting the vibration environment for an entirely new vehicle. The second method is a specific extrapolation technique, and is suggested when measured data are available from a previous vehicle similar to the new vehicle of interest. The first procedure is presented in this section. The second is covered in Section 6.3.

### 5.7.1 Description

Method No. 1 was designed to predict the acoustically and aerodynamically induced vibration of space vehicle structures based upon a generalized acoustic-vibration frequency response function developed using data from the JUPITER, TITAN, MINUTEMAN, SKYBOLT, and GENIE vehicles. The vibration measurements from these vehicles were individually identified with a 1/3 octave band acoustic pressure spectrum acting on the structure, and an average surface weight density for the structure. The resulting frequency response function, based on 1/3 octave band data and normalized to a vehicle diameter of 10 feet, is shown in Figure 23. This frequency response function was then converted

Surface Weight Density = 1 psf

Incident Sound Pressure Level in each 1/3 octave band = 171 dB = 1 psi.

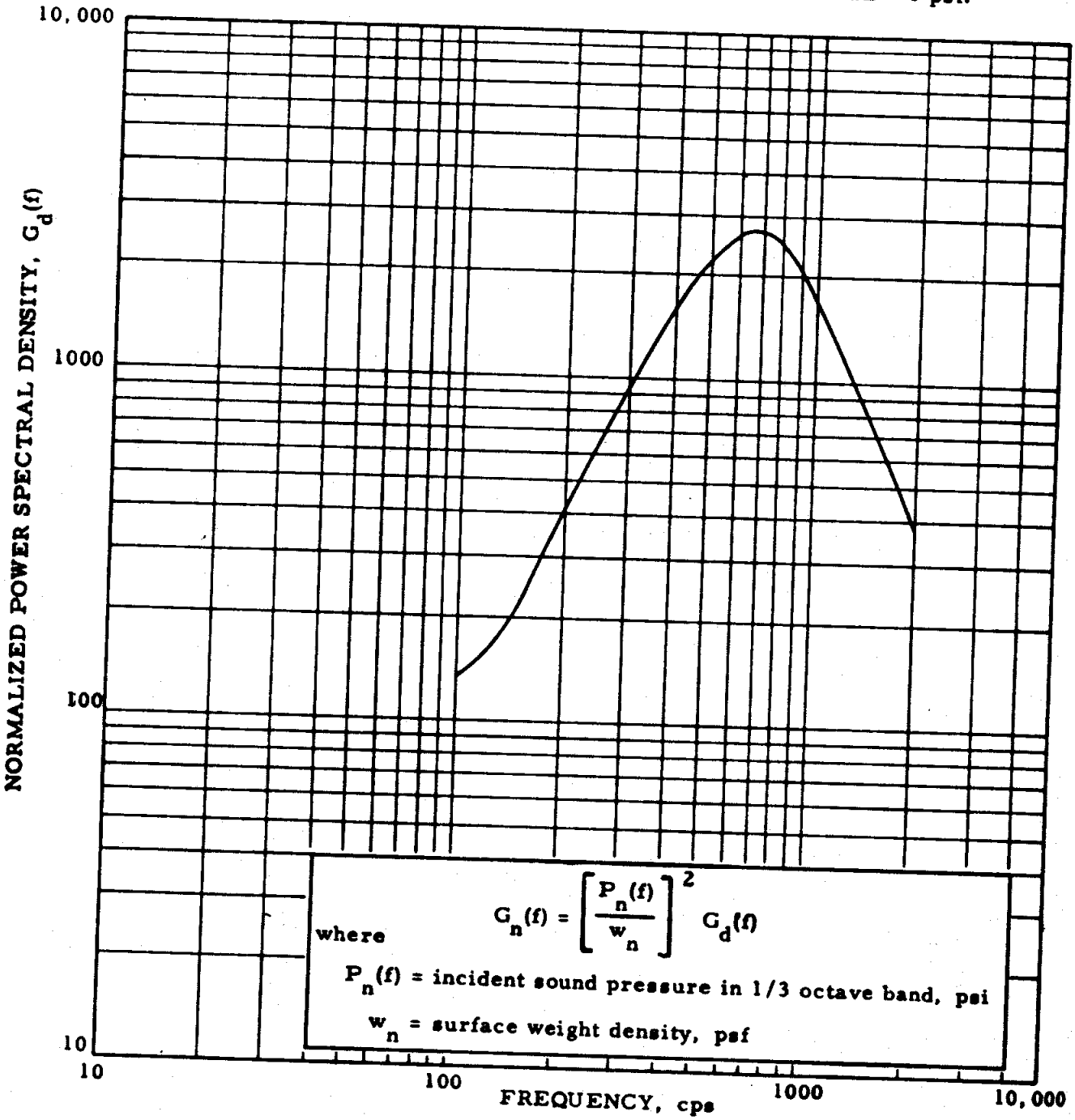


Figure 24. Modified Frequency Response Function for Winter Method

where

$G_d(f)$ = ordinate value of Figure 24

$P_n(f)$ = predicted 1/3 octave band excitation pressure level for new vehicle in psi

$w$ = average surface weight density for new vehicle structure in psf

$G_n(f)$ = power spectral density function for vibration of new vehicle structure in $g^2/cps$

To aid in the application of Eq. (19), Figures 25 through 27 are provided. Figure 25 relates material thickness to surface weight density. Figure 26 converts pressure levels in dB to pressure levels in psi. Figure 27, which is based upon unpublished studies, converts boundary layer turbulence levels to equivalent "effective" acoustic pressure levels. In other words, this figure attempts to account for differences in the efficiency with which boundary layer and acoustic pressures induce structural vibration. This permits Eq. (19) to be used to predict aerodynamically induced vibration during flight as well as acoustically induced vibration during liftoff. Note that Figure 27 presents the conversion in terms of a relatively wide range, indicating the uncertainty associated with this step.

The data used to develop Figures 23 and 24 have been normalized to a reference vehicle diameter of 10 feet. Figure 24 can be used directly for vehicle diameters between approximately 5 and 20 feet. Otherwise, Figure 23 must be used with the frequency scale (abscissa) shifted in accordance with the following empirically determined relationship:

$$f_n = f_d \left( \frac{10}{D_n} \right)^{1/2} \qquad (20)$$

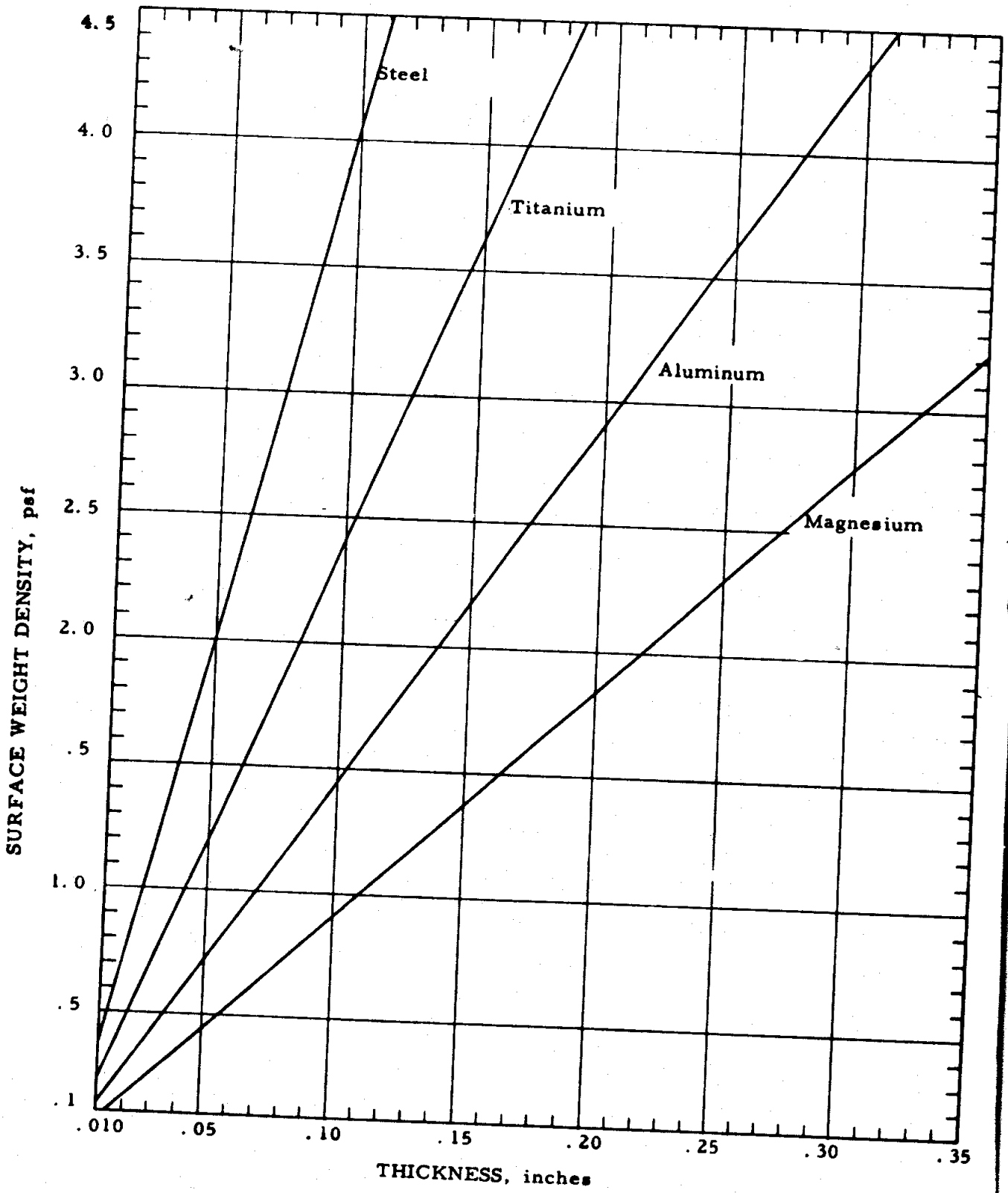


Figure 25. Relationship Between Skin Thickness And Surface Weight Density For Various Materials

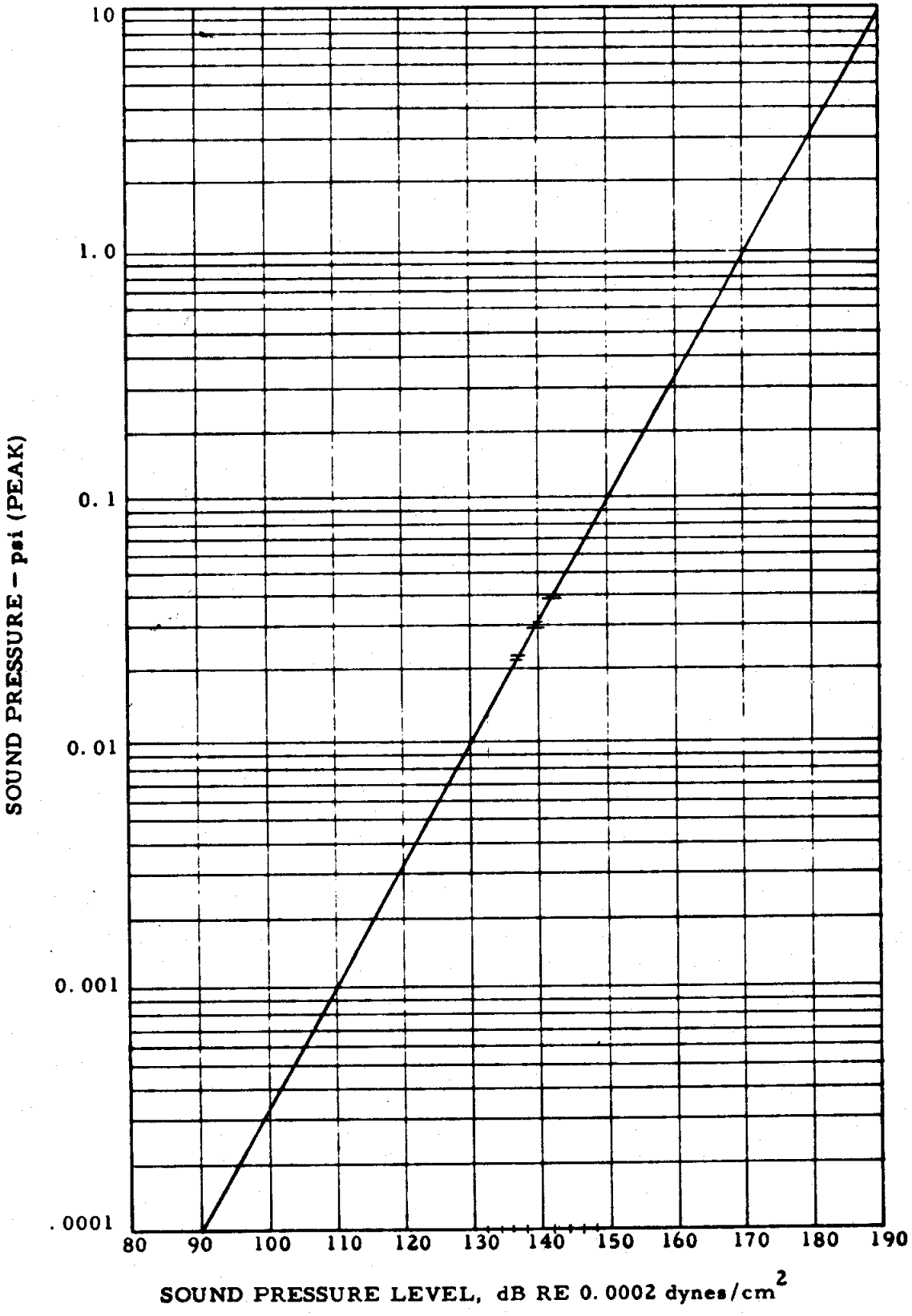


Figure 26. Conversion of Sound Pressure Level in dB to Sound Pressure in Psi

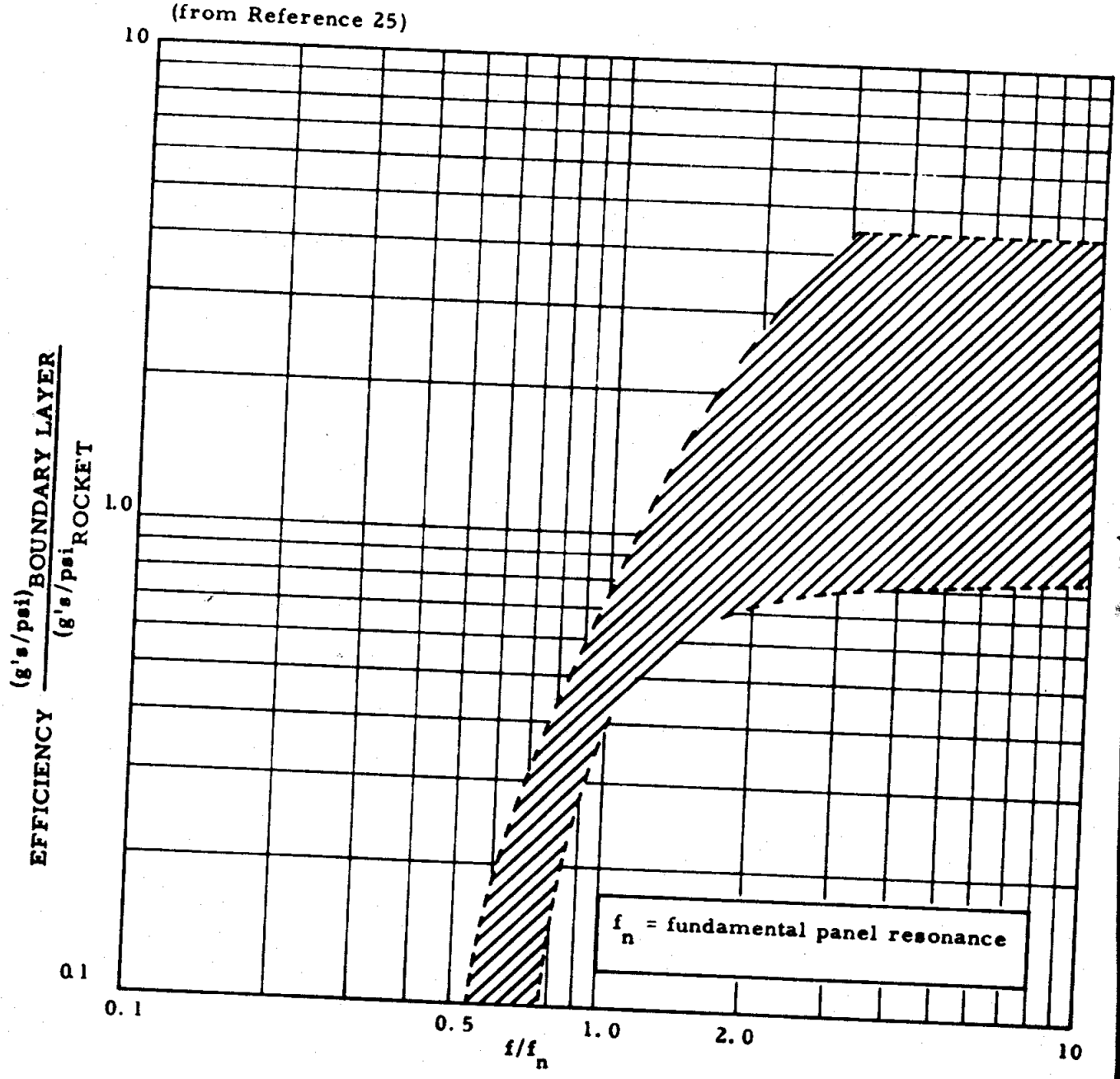


Figure 27. Summary of Data on the Relative Efficiency of "Rocket" Noise and Boundary Layer Pressure Fluctuations in Inducing Structural Vibration

where

$f_n$ = frequency for predicted level

$f_d$ = frequency given in Figure 23

$D_n$ = diameter of new vehicle

For the case where vibration predictions are desired at points where heavy components will be mounted, a weight correction factor is suggested as follows:

$$G_{nc}(f) = \frac{W_n}{W_n + W_c} G_n(f) \qquad (21)$$

where

$G_n(f)$ = predicted power spectral density function for acceleration response of new vehicle structure

$W_n$ = weight of new vehicle structure in general region of interest

$W_c$ = weight of all attached components in general region of interest

$G_{nc}(f)$ = predicted power spectral density function for acceleration response of new vehicle structure with components attached

The inclusion of an unusually large amount of damping in a design should also be accounted for since the result will be to lower the vibration levels significantly. This is especially important for those cases where the predicted environment would normally be severe, and any reduction in level would be advantageous to the program. For example,

high performance missiles often are designed with an external additive coating which reduces vibration in two ways; first by the added mass, and second by the added damping. It is suggested that the effect of such damping be accounted for by a correction factor as follows:

$$G_{n\zeta}(f) = \frac{\zeta_d}{\zeta_n} G_n(f) \tag{22}$$

where

$G_n(f)$ = predicted power spectral density function for acceleration response of new vehicle

$\zeta_n$ = estimated damping ratio for normal modes of new vehicle

$\zeta_d$ = estimated damping ratio for normal modes of data vehicle

$G_{n\zeta}(f)$ = predicted power spectral density function for acceleration response of new vehicle with added damping

A final correction factor is suggested for those cases where vibration predictions for beam and truss type structure are required. Specifically, it is proposed that beam and truss vibration in the frequency range above approximately 500 cps be obtained by taking one-seventh of the levels predicted by Eq. (19). As the frequency reduces below 500 cps, the beam and truss vibration predictions should be slowly faired into levels predicted by Eq. (19) until they are equivalent at approximately 100 cps.

The method was evaluated in Reference 7 by comparing predictions for vibration in the SKYBOLT missile to actual measurements. The

agreement is fair in the frequency range from 300 to 1200 cps. At the higher and lower frequencies, however, the predictions are up to 15 dB too high. A second evaluation was made in Reference 22 where predictions for vibration in the SATURN I are compared to actual measurements. The agreement is quite good (within 3 dB in most cases).

### 5.7.2 Summary

#### Assumptions

1. All flight vehicles to which the procedure is applied have characteristics similar to the various vehicles used to develop the procedure.
2. Vibration is due principally to acoustic noise during liftoff and aerodynamic sources during flight.
3. Vibration magnitude is directly proportional to the pressure level of the excitation and inversely proportional to the surface weight density of the structure.
4. Predominant vibration frequencies are inversely proportional to the square root of the diameter of the vehicle.
5. Spatial variations in the vibration can be considered a random variable.

#### Information Required

1. Predictions for the acoustic noise or aerodynamic noise environment
2. Average surface weight density of the structure
3. Diameter of the vehicle

#### Advantages

1. The procedure is simple and easy to use.
2. Only rudimentary structural details are required.

3. The procedure includes suggestions for predicting beam and truss vibration, and for predicting vibration with and without component loading and additive damping.

Limitations

1. The procedure is based upon space vehicle data only. Its application to other types of flight vehicles is questionable.
2. No excitation factors other than acoustic noise and boundary layer turbulence are considered.
3. No distinction is made between different orthogonal directions.
4. Statistical considerations are not clearly defined.

# 6. SPECIFIC EXTRAPOLATION APPROACH

The specific extrapolation approach includes those procedures which predict vibration environments in future vehicles by scaling measured data from a similar previous vehicle. This approach differs from the general extrapolation procedures discussed previously in Section 5 in the following ways. The specific extrapolation approach is more flexible in that vibration levels may be predicted for any desired type of structure by extrapolating data measured on that type of structure in the data vehicle. Furthermore, predictions may be obtained for any desired flight condition by extrapolating the measurements from the data vehicle for that flight condition.

Three of the better known specific extrapolation techniques are presented in this section.

## 6.1 CONDOS AND BUTLER METHOD

### 6.1.1 Description

This method, which is presented in Reference 23, employs a scaling formula to extrapolate vibration data measured on some previous vehicle to predict vibration levels on a new vehicle of similar design based upon differences in the excitation pressures and surface weight densities for the two vehicles. The specific extrapolation rule suggested in Reference 23 is

$$G_n(f) = G_d(f)\left(\frac{w_d}{w_n}\right)^2 \frac{G_{pn}(f)}{G_{pd}(f)} \qquad (23)$$

where

Subscript n denotes the new vehicle

Subscript d denotes the data vehicle

$G(f)$ = power spectral density for the acceleration response

$G_p(f)$ = power spectral density for the pressure excitation

$w$ = average surface weight density of the vehicle structure

Although the method was originally suggested in Reference 23 as a technique for predicting missile vibration environments, it is equally applicable to any other type of flight vehicle.

Reference 23 suggests that predictions be based upon the 95th percentile of a lognormal distribution fitted to the measurements in each structural zone of concern. Note that the actual procedure used by the authors to arrive at a 95th percentile level involves some unusual manipulations, but this is due to the specialized formats of their data and has no bearing on the general applicability of Eq. (23).

The principal difficulty in applying Eq. (23) is the determination of the $G_p(f)$ functions (the spectral densities for the pressure excitations on the new and reference vehicles). For the case of acoustic excitation during liftoff of rocket powered vehicles, Reference 23 suggests a detailed procedure for estimating these functions, as follows.

Step 1 Determine for both the data vehicle and the new vehicle the overall sound power levels generated by the rocket motor using the formula

$$SPL = 78 + 13.5 \log 21.8\ T^2/W_e \qquad (24)$$

where

SPL = overall sound power level in decibels

T = engine thrust in pounds

$W_e$ = exhaust weight flow per second

Step 2 Determine the shift in spectrum frequencies between the data missile and new vehicle by taking the ratio of the dimensionless frequency parameters for each engine, given by

$$f D_e / V \qquad (25)$$

where

f = frequency in cps

$D_e$ = rocket nozzle exit plane diameter in ft.

V = exit velocity of exhaust gases in ft/sec

Step 3 Determine, on the new vehicle, the distance of the structural region under study to the rocket nozzle exit plane, and choose from the data vehicle a measured or estimated sound pressure level spectrum corresponding to this distance.

Step 4 Shift the level of the acoustic spectrum found in Step 3 by the difference in overall SPL's determined in Step 1, and the frequency by the ratio determined in Step 2. The resulting curve is the predicted acoustic spectrum on the new vehicle. The acoustic spectrum for the data vehicle is as measured or estimated in Step 3.

Another approach to establishing appropriate values for the $G_p(f)$ functions is to use the estimation procedures outlined in Section 5.2.1. These procedures apply to boundary layer pressure predictions as well as acoustic pressure predictions. Additional information on the prediction

of acoustic and aerodynamic induced pressure fields is presented in the Appendix.

In Reference 23, vibration levels measured on an unidentified missile are compared to the levels predicted using the Condos-Butler method. The agreement between measurements and predictions is relatively good (within 5 dB in most cases) in the frequency range between 100 and 500 cps. Above and below this frequency range, the method generally overpredicted the vibration levels by up to 15 dB. At one location where a heavy component was mounted, the overprediction was as high as 25 dB.

### 6.1.2 Summary

#### Assumptions

1. The data vehicle and the new vehicle of interest have similar missions and structural designs.
2. Vibration magnitude is directly proportional to the pressure level of the excitation and inversely proportional to the surface weight density of the structure.
3. Spatial variations in the vibration can be considered a random variable.

#### Information Required

1. Vibration measurements for the data vehicle.
2. Measurements or predictions for the acoustic noise, aerodynamic turbulence, or other pressure environments of interest for the data vehicle.
3. Predictions for the corresponding pressure environment for the new vehicle.
4. Average surface weight densities for the structures of the new and data vehicles.

Advantages

1. The procedure is relatively easy to use.
2. Only rudimentary structural details are required.
3. The procedure yields reasonably accurate results if the new and data vehicles are quite similar.
4. The procedure is flexible and can be applied to any type of structure in any flight vehicle for any flight condition, so long as appropriate measurements are available from the data vehicle.

Limitations

1. Extensive vibration measurements from experiments on a previous similar vehicle are required.
2. The accuracy of the predictions are heavily dependent upon the quantity and quality of the measurements from the data vehicle, and upon the similarity of the data vehicle to the new vehicle.

## 6.2 BARRETT METHOD

### 6.2.1 Description

This method, which is presented in Reference 24, was originally proposed for applications to rocket powered space vehicles. It is similar to the Condos-Butler method discussed in Section 6.1, except that this method includes suggestions for predicting the structural vibration induced by direct mechanical transmission from rocket motor vibration.

The method initially assumes that the structure for a vehicle of interest can be divided into two distinct categories as follows:

1. Structure susceptible to acoustic and aerodynamic pressure fluctuations
2. Structure not susceptible to acoustic and aerodynamic pressure fluctuations

The first category would include skin panels, skin stiffeners (ring frames and stringers), and bulkheads. The second category would include structural beams and components mounted on the rocket engine.

For category No. 1 predictions (structures susceptible to pressure fluctuations), the extrapolation rule suggested in Reference 24 is

$$G_n(f) = G_d(f)\left[\frac{\rho_d\, t_d}{\rho_n\, t_n}\right]^2 \frac{G_{pn}(f)}{G_{pd}(f)}\, F \qquad (26)$$

where

Subscript n denotes the new vehicle

Subscript d denotes the data vehicle

$G(f)$ = power spectral density function for the acceleration response

$G_p(f)$ = power spectral density function for the pressure excitation

$\rho$ = weight density of structural material

$t$ = average thickness of structure

$F$ = $W_n/(W_n + W_c)$, an attenuation factor to account for component loading

$W_n$ = weight of structure in area where component is to be mounted

$W_c$ = weight of component to be mounted

Note that Reference 24 actually presents the extrapolation rule in terms of rms values rather than mean square (power spectra) values. Hence, Eq. (26) is effectively the square of the formula in Reference 24. Further note that Eq. (26) is very similar to the extrapolation formula suggested by Condos and Butler in Eq. (23). Although originally proposed for rocket powered space vehicles, Eq. (26) is applicable to any other type of flight vehicle as well.

For category No. 2 predictions (structure not susceptible to pressure fluctuations), the extrapolation rule suggested in Reference 24 is

$$G_n(f) = G_d(f) \frac{(NVT)_n \, W_d}{(NVT)_d \, W_n} F \qquad (27)$$

where

Subscript n denotes new vehicle

Subscript d denotes data vehicle

$G(f)$ = power spectral density function for acceleration response

$N$ = number of rocket motors

$V$ = exhaust gas velocity for each rocket motor

$T$ = thrust for each rocket motor

$W$ = overall weight of structure

$F$ = attenuation factor for component loading, as defined in Eq. (26)

Again note that Eq. (27) is the square of the actual extrapolation rule presented in Reference 24.

Reference 25, which is a companion to Reference 24, suggests predictions be based upon a 97.5 percentile level for the vibration measurements in each structural zone of interest. As for the Condos and Butler Method, some unusual manipulations are made to arrive at a 97.5 percentile level, including the use of a special empirical distribution function which is fitted to the individual measurements. However, these details have no direct bearing on the applicability of Eqs. (26) and (27).

Reference 24 provides numerous detailed guidelines for the application of Eqs. (26) and (27), and detailed reference vehicle scaling parameters for scaling SATURN I data to other similar vehicles. Included are plots of the overall acoustic pressure level to be expected on a space vehicle structure during liftoff, versus distance from the rocket exit for various contemporary rocket motors. A collection of these acoustic plots is presented in Figures 28 through 34. Also included is a plot of the overall boundary layer pressure level to be expected on a clean structure during flight, versus distance from the leading edge of the vehicle. This plot is presented in Figure 35. The detailed SATURN I scaling data is not presented here because of its limited application to SATURN I type vehicles, and because it is only a specific example of the general technique presented by Barrett.

The adequacy of the Barrett method has been evaluated in an unpublished document where vibration measurements on the SATURN V vehicle (S-IC Stage) were compared to predictions obtained using Eqs. (26) and (27). The data vehicle used for the predictions was the SATURN I vehicle. The results indicate that the predictions for category No. 1 type structure using Eq. (26) were reasonably accurate (the predictions would just envelope most of the measurements). The predictions for

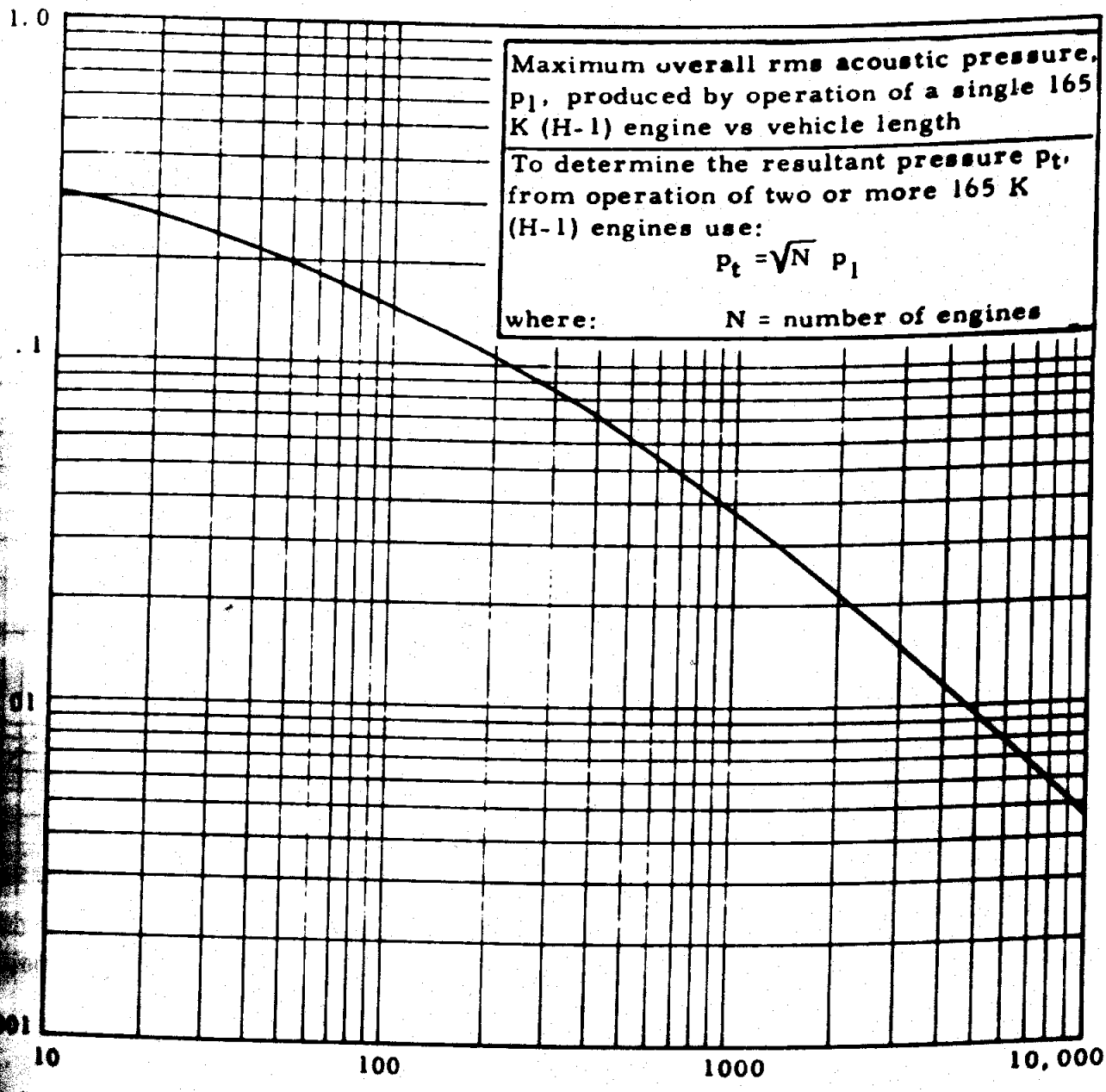


Figure 28. Acoustic Pressure vs Vehicle Length 165K H-1 Engine

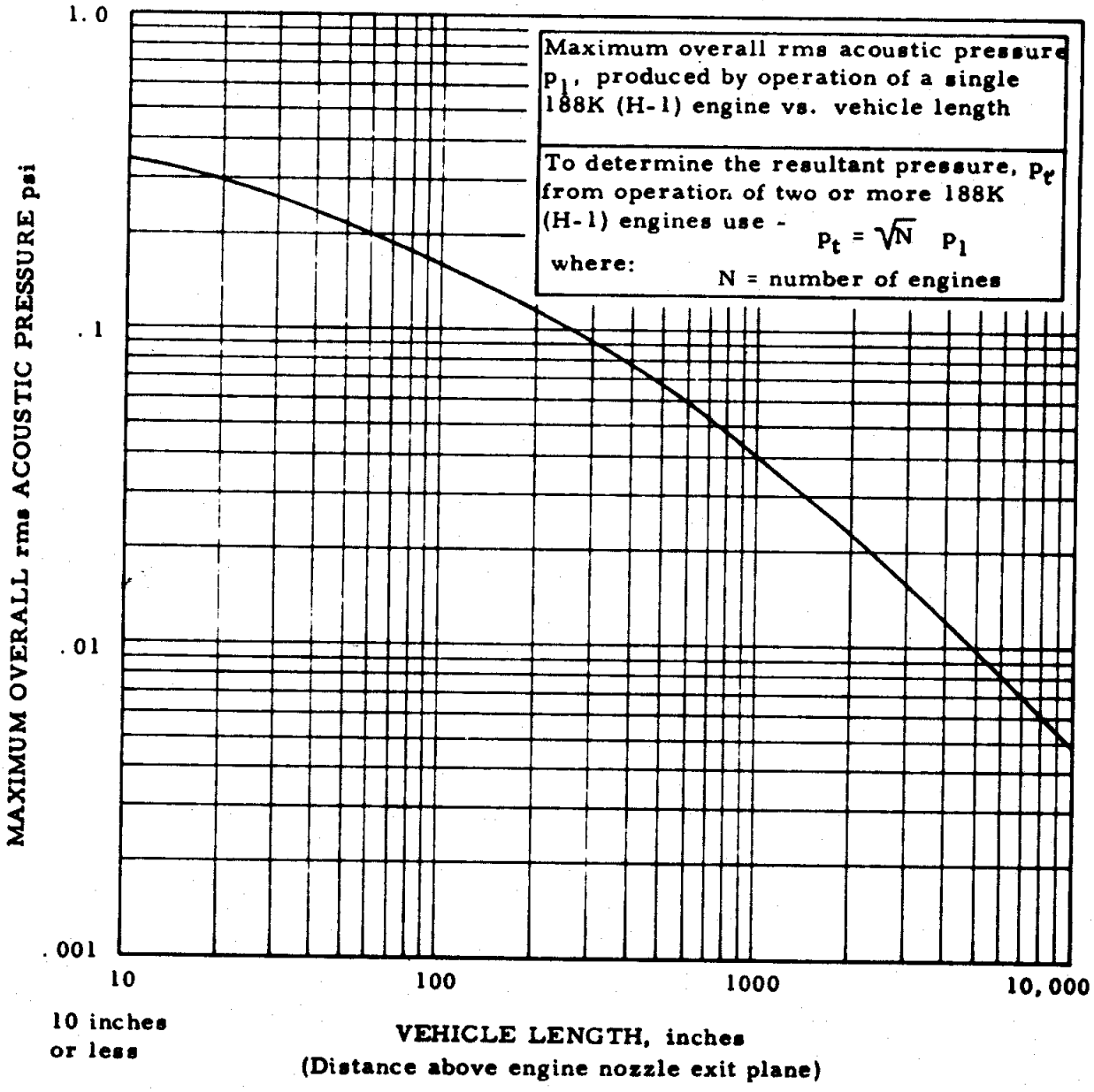


Figure 29. Acoustic Pressure vs. Vehicle Length 188K H-1 Engine

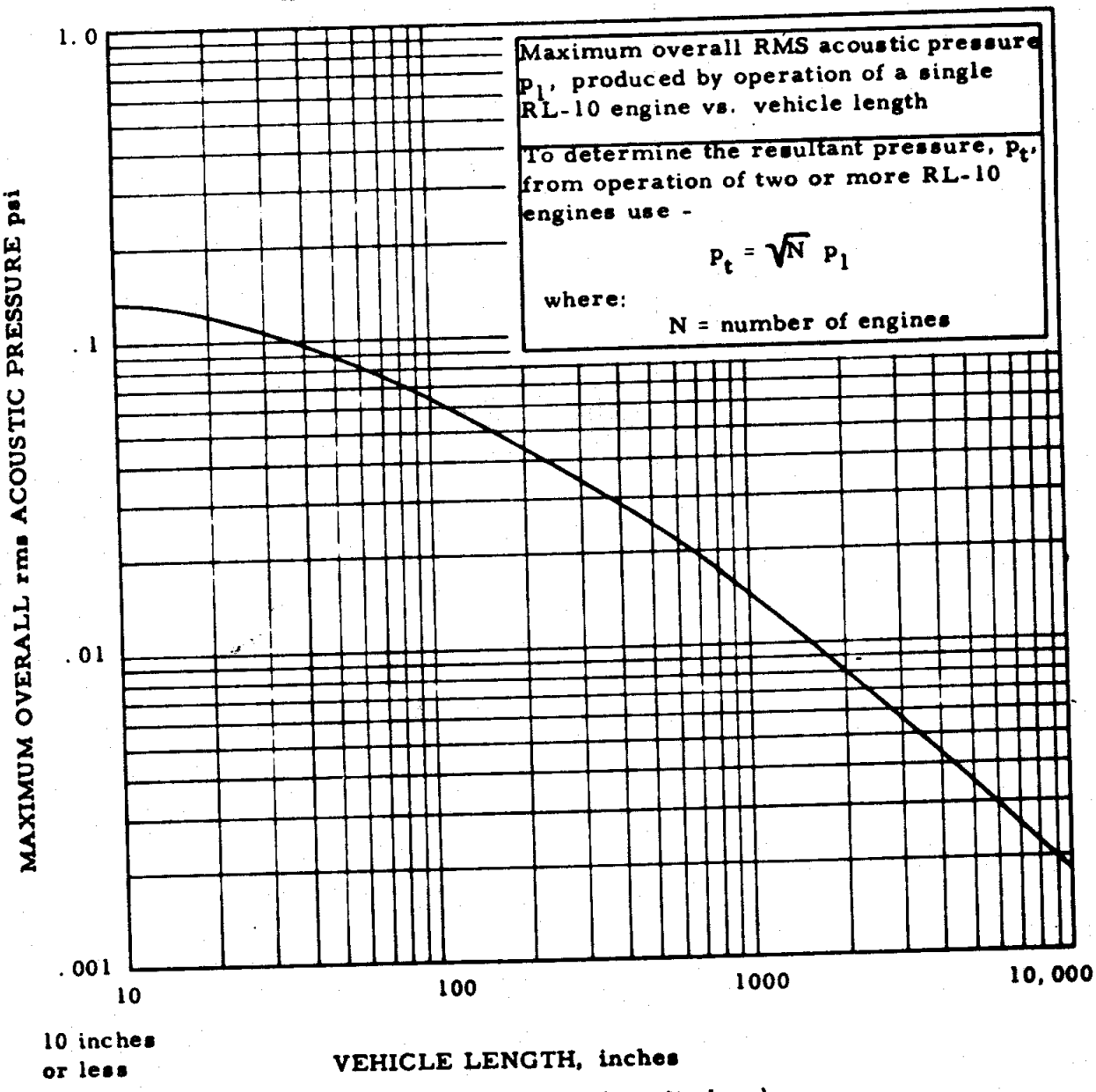


Figure 30. Acoustic Pressure vs. Vehicle Length RL-10 Engine

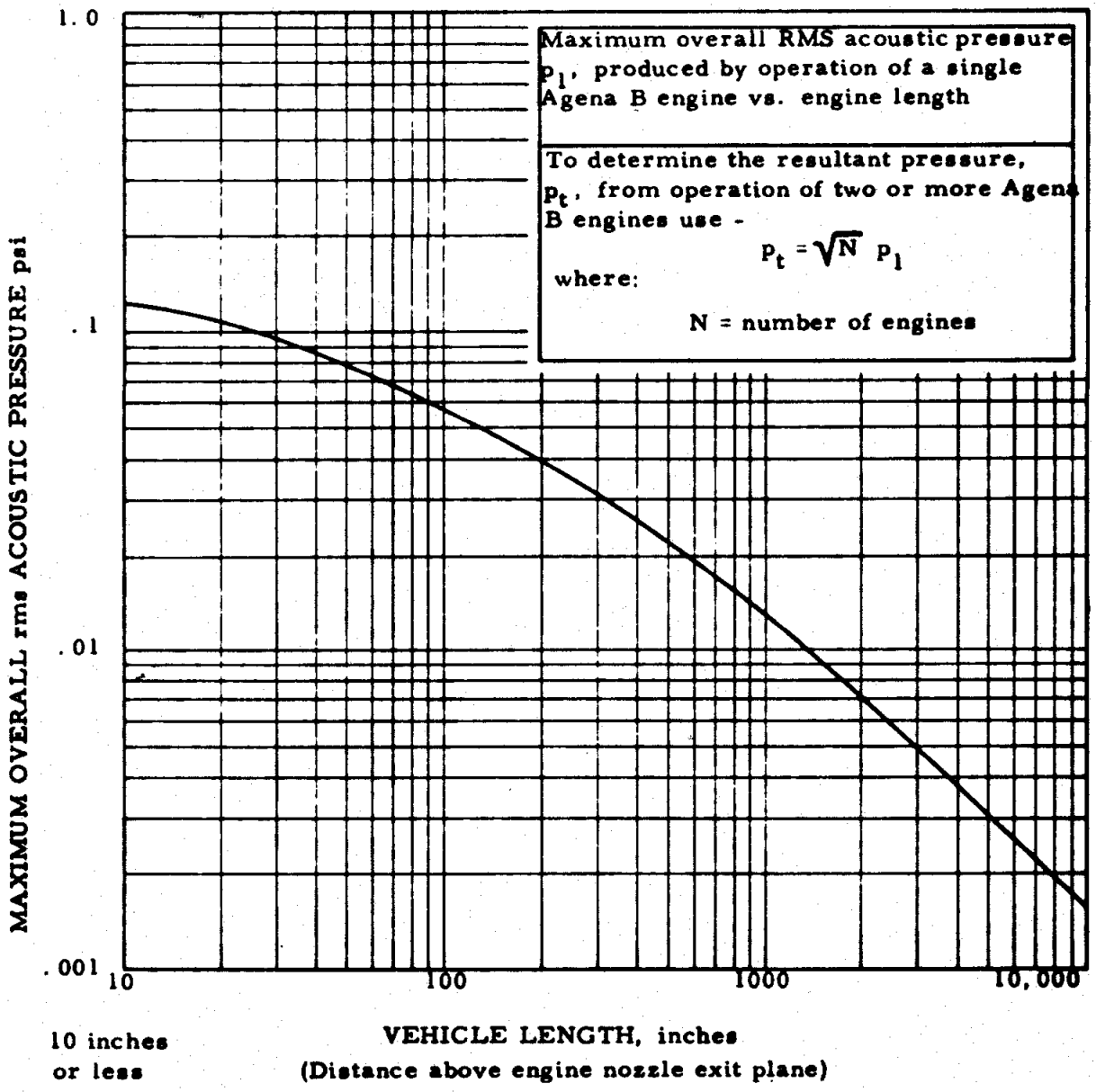


Figure 31. Acoustic Pressure vs. Vehicle Length Agena R & D Engine

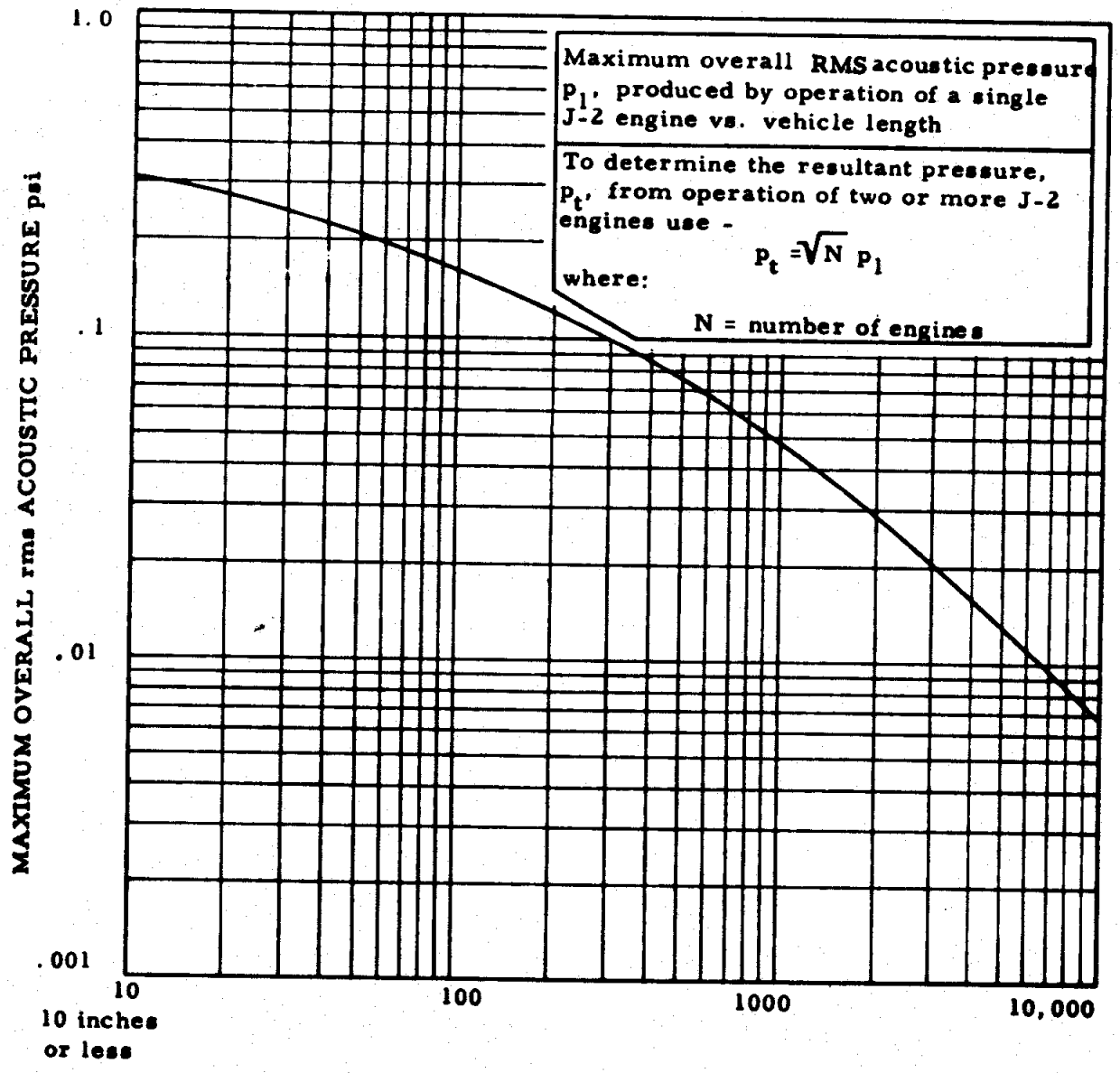


Figure 32. Acoustic Pressure vs. Vehicle Length J-2 Engine

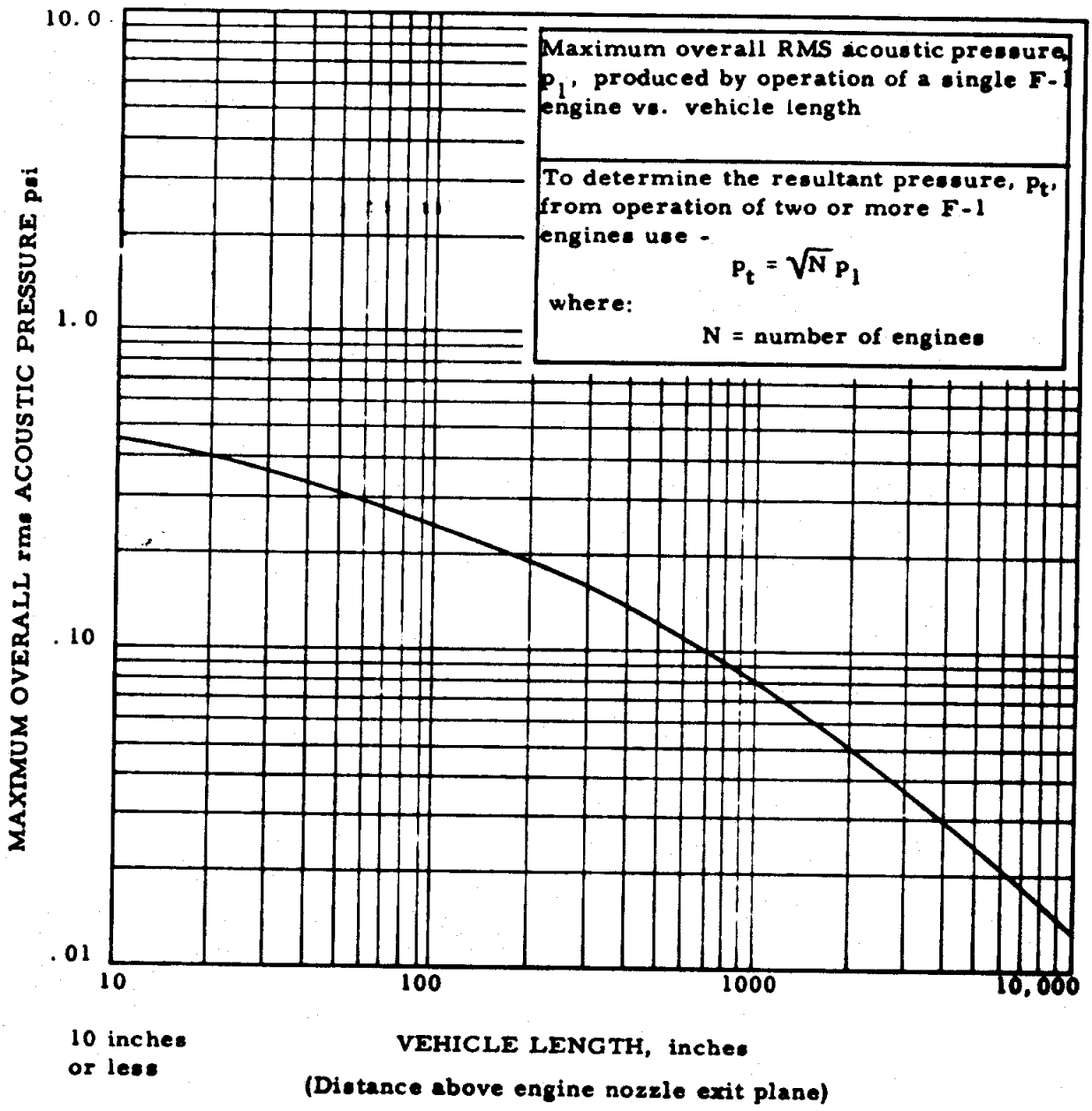


Figure 33. Acoustic Pressure vs. Vehicle Length F-1 Engine

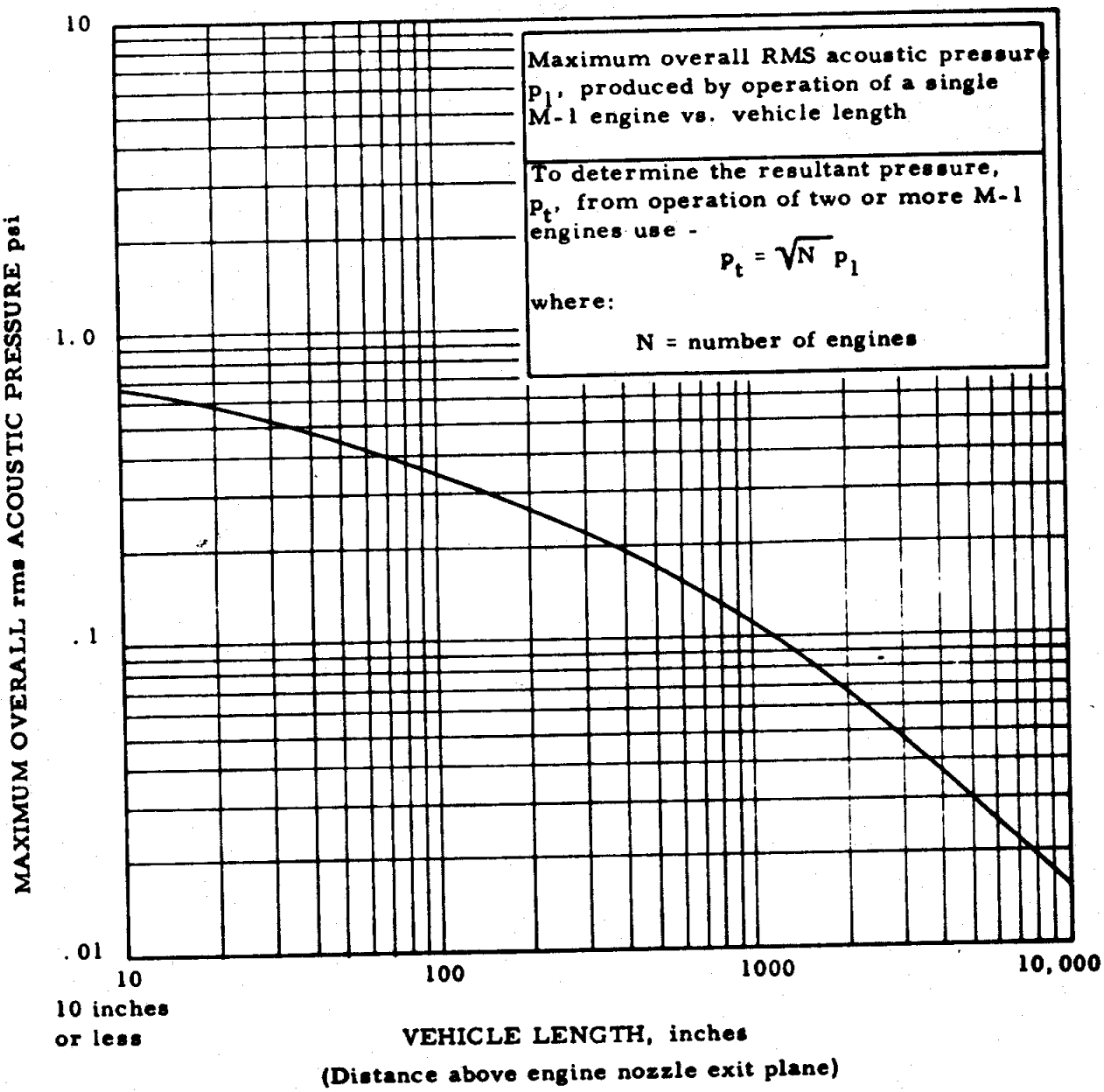


Figure 34. Acoustic Pressure vs. Vehicle Length M-1 Engine

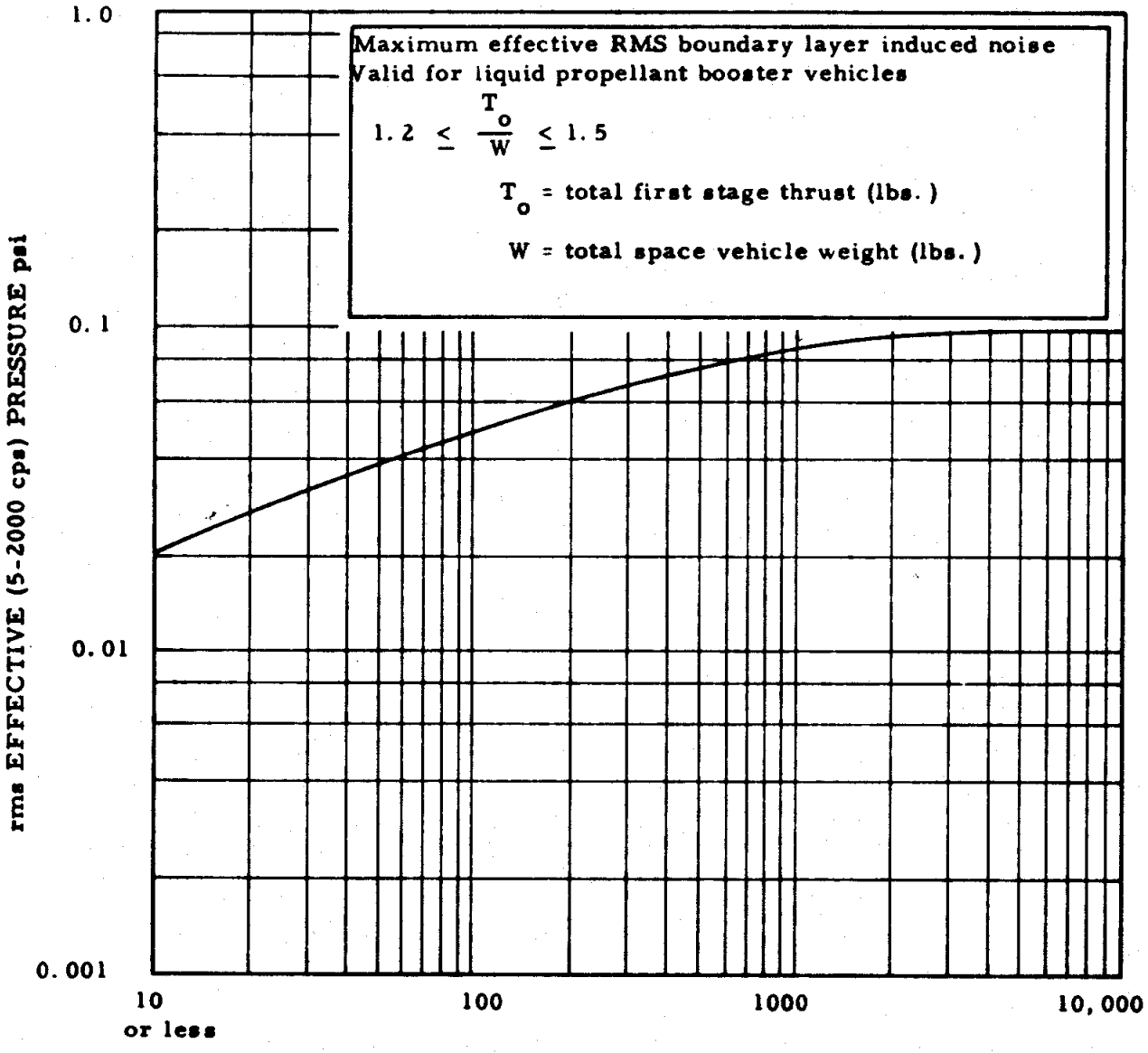


Figure 35. Boundary Layer Induced Noise vs. Vehicle Length

Category No. 2 type structure using Eq. (27), however, were sometimes overly conservative by 10 dB or more. These discrepancies are believed to be due to the lack of similarity between the category No. 2 structures in the SATURN I and SATURN V vehicles.

### 6.2.2 Summary

#### Assumptions

1. The data vehicle and the new vehicle of interest have similar missions and structural designs.
2. The vehicle structure can be divided into structure susceptible to acoustic and aerodynamic pressure fluctuations, and structure not susceptible to acoustic and aerodynamic pressure fluctuations.
3. For structure susceptible to acoustic and aerodynamic pressure fluctuations, vibration is directly proportional to the pressure level, and inversely proportional to the surface weight density of the structure.
4. For other structures, vibration is directly proportional to the number of rocket motors and the exhaust gas velocity and thrust of each motor, and inversely proportional to overall structural weight.
5. Spatial variations in the vibration can be considered a random variable.

#### Information Required

1. Vibration measurements for the data vehicle.
2. Measurements or predictions for the acoustic noise, aerodynamic turbulence, rocket motor exhaust gas velocity, and thrust for the data vehicle.
3. Predictions for the corresponding pressure environments and rocket motor performance for the new vehicle.

4. Average surface weight densities or overall weights for the structures of the data and new vehicles.

Advantages

1. The procedure is relatively easy to use.
2. Only rudimentary structural information is required.
3. The procedure yields reasonably accurate results if the data and new vehicles are quite similar.
4. The procedure includes suggestions for predicting beam and truss vibration, and for predicting vibration with and without component loading.
5. The procedure is flexible. At least part of the procedure can be applied to any type of structure in any flight vehicle for any flight condition, so long as appropriate measurements are available from the data vehicle.

Limitations

1. Extensive vibration measurements from experiments on a previous similar vehicle are required.
2. The accuracy of the predictions is heavily dependent upon the quantity and quality of the measurements from the data vehicle, and upon the similarity of the data vehicle to the new vehicle.

## 6.3 WINTER METHOD NO. 2

### 6.3.1 Description

Winter Method No. 2 is the same as Method No. 1, discussed in Section 5.7, except the generalized frequency response function used for the predictions is developed in each case by evaluating data measured on a particular vehicle which is similar in mission and structural design to the new vehicle of interest. Specifically, data from a previous

vehicle of similar performance and design is measured, and a prediction curve similar to Figure 24 is developed using Eq. (18). Predictions are then obtained using Eq. (19), and modified as required using Eqs. (20) through (22). If desired, several prediction curves may be developed to distinguish between different classes of structure or different orthogonal directions. The accuracy of the procedure should be equal to or better than the accuracy of Method No. 1, as discussed in Section 5.7.

### 6.3.2 Summary

#### Assumptions

1. The data vehicle and the new vehicle of interest have similar missions and structural designs.
2. Vibration is due principally to acoustic noise during liftoff and aerodynamic noise during flight.
3. Vibration magnitude is directly proportional to the pressure level of the excitation and inversely proportional to the surface mass density of the structure.
4. Predominant vibration frequencies are inversely proportional to the square root of the diameter of the vehicle.
5. Spatial variations in the vibration can be considered a random variable.

#### Information Required

1. Vibration measurements for the data vehicle
2. Measurements or predictions for the acoustic noise and aerodynamic noise for the data vehicle
3. Predictions for the acoustic noise and aerodynamic noise for the new vehicle

4. Average surface weight densities for the structures of the data and new vehicles

5. Diameters of the data and new vehicles

Advantages

1. The procedure is relatively easy to use.

2. Only rudimentary structural information is required.

3. The procedure yields reasonably accurate results if the data and new vehicles are quite similar.

4. The procedure includes suggestions for predicting beam and truss vibration and for predicting vibration with and without component loading.

5. The procedure is flexible and can be applied to any type of structure in any flight vehicle for any flight condition; so long as appropriate measurements are available from the data vehicle.

Limitations

1. Extensive vibration measurements from experiments on a previous similar vehicle are required.

2. The accuracy of the predictions is heavily dependent upon the quantity and quality of the measurements from the data vehicle, and upon the similarity of the data vehicle to the new vehicle.

# 7. STATISTICAL ENERGY APPROACH

## 7.1 DESCRIPTION

As discussed in Section 3, classical methods of analysis have not proven adequate as tools for the prediction of high frequency random vibration of complex structures. A modification of the classical approach, known generally as the "statistical energy" approach, has been proposed to overcome some of the difficulties. Although not widely used to date as a practical tool for flight vehicle vibration predictions, the statistical energy approach is believed to have considerable promise. Because the approach is relatively new and nontrivial in concept, many details concerning the development of the approach are included in the discussions to follow.

### 7.1.1 Directly Excited Structures

Consider a distributed elastic structure which is exposed to a distributed random pressure field with a spatial cross spectral density function as defined in Eq. (2). The classical solution for the response of the structure at any point $\underline{x}$ will be as given in Eq. (4), which is repeated below.

$$G_y(\underline{x}, f) = \sum_i \sum_k \frac{\phi_i(\underline{x})\, \phi_k(\underline{x})}{4\pi^2 f^2\, Z_i(f)\, Z_k^*(f)} \iint G_p(\underline{\xi}, \underline{\xi}', f)\, \phi_i(\underline{\xi})\, \phi_k(\underline{\xi}')\, d\xi\, d\xi' \tag{4}$$

Now let the average of $G_y(\underline{x}, f)$ over the entire structure be determined by integrating Eq. (4) with respect to $\underline{x}$ and dividing by the total area. Because of the orthogonality of normal modes*

$$\left\langle G_y(\underline{x}, f) \right\rangle_A = \sum_i \frac{\left\langle \phi_i^2(\underline{x}) \right\rangle_A}{4\pi^2 f^2 Z_i^2(f)} \iint G_p(\underline{\xi}, \underline{\xi}', f)\, \phi_i(\underline{\xi})\, \phi_i(\underline{\xi}')\, d\underline{\xi}\, d\underline{\xi}' \tag{28}$$

The spectrum of the vibration energy is

$$G_E(f) = \int \rho(\underline{x})\, G_v(\underline{x}, f)\, d\underline{x} \tag{29}$$

or

$$G_E(f) = M \left\langle G_v(\underline{x}, f) \right\rangle_M \tag{30}$$

By the definition of modal mass

$$M_i = \int \rho(\underline{x})\, \phi_i^2(\underline{x})\, d\underline{x} \tag{31}$$

*If the structure had been nonuniform, then the appropriate weighting function would have to be used in the orthogonalization, and we would obtain $\left\langle \rho(\underline{x})\, G_y(\underline{x}, f) \right\rangle_M$, averaged over the total mass.

We now have

$$G_E(f) = \sum_i \frac{M_i}{\left|Z_i(f)\right|^2} \iint G_p(\underline{\xi}, \underline{\xi}', f)\, \phi_i(\underline{\xi})\, \phi_i(\underline{\xi}')\, d\underline{\xi}\, d\underline{\xi}' \qquad (32)$$

or

$$G_v(f) = \sum_i \frac{M_i/M}{\left|Z_i(f)\right|^2} \iint G_p(\underline{\xi}, \underline{\xi}', f)\, \phi_i(\underline{\xi})\, \phi_i(\underline{\xi}')\, d\underline{\xi}\, d\underline{\xi}' \qquad (33)$$

Now consider the double integral in Eq. (33). This double integral can be normalized by the power spectrum of pressure at some arbitrary reference point and the squared area of the structure to give a function which will be called the joint acceptance, $j_i^2(f)$. That is,

$$j_i^2(f) = \frac{1}{G_0(f)\, A^2} \iint G_p(\underline{\xi}, \underline{\xi}', f)\, \phi_i(\underline{\xi})\, \phi_i(\underline{\xi}')\, d\underline{\xi}\, d\underline{\xi}' \qquad (34)$$

where $G_0(f)$ is reference point power spectrum and A is the area. The joint acceptance is a measure of how well the pressure field couples with the mode shape. Even though the integral is difficult to evaluate, there are a number of approximations and bounds which can be applied to estimate it, as discussed in References 26 and 27.

The spectrum of the vibration energy is now given by

$$G_E(f) = \sum_i \frac{M_i}{\left|Z_i(f)\right|^2} G_0(f) A^2 j_i^2 \tag{35}$$

Before going further, let Eq. (35) be compared to the original response relationship given by Eq. (4) to see what has been gained and lost. First, the double series has been reduced to a single series, thus reducing computation. To achieve this reduction, a definition of the detailed response at any predetermined point $\underline{x}$ has been forfeited. That is, only the average response over the vibrating surface is now known. The second gain is the ability to use the modal mass and joint acceptance. Both of these functions are relatively easier to compute and less sensitive to changes in the structure than the individual mode shapes. Approximations for them can be treated with greater confidence.

To this point, no approximations or assumptions have been required in the analysis. To proceed further, however, some assumptions must be made which are justified under certain conditions. It will be shown later, however, that these conditions are not very restrictive. Hence, the approximations will be valid in the majority of cases.

When the modal damping is rather low, as it is for most aerospace structures, and the product of $G_0(f)\, j_i^2$ is reasonably constant in the neighborhood of the ith natural frequency, then the mean square velocity response of the ith mode is given by References 3 and 4 as

$$\left\langle \dot{q}_i^2 \right\rangle_t \approx \frac{G_0(f_i)\, j_i^2 A^2}{8 R_i M_i} \tag{36}$$

The contribution to the total energy due to this mode of vibration is

$$E_i \simeq \frac{G_0(f_i)\, j_i^2\, A^2}{8R_i} \tag{37}$$

The mean square velocity of the mode, when averaged over the mass of the system is

$$\left\langle V_i^2 \right\rangle_{x,\,t} \simeq \left(\frac{M_i}{M}\right) \frac{G_0(f_i)\, j_i^2\, A^2}{8R_i\, M_i} \tag{38}$$

Consider a frequency band which is wide enough to admit several (perhaps 5 or more) modes of the system. The energy of vibration in this frequency band is thus

$$E(\Delta f, f) \simeq \sum \frac{G_0(f_i)\, j_i^2\, A^2}{8R_i} \tag{39}$$

where the summation is made only over those modes having natural frequencies in the band of interest. This summation may be replaced by the expression

$$\sum \frac{G_0(f_i)\, j_i^2\, A^2}{8R_i} = N \left\langle \frac{G_0(f_i)\, j_i^2}{R_i} \right\rangle \frac{A^2}{8} \tag{40}$$

where the average is taken over the ensemble of modes in the frequency band and N is the number of modes in the band (see References 28 and 29). Upon dividing by the band width, we return to a form of energy spectral density, but averaged over the band.

$$G_E(f) \approx n(f) \left\langle \frac{G_0(f)\, j_i^2(f)}{R} \right\rangle \frac{A^2}{8} \tag{41}$$

where n(f) is the modal density of the system. If the excitation spectrum is rather flat, and the joint acceptance and modal resistance do not vary greatly from mode to mode in the band, then

$$G_E(f) \simeq \frac{n(f)\, G_0(f) \left\langle j_i^2 \right\rangle A^2}{8 \left\langle R \right\rangle} \tag{42}$$

The average resistance can be estimated experimentally by exciting the structure with a band of random noise and then measuring the vibration decay when the excitation is suddenly turned off. The average joint acceptance may be found by calculating the joint acceptance for a typical mode in the band, and then averaging over all modes. In some instances where there may be large differences in the types of modes resonating in a band, it may be necessary to subdivide the modes into similar groups so that a proper and representative $\left\langle j_i^2 \right\rangle$ and $\left\langle R_i \right\rangle$ can be used for each group.

### 7.1.2 Indirectly Excited Systems

In the preceding section, the response of structures which were directly excited by external pressure fields was discussed. Now consider a structure which may be divided into sub-structures. One or more of the sub-structures is excited by an external force, and the resulting vibration is distributed among the structures as a result of their coupling. The statistical energy analysis has been applied with success to structural systems of this type, such as panels in an acoustic field (References 30 and 31), transmission of sound through double walls (Reference 32), enclosures (Reference 33 and 34) or cylinders (References 35 and 36), and vibration between coupled plates (Reference 37).

There are several derivations and developments which serve to explain the concepts of the statistical energy approach. The original concepts of Lyon and Maidanik (Reference 38) have been expanded to be applicable to a very broad class of structural systems. Some of the original restrictions on the use of the method have been removed, but other restrictions remain or have been introduced for special cases. In the development which follows, the basic ideas will be put forth as well as the conditions or restrictions which limit their applicability.

#### Two Mode System

Consider a simple two degree-of-freedom system as shown in Figure 36. Assume for the moment that there are no restrictions on the system other than it be linear and the coupling element be nondissipative. This latter condition implies that the coupling element can be any combination of springs, masses, or gyroscopic devices which dissipate no energy (see References 37, 38 and 39). The quantities of interest in this section are the energies of each oscillator and the energy flow between them.

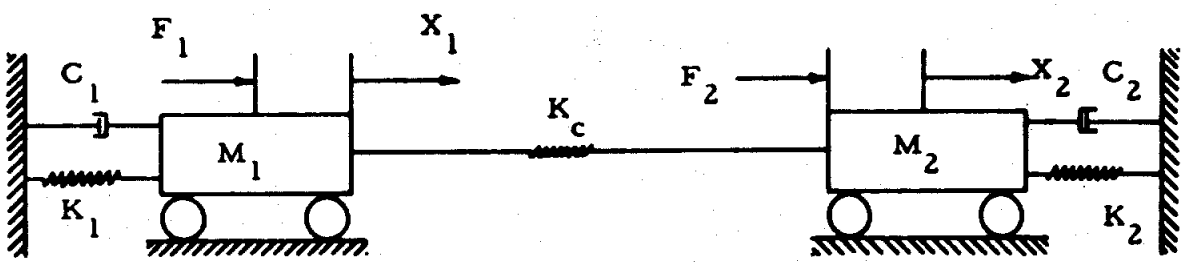


Figure 36. Two Degree-of-Freedom System

The velocity of System 1 due to forces $F_1$ and $F_2$ is given by

$$V_1(t) = \int_{-\infty}^{\infty} y_{11}(\tau)\, F_1(t - \tau)\, d\tau + \int_{-\infty}^{\infty} y_{12}(\lambda)\, F_2(t - \lambda)\, d\lambda \qquad (43)$$

where $y_{11}$ is the velocity response of System 1 due to an impulsive force acting on it, and $y_{12}$ is the velocity response of System 1 due to an impulsive force acting on System 2. We may express the response of System 2 in a similar way:

$$V_2(t) = \int_{-\infty}^{\infty} y_{22}(\tau)\, F_2(t - \tau)\, d\tau + \int_{-\infty}^{\infty} y_{21}(\lambda)\, F_1(t - \lambda)\, d\lambda \qquad (44)$$

Taking the Fourier transform of a finite sample of both values of the above equations gives

$$V_1(f) = Y_{11}(f)\, F_1(f) + Y_{12}(f)\, F_2(f) \tag{45}$$

$$V_2(f) = Y_{21}(f)\, F_1(f) + Y_{22}(f)\, F_2(f) \tag{46}$$

By the relation

$$G(f) = \lim_{T \to \infty} \frac{2}{T}\, X_T(f)\, X_T^*(f) \quad ; \quad f \geq 0 \tag{47}$$

the spectra of velocity of the two masses is easily found

$$G_{v,1}(f) = \left|Y_{11}(f)\right|^2 G_1(f) + \left|Y_{12}(f)\right|^2 G_2(f) + 2\mathrm{Re}\left[Y_{11}(f)\, Y_{12}^*(f)\, G_{12}(f)\right] \tag{48}$$

$$G_{v,2}(f) = \left|Y_{22}(f)\right|^2 G_2(f) + \left|Y_{21}(f)\right|^2 G_1(f) + 2\mathrm{Re}\left[Y_{22}(f)\, Y_{21}^*(f)\, G_{21}(f)\right] \tag{49}$$

At this stage, the computations become extremely arduous if the last terms in the above equations do not vanish. For this reason, the statistical energy analysis requires that the forces $F_1$ and $F_2$ be uncorrelated so that $G_{12}(f) = G_{21}(f) = 0$. This assumption is apparently justified under most conditions, but it must be recognized that the validity is open to question in some cases. When only one oscillator is directly excited, the assumption is always correct.

The average power dissipated by the first oscillator is

$$P_1 = C_1 \left\langle v_1^2 \right\rangle \tag{50}$$

and by the second

$$P_2 = C_2 \left\langle v_2^2 \right\rangle \tag{51}$$

In terms of spectra, these equations would be

$$G_{p1}(f) = C_1 G_{v1}(f) \tag{52}$$

$$G_{p2}(f) = C_2 G_{v2}(f) \tag{53}$$

The power dissipated by the second oscillator must come entirely through the coupling element. Hence, the power flow in the coupling element when only System 1 is excited is

$$P_{12,1} = C_2 \left\langle V_2^2 \right\rangle_1 \tag{54}$$

By a similar argument, when only System 2 is excited, the power flow in the element is

$$P_{21,2} = C_1 \left\langle V_1^2 \right\rangle_2 \tag{55}$$

Combining Eqs. (48), (49), (54) and (55), the spectra of power flow may be written as

$$G_{1,2}(f) = C_2 G_1(f) \left| Y_{21}(f) \right|^2 - C_1 G_2(f) \left| Y_{12}(f) \right|^2 \tag{56}$$

Under the restriction that the coupling is conservative and no energy is dissipated in the coupling element

$$\left| Y_{12}(f) \right|^2 = \left| Y_{21}(f) \right|^2 \tag{57}$$

Thus,

$$G_{1,2}(f) = \left[ C_2 G_1(f) - C_1 G_2(f) \right] \left| Y_{12}(f) \right|^2 \tag{58}$$

The mean square power flow is the integral of Eq. (58) over frequency. That is,

$$P_{12} = \int_{-\infty}^{\infty} \left[ C_2 G_1(f) - C_1 G_2(f) \right] \left| Y_{12}(f) \right|^2 df \qquad (59)$$

Equations (47) and (48) may be rewritten (when $G_{12} = 0$) as

$$G_{v1}(f) = \left| Y_{11}(f) \right|^2 G_1 + \left| Y_{12}(f) \right|^2 G_2 \qquad (60)$$

$$G_{v2}(f) = \left| Y_{12}(f) \right|^2 G_1 + \left| Y_{22}(f) \right|^2 G_2 \qquad (61)$$

These may be solved simultaneously to obtain $G_1$ and $G_2$, as follows.

$$G_1(f) = \frac{\left| Y_{12} \right|^2 G_{v2} - \left| Y_{22} \right|^2 G_{v1}}{\left[ \left| Y_{12} \right|^4 - \left| Y_{11} \right|^2 \left| Y_{22} \right|^2 \right]} \qquad (62)$$

$$G_2(f) = \frac{\left| Y_{12} \right|^2 G_{v1} - \left| Y_{11} \right|^2 G_{v2}}{\left[ \left| Y_{12} \right|^4 - \left| Y_{11} \right|^2 \left| Y_{22} \right|^2 \right]} \qquad (63)$$

These values may be substituted in Eq. (58) or (59) to give

$$G_{12}(f) = A_{12}\, G_{v1} - A_{21}\, G_{v2} \tag{64}$$

where

$$A_{12} = \frac{\left[C_2 \left|Y_{22}\right|^2 + C_1 \left|Y_{12}\right|^2\right] \left|Y_{12}\right|^2}{\left[\left|Y_{11}\right|^2 \left|Y_{22}\right|^2 - \left|Y_{12}\right|^4\right]} \tag{65}$$

$$A_{21} = \frac{\left[C_2 \left|Y_{12}\right|^2 + C_1 \left|Y_{11}\right|^2\right] \left|Y_{12}\right|^2}{\left[\left|Y_{11}\right|^2 \left|Y_{22}\right|^2 - \left|Y_{12}\right|^4\right]} \tag{66}$$

At this stage, additional assumptions may be made to simplify further the results. The first assumption is that the coupling between the modes is light so that

$$\left|Y_{11}\right|^2 \gg \left|Y_{12}\right|^2 , \left|Y_{22}\right|^2 \gg \left|Y_{12}\right|^2$$

This modifies Eq. (36) to

$$G_{12}(f) \approx \left[\frac{C_2}{\left|Y_{11}\right|^2}\, G_{v1}(f) - \frac{C_2\, G_{v2}(f)}{\left|Y_{22}\right|^2}\right] \left|Y_{12}\right|^2 \tag{67}$$

If we make the substitution

$$B_1(f) = \frac{C_2 \left|Y_{12}\right|^2}{m_1 \left|Y_{11}\right|^2} \tag{68}$$

$$B_2(f) = \frac{C_1 \left|Y_{12}\right|^2}{m_2 \left|Y_{22}\right|^2} \tag{69}$$

Then

$$G_{12}(f) = B_1(f)\, G_{E1}(f) - B_2(f)\, G_{E2}(f) \tag{70}$$

where

$$G_{E1}(f) = m_1\, G_{v1}(f) \tag{71}$$

$$G_{E2}(f) = m_2\, G_{v2}(f) \tag{72}$$

are the vibration energies of each oscillator.

It is seen from Eq. (70) that the spectrum of energy flow will be proportional to the energy differences only if $B_1(f) = B_2(f)$. This would imply that the two oscillators are identical. From this we can make the following statement:

"If two identical oscillators are coupled by any conservative coupling mechanism, and excited by statistically independent random forces, then the spectrum of energy flow between the oscillators will be proportional to the difference in energy spectra of the two oscillators."

A slightly different approach to the problem is to integrate over frequency at a much earlier stage in the development, and deal only with mean square values. Integrating Eqs. (60) and (61) (under the assumption that $G_1(f)$ and $G_2(f)$ are white noise, or do not change much in the vicinity of any system resonances) gives

$$\left\langle V_1^2 \right\rangle = G_1 I_{11} + G_2 I_{12} \tag{73}$$

$$\left\langle V_2^2 \right\rangle = G_1 I_{12} + G_2 I_{22} \tag{74}$$

when

$$I_{ij} = \int_0^\infty \left| Y_{ij}(f) \right|^2 df \tag{75}$$

Equations (73) and (74) may be solved for $G_1$ and $G_2$ in terms of $\left\langle V_1^2 \right\rangle$ and $\left\langle V_2^2 \right\rangle$. When this is done and the appropriate substitution is made in the integral of Eq. (75), the result is

$$P_{12} = \left[ \frac{C_2 I_{22} + C_1 I_{12}}{I_{11} I_{22} - I_{12}^2} \right] I_{12} \left\langle V_1^2 \right\rangle - \left[ \frac{C_1 I_{11}^2 + C_2 I_{12}}{I_{11} I_{22} - I_{12}^2} \right] I_{12} \left\langle V_2^2 \right\rangle \tag{76}$$

Again it is seen that if the two systems are identical, the average power flow will be proportional to the difference in their energies. By defining the time average kinetic energies by

$$\langle T_j \rangle = \frac{m_j \langle V_j^2 \rangle}{2} \tag{77}$$

and a coupling coefficient $\phi_{ij}$ by

$$\phi_{12} = \frac{(C_2 I_{22} + C_1 I_{12})\, 2I_{12}}{m_1 \left[ I_{11} I_{22} - I_{12}^2 \right]} \tag{78}$$

$$\phi_{21} = \frac{(C_1 I_{11} + C_2 I_{12})\, 2I_{12}}{m_2 \left[ I_{11} I_{22} - I_{12} \right]} \tag{79}$$

then

$$P_{12} = \phi_{12} \langle T_1 \rangle - \phi_{21} \langle T_2 \rangle \tag{80}$$

The integrals $I_{ij}$ have been calculated for the case of stiffness or gyroscopic coupling in Reference 39. Use of the proper integrals in Eqs. (78) and (79) give

$$\phi_{12} = \phi_{21} = \frac{2}{m_1 m_2} \frac{k_c^2 \alpha_k + C_g^2 \alpha_c}{\alpha_k \alpha_c + 16\pi^4 (f_2^2 - f_1^2)^2} \tag{81}$$

where

$$\alpha_k \equiv 4\pi(\xi_1 f_1 + \xi_2 f_2) = \frac{C_1}{m_1} + \frac{C_2}{m_2}$$

$$\alpha_c \equiv \frac{C_1 k_1 + C_2 k_2}{m_1 m_2} = 16\pi^3 f_1 f_2 (\xi_1 f_2 + \xi_2 f_1)$$

$$4\pi^2 f_1^2 \equiv (k_1 + k_c)/m_1$$

$$4\pi^2 f_2^2 \equiv (k_2 + k_c)/m_2$$

$$\xi_1 \equiv C_1/(4\pi m_1 f_1)$$

$$\xi_2 \equiv C_2/(4\pi m_2 f_2)$$

$C_g$ = gyroscopic coupling coefficient

This means that the energy flow is proportional to the difference in kinetic energies, regardless of the coupling strength. The coupling coefficient $\phi_{12}$ will be largest for modes having nearly the same natural frequencies and decrease as the frequency difference becomes large (see Reference 40).

The material which has been presented up to now can be summarized quite simply as follows.

> "If two conservatively coupled oscillators are identical and excited by independent random forces, the spectrum of power flow between them is proportional to the difference in the spectra of their energies. For oscillators which are not identical, the total energy flow will be proportional to the difference in energies, provided the excitation spectra are relatively flat near the resonance frequencies."

If only one oscillator is excited directly from an outside source, energy will flow through this directly excited oscillator to the other oscillator.

## Multi-Mode Systems

Most mechanical or structural systems of practical interest are multi-modal with many mode shapes and natural frequencies. In analyzing the response of these structures to random pressure fields, it is informative to take into account the material presented in the previous discussion. Because each mode may be considered to be a single oscillator coupled to other oscillators, the energy flow considerations may be of significant use. The general approach is to examine the modes of the system or subsystem and to group them into similar sets. By this we mean that the modes in a particular group will have similar dynamic properties such as modal mass, stiffness, and damping. It also is necessary to assume that the modal generalized forces are uncorrelated, as well as the fact that the modes in the group are not coupled to each other. All the member modes of the set, while uncoupled among themselves (to the first order of approximation) will be coupled to the modes in a different group. This type of a system is illustrated in Figure 37.

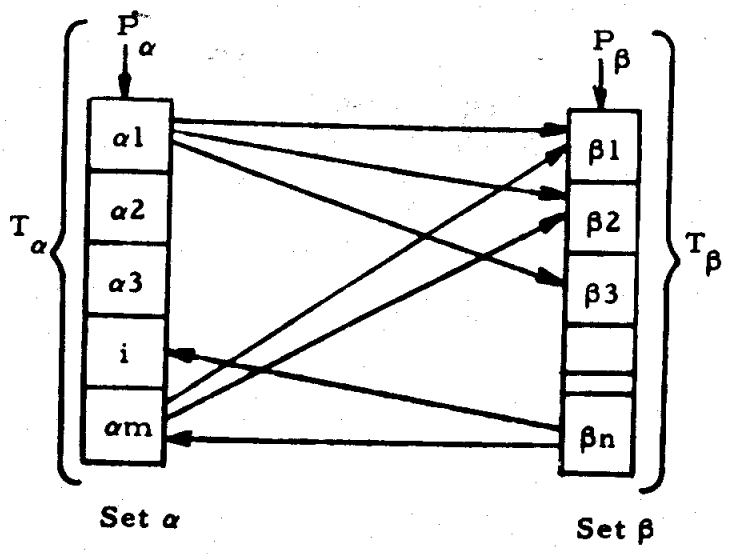


Figure 37. Illustration of Energy Flow in Multi-Mode System

There is assumed to be no energy flow between members of a set because they are uncoupled or because their energies are the same. This assumption is essential to the success of the method, and must be examined for each system of grouping of modes.

The power flow from set $\alpha$ to set $\beta$ can be computed by the statistical energy approach only in the time average sense and not on the basis of spectra. If the oscillator bandwidths are small, and one takes an average over some moderate bandwidth encompassing many modes (say one-third octave), and the excitation spectra are reasonably flat in this band, then an "average" spectrum of energy flow may be found by dividing the total power flow by the broad band width.

The total power flow from set $\alpha$ to set $\beta$ is the sum of the individual power flows. Thus

$$P_{\alpha\beta} = \sum_{i=1}^{N_\alpha} \sum_{k=1}^{N_\beta} P_{\alpha i, \beta k}$$

$$= \sum_{i=1}^{N_\alpha} \sum_{k=1}^{N_\beta} \phi_{\alpha i, \beta k} (T_{\alpha i} - T_{\beta k}) \tag{82}$$

where $N_\alpha$ and $N_\beta$ are the total number of modes in each set respectively. The average (over the set) kinetic energies are given by

$$T_\alpha = \sum_{i=1}^{N_\alpha} \frac{T_{\alpha i}}{N_\alpha} \tag{83}$$

$$T_\beta = \sum_{k=1}^{N_\beta} \frac{T_{\beta k}}{N_\beta}$$

At this point, it is recalled that the power flow between two oscillators is proportional to the difference in kinetic energies. It would be desirable for this also to be true on a mode set basis. By assuming it to be so, a set of conditions can be set up which, when satisfied, will allow the desired assumption to be satisfied.

By analogy to Eq. (70) it follows that

$$P_{\alpha\beta} = \phi_{\alpha\beta} T_\alpha - \phi_{\beta\alpha} T_\beta \tag{84}$$

$$P_{\alpha\beta} = \phi_{\alpha\beta} \sum_{i=1}^{N_\alpha} \frac{T_{\alpha i}}{N_\alpha} - \phi_{\beta\alpha} \sum_{k=1}^{N_\beta} \frac{T_{\beta k}}{N_\beta} \tag{85}$$

or

$$\sum_{i=1}^{N_\alpha} \sum_{k=1}^{N_\beta} \phi_{\alpha i, \beta k} \left( T_{\alpha i} - T_{\beta k} \right) = \frac{\phi_{\alpha\beta}}{N_\alpha} \sum_{i=1}^{N_\alpha} T_{\alpha i} - \frac{\phi_{\beta\alpha}}{N_\beta} \sum_{k}^{N_\beta} T_{\beta k} \quad (86)$$

This must be true for all $T_{\alpha i}$ and $T_{\beta k}$, thus

$$\phi_{\alpha\beta} = \frac{N_\alpha \sum_{i}^{N_\alpha} \sum_{k}^{N_\beta} \phi_{\alpha i, \beta k} T_{\alpha i}}{\sum_{i}^{N_\alpha} T_{\alpha i}} \quad (87)$$

$$\phi_{\beta\alpha} = \frac{N_\beta \sum_{i}^{N_\alpha} \sum_{k}^{N_\beta} \phi_{\alpha i, \beta k} T_{\beta k}}{\sum_{k}^{N_\beta} T_{\beta k}} \quad (88)$$

The quantities $\phi_{\alpha\beta}/N_\alpha$ and $\phi_{\beta\alpha}/N_\beta$ are average modal coupling factors, with averaging weights of $T_{\alpha i}$ and $T_{\beta k}$ respectively. This relation then brings out the fact that the total power flow between the sets is the average mode to mode flow times the number of mode pairs.

$$\begin{aligned} P_{\alpha\beta} &= N_\alpha N_\beta \left\langle \phi_{\alpha\beta} \right\rangle T_\alpha - N_\alpha N_\beta \left\langle \phi_{\beta\alpha} \right\rangle T_\beta \\ &= N_\alpha N_\beta \left[ \left\langle \phi_{\alpha\beta} \right\rangle T_\alpha - \left\langle \phi_{\beta\alpha} \right\rangle T_\beta \right] \end{aligned} \quad (89)$$

When the individual coupling factors $\phi_{\alpha i, \beta k}$ are equal, then

$$\phi_{\alpha\beta} = \phi_{\beta\alpha} = N_\alpha N_\beta \phi_0 \tag{90}$$

where $\phi_0$ is the value of the individual mode coupling factor. In this case, the power flow between the mode sets is dependent only upon their kinetic energy difference.

$$P_{\alpha\beta} = N_\alpha N_\beta \phi_0 (T_\alpha - T_\beta) \tag{91}$$

Thus, the necessity for grouping modes so that their dynamic properties and coupling coefficients are the same is borne out. Only by making this assumption can a reasonably tractable solution be obtained.

In summary, the requirements for the validity of Eq. (91) are as follows.

1. Modes in each group must be uncoupled among themselves or have equal energies.
2. Mode to mode coupling between groups must be conservative.
3. Modal damping is small and primary response is in the neighborhood of resonance.
4. Coupling factors between modes must be constant for all modes and not strongly frequency dependent.
5. Kinetic energy in the coupling must be small.

There are many variations and special cases of this statistical energy approach. In many of these instances, some term may be rearranged or redefined into more meaningful parameters. Nevertheless, the principles remain essentially the same, and the noted restrictions must apply.

One of the major difficulties of the statistical energy approach is the assignment of values to the coupling parameters. The other terms such as mass, frequency, damping, etc., can be calculated or estimated, but the coupling remains a very difficult term to determine. The coupling parameter has been found for special cases such as between structural modes and room acoustic modes (Reference 38), and between certain classes of structural modes (References 34 and 41).

To date, the statistical energy approach has been used to predict actual flight vehicle vibration environments only by a small number of highly skilled analysts. There is still a great deal of art involved in its use which requires a thorough understanding of the material in the appropriate reference. It is believed, however, that the approach will come into wider use in the future as the art becomes better defined and more understood.

## 7.2 SUMMARY

### Assumptions

1. The modes of each structure or substructure of interest must be grouped into similar sets.
2. The coupling between modes in a group is negligible.
3. The coupling between groups is conservative.

4. Modal damping is light and modal response is mostly resonant.
5. The power spectrum of force is approximately constant over the bandwidth of interest.
6. Kinetic energy is evenly divided among modes in a set.
7. Kinetic energy in coupling must be small compared to modal kinetic energy.
8. The coupling factors between modes is constant and not strongly frequency dependent near the resonance condition.

Information Required

1. Estimates for the modal density and modal damping of the structure.
2. Estimates for the joint acceptance function for the structure.
3. Predictions for the power spectral density function of the excitation.

Advantages

When properly utilized, the procedure can yield accurate predictions for structural vibration in the higher frequencies (where the wave number of the mode is very small compared to the dimensions of the structure). Accurate predictions in this frequency range are not feasible by the direct classical approach.

Limitations

1. The procedure must be used with great caution. Violations of its central assumptions can lead to serious errors.
2. The joint acceptance function is difficult to calculate. Previous determinations of joint acceptance functions for common structure-excitation configurations are not widely available at this time.

## 8. MODEL STUDY APPROACH

A model of a mechanical prototype system is defined as a configuration with properties equivalent to the properties of interest for the prototype system. By examining the behavior of such a model, the behavior of the prototype system can be predicted with a known accuracy. Referring to Figure 38, a model need not be a scaled replica of the prototype system, but may be a physically dissimilar mechanical model, an assembly of electrical components, a nontopological configuration with equivalent physical properties, or a collection of mathematical expressions. It is obviously true that

1. no particular form of modeling is an efficient technique for all problems
2. the particular form of modeling used is indicative of the interests and biases of the technical personnel involved.

Since the topic of interest is the prediction of structural vibration environments in modern flight vehicles, only those modeling techniques relevant to this subject will be discussed. A brief review of the technical literature suggests the following types of models are applicable.

1. Scaled Physical Models
2. Dynamically Equivalent Physical Models
3. Analytical Models
4. Electrical Models

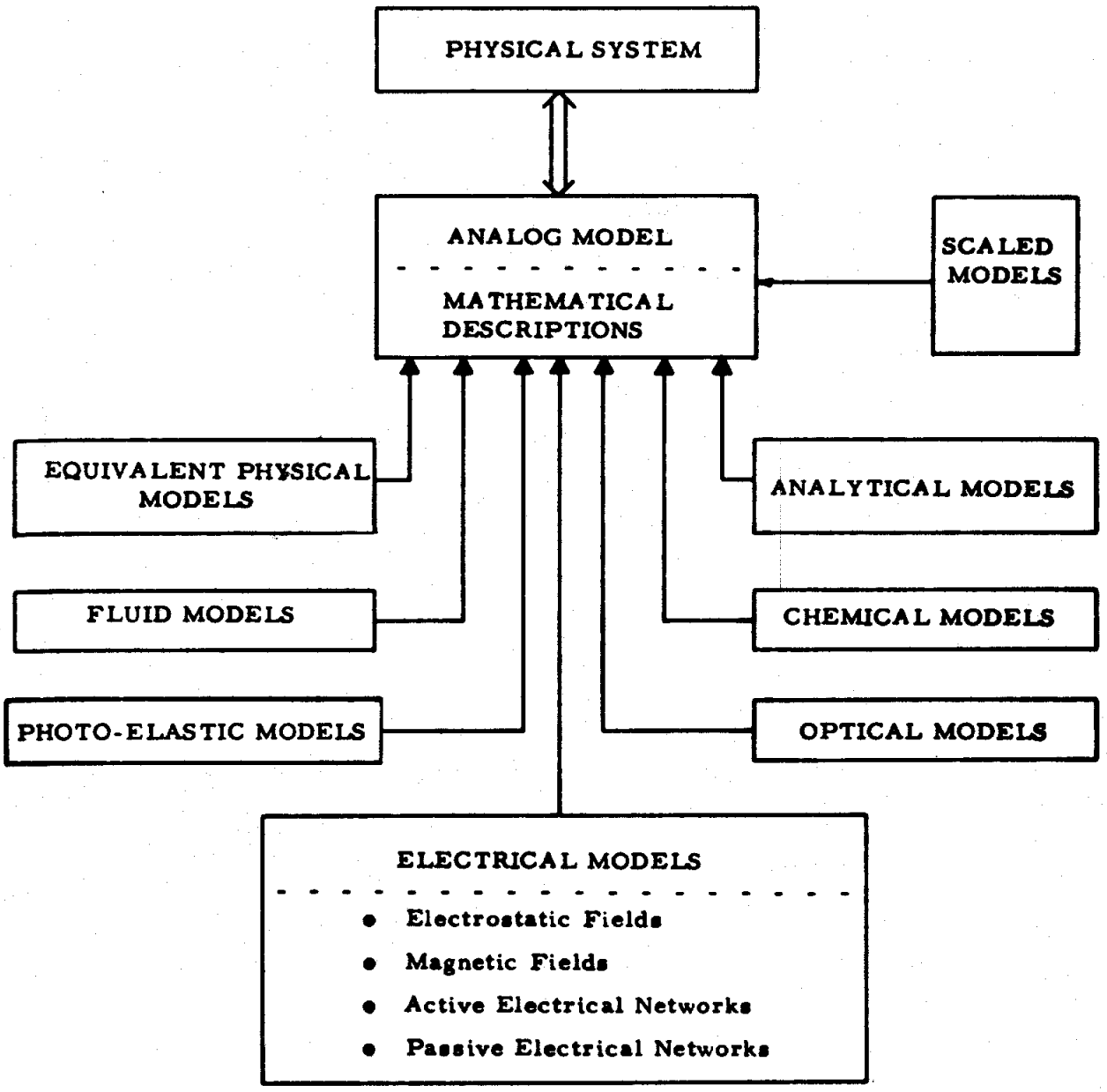


Figure 38. Perspective of Analog Models

The first two items will be considered collectively since they both require construction of a physical model and the existence of a test facility. The third item has already been covered in Section 3, and will not be discussed further. The last item will be considered separately.

## 8.1 PHYSICAL MODEL METHOD

### 8.1.1 Description

The basis of model theory is embodied in concepts of similitude and approximation theory. Perhaps the most widely quoted statement associated with modeling is the Buckingham pi theorem (Reference 42). This theorem is a formal statement which implies that the laws of mechanics are invariant with respect to the units used. The pi theorem thus allows one to express a functional statement with dimensional parameters in terms of an equivalent statement with dimensionless parameters. It is frequently quoted as follows:

> "A physical equation having "n" variables in N fundamental units can be written as
>
> $$\phi(\pi_1, \pi_2, \ldots, \pi_{n-N}) = 0 \qquad (92)$$
>
> where the $\pi$ factors are independent dimensionless terms having the form of products of powers of the variables. The number of such $\pi$ terms will not be less than (n - N)."

The use of dimensionless parameters provides one of the most efficient ways to categorize the physics involved for a specified problem. Although the number of dimensionless parameters are fixed, the forms of the dimensionless parameters are not unique. That is, there are a variety

of ways to arrange the dimensionless quantities, all being "correct." Illustrative examples involving applications of Eq. (92) to physical problems are given in References 42 through 47.

If little is known about the physics of the problem except that the variables can be identified, then complete geometric similarity between the system prototype and the model is desirable. It is understood that such requirements demand a scaling of the boundary conditions and the excitation, as well as the prototype structure. Additional information of the physics involved generally allows a relaxation of the symmetry requirement, and results in a so-called "distorted" or equivalent physical model. An example of a distorted model is a rectangular beam configuration which is dynamically similar (in the first two bending modes) to a full scale rocket vehicle.

In the construction of a physical replica of a prototype system, damping usually cannot be controlled, and size reduction tends to introduce scale effect problems. For example, failures to scale precisely rivet hole sizes, intricate geometric details, and fabrication methods may result in different directional properties and/or local behavior between the model and the prototype system. For gross vehicle studies, these details may be unimportant. For local structural vibration studies, however, such departures could produce serious errors. As mentioned earlier, the applied excitation must be scaled to be compatible with the reduced model, and appropriate instrumentation must be available to measure and to monitor the quantities of interest. This requires careful experimental design and often elaborate instrumentation.

In short, the use of physical models for spacecraft and launch vehicle vibration prediction is a relatively expensive approach. However,

such models provide a useful method for studying vibration environments in detail, and with great accuracy if the experiments are performed carefully.

### 8.1.2 Summary

#### Assumptions

1. The structure can be modeled in acceptable detail.
2. The excitation can be modeled and simulated in the laboratory.

#### Information Required

1. Sufficient knowledge of the structure to permit the fabrication of an accurate physical model.
2. The spatial cross-spectral density function of the excitation.

#### Advantages

The procedure yields accurate results if all required information is available.

#### Limitations

1. Accurate physical models are expensive to fabricate.
2. Extensive instrumentation and careful laboratory experiments are required.
3. Certain structural details, such as damping and fabrication details, are often difficult to model.
4. The excitation is often difficult to model and/or simulate.

## 8.2 ELECTRICAL MODEL METHOD

### 8.2.1 Description

Since structural models are a chief concern, only passive analog modeling techniques will be considered. These techniques involve the use of networks which conceptually simulate a structural configuration by an appropriate assembly of passive electrical components, i.e., resistors, inductors, capacitors, and transformers. By considering force to be equivalent to current and velocity to be equivalent to voltage, resistance corresponds to an equivalent viscous damping, inductance to a flexibility, and capacitance to mass. Transformers are used to describe the spatial geometry. These electrical models commonly are topologically similar to the physical system. They correspond mechanically to a type of lumped parameter model, and correspond mathematically to a finite difference model. Such basic models for discrete multi-degree-of-freedom systems including rods, beams, plates, and cylindrical shells are discussed in References 48 and 49.

In principle, analog models are used to synthesize an electrical network of a physical system. An electrical experiment is then conducted in much the same manner as a physical experiment is conducted with physical models. Arbitrary boundary conditions can be satisfied, non-uniform mass and stiffness distributions can be accommodated, irregular geometry can be treated, and random excitation can be applied as required. Parametric studies may be carried out swiftly by simply adjusting a parameter value, and recording the desired response. Similarly, by reading a meter, internal moments, torques, shear forces, etc., can be obtained as readily as spatial deflections, velocities, and/or accelerations. Large computers for such simulations are not widely available.

The three largest installations are located at the McDonnell-Douglas Company, St. Louis, Missouri; Convair, Fort Worth, Texas; and North American Aviation, Los Angeles Division, Los Angeles, California. Furthermore, since the size of such computers is finite, the difference grid that can be constructed for any problem is limited. These are obvious practical limitations on the use of the approach.

Other than use in conjunction with a passive analog computer, such analog models or associated techniques have additional application to problems of structural dynamics. The concepts of designing the analog model can be applied to improve current methods of developing equivalent mechanical models. For example, experimental measurements such as mechanical impedance plots can be applied directly to structural modeling, and localized damping effects on modal damping can be quickly calculated. By being able to cast the mechanical system into an equivalent electrical network, techniques of circuit analysis as well as those common to vibrations can be used to solve for a desired response. In this way, perhaps more efficient analysis techniques can be formulated. Furthermore, by simply providing another perspective of examining the dynamics of elastic systems, an understanding of mechanical vibrations for such systems is often advanced.

For example, consider a matrix formulation for the modal frequencies and mode shapes of a cantilevered beam with nonuniform mass and stiffness properties. A six-cell passive analog model for this configuration is shown in Figure 39. Consistent with mobility definitions, all voltages are proportional to velocities, so that it is proper to speak of slope velocities ($\dot{\theta}$) and lateral velocities ($\dot{y}$). The current flows ($M_n$'s) in the slope circuit correspond to bending moments, while current flows in the deflection circuit correspond to shear flows ($V_n$'s) and inertial forces ($F_n$'s) of the lumped masses. The bending flexibility of an

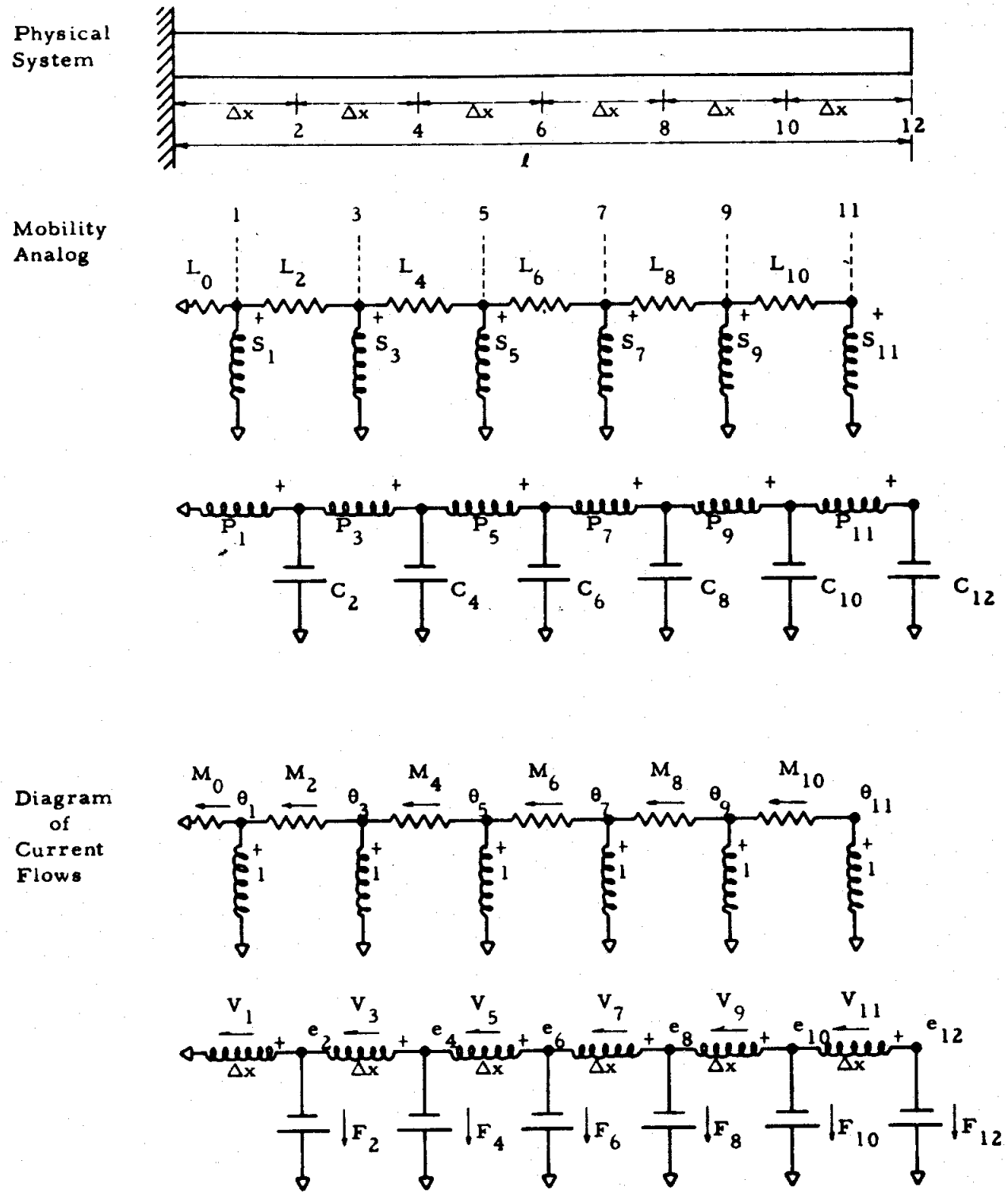


Figure 39. Six-Cell Mobility Analog of a Bernoulli-Euler Cantilever Beam

nth beam segment is shown as the inductor $L_n$, the mass of an nth segment as the capacitor $C_n$, and the geometry relating the slope and lateral deflection by the transformer $P/S_n$. The relationships between these electrical components and their mechanical counterparts are

$$L_n \propto \left.\frac{\Delta x}{EI}\right|_n \qquad \left.\frac{P}{S}\right|_n \simeq \Delta x_n \qquad C_n \propto \left. m\Delta x\right|_n \tag{93}$$

where the subscript 'n' refers to the nth difference segment and the symbolism $|_n$ imposes an integration over the length of the nth segment.

From elementary circuit analysis procedures, the iterative form for convergence to the lowest mode of the system appears as

$$\{e\} = -(\Delta x)^2 \begin{bmatrix} 1 & & \\ -1 & 1 & \\ & -1 & 1 \end{bmatrix}^{-1} \begin{bmatrix} 1 & & \\ -1 & 1 & \\ & -1 & 1 \end{bmatrix}^{-1} \begin{bmatrix} Z(\theta) & & \\ & & \\ & & \end{bmatrix} \begin{bmatrix} 1 & & \\ -1 & 1 & \\ & -1 & 1 \end{bmatrix}^{-1} \begin{bmatrix} 1 & & \\ -1 & 1 & \\ & -1 & 1 \end{bmatrix}^{-1} \begin{bmatrix} Z(V) & & \\ & & \\ & & \end{bmatrix}^{-1} \{e\} \tag{94}$$

where $\{e\}$ is a column matrix denoting the deflections at the spatial positions, and $\Delta x$ the finite difference length. In this expression, all difference lengths are assumed uniform. Removing this restriction is a trivial analytical task, and the form of Eq. (93) remains unchanged. The remaining matrices are square consisting of either diagonal elements

$X_n(\theta)$ and $Z(V)$, or elements sparsely spaced about the diagonal. For a beam described by Bernoulli-Euler theory, the impedances in the slope and shear circuits are given by

$$Z_n(\theta) = i\omega L_n \simeq i\omega \frac{\Delta x}{EI}\bigg|_n$$

$$Z_n(V) = \frac{1}{i\omega C_u} \simeq \frac{1}{\omega m \Delta x}\bigg|_n \qquad (95)$$

With this formulation, viscoelastic properties, added masses, elastic and/or viscoelastic foundations, may be treated immediately by converting the impedance functions to reflect these phenomena. Such a conversion may require a complex quantity and/or a slightly more complicated form of Eq. (94). In addition, local or regional damping may be related to the modal damping of the overall vehicle. Such information is of use in optimizing the effects of local damping on the overall motion of the vehicle.

The formulation shown as Eq. (94) could have been made by applying difference techniques to the Bernoulli-Euler equation of motion. However, neither the impedance relationships nor the obvious procedures for including viscoelastic effects, additional masses, etc., would be as immediately evident, although these same relationships could have been determined.

Such analog modeling appears to have promise as an analysis and prediction tool pertinent to structural design in a random environment. This approach is amenable to conventional analysis techniques, can make direct use of experimental data, and can be used in analog simulation.

14. P. A. Franken, "Review of Information on Jet Noise," Noise Control, Vol. 4, No. 3, pp 8-16, May 1958.

15. I. Dyer, P. A. Franken, and E. E. Ungar, "Noise Environments of Flight Vehicles," Noise Control, Vol. 6, No. 1, pp 31-40, 51, January 1960.

16. D. A. Bies, "A Review of Flight and Wind Tunnel Measurements of Boundary Layer Pressure Fluctuations and Induced Structural Response," NASA CR-626, October 1966.

17. D. A. Hilton, "Scout-Vehicle Aerodynamic-Noise Measurements," Sound, Vol. 2, No. 5, pp 28-31, October 1963.

18. H. Schlichting, Boundary Layer Theory, p 35, Pergamon Press, New York, 1955.

19. A. J. Curtis, "A Statistical Approach to Prediction of the Aircraft Flight Environment," Shock and Vibration, Bulletin No. 33, Part I, February 1964.

20. P. A. Franken, "Sound Induced Vibrations of Cylindrical Vehicles," Journal of the Acoustical Society of America, Vol. 34, No. 4, pp 453-454, April 1962.

21. R. A. Schiffer, "Correlation of Launch-Vehicle Wind Tunnel Aerodynamic Noise with Spacecraft Flight Vibration Data" (Revision No. 1), Jet Propulsion Laboratory, Cal Tech, Technical Report No. 32-619, September 15, 1964.

22. E. F. Winter and W. F. Van Der Laan, "Recommended Procedures for Predicting Random Vibration Environments in MSFC Aerospace Vehicles," Measurement Analysis Corporation Report MAC 504-19, September 1967.

23. F. Condos and W. Butler, "A Critical Analysis of Vibration Prediction Techniques," Proceedings of the IES Annual Technical Meeting in Los Angeles, 1963.

24. R. E. Barrett, "Techniques for Predicting Localized Vibration Environments of Rocket Vehicles," NASA TN D-1836, October 1963.

25. R. E. Barrett, "Statistical Techniques for Describing Localized Vibration Environments in Rocket Vehicles," NASA TN D-2158, July 1964.

26. F. S. Mayer, "Calculation of the Generalized Load for Random Pressure Fields with Applications," Douglas Aircraft Company Engineering Paper No. 1739, 1963.

27. P. H. White, "Some Useful Approximations for Determining the Vibration of Structures Excited by Random Pressure Fields," Journal of the Acoustical Society of America, Vol. 36, No. 4, pp 784-785, 1964.

28. I. Dyer, "Response of Structures to Rocket Noise," Random Vibration, Vol. 2 (Ed. by S. H. Crandall), Chap. 7, MIT Press, Cambridge, Mass., 1963.

29. M. Heckl, et al., "New Methods for Understanding and Controlling Vibration of Complex Structures," Bolt Beranek and Newman, Inc., Report No. 875, 1961.

30. P. Smith, "Response and Radiation of Structural Modes Excited by Sound," Journal of the Acoustical Society of America, Vol. 34, No. 5, p 640, 1962.

31. G. Maidanik, "Response of Radiation of Ribbed Panels," Journal of the Acoustical Society of America, Vol. 34, No. 6, p 809, June 1962.

32. P. H. White and A. Powell, "Transmission of Random Sound and Vibration Through a Rectangular Double Wall," Journal of the Acoustical Society of America, Vol. 40, No. 4, p 821, October 1966.

33. E. Eichler, "Thermal Circuit Approach to Vibrations in Coupled Systems," Journal of the Acoustical Society of America, Vol. 37, No. 6, p 995-1007, 1965.

34. R. H. Lyon and E. Eichler, "Random Vibration of Connected Structures," Journal of the Acoustical Society of America, Vol. 36, No. 7, pp 1344-1354, 1964.

35. J. E. Manning and G. Maidanik, "Radiation Properties of Cylindrical Shells," Journal of the Acoustical Society of America, Vol. 36, No. 9, pp 1691-1698, 1964.

36. P. H. White, "Sound Transmission Through a Closed Finite Cylindrical Shell," Journal of the Acoustical Society of America, Vol. 40, No. 5, p 1124, November 1966.

37. R. H. Lyon and T. D. Scharton, "Vibrational Energy Transmission in a Three Element Structure," Journal of the Acoustical Society of America, Vol. 38, No. 2, pp 253-261, 1965.

38. R. H. Lyon and G. Maidanik, "Power Flow Between Linearly Coupled Oscillators," Journal of the Acoustical Society of America, Vol. 34, No. 5, pp 623-639, 1962.

The possible return (in information per dollar) is competitive with other analytical methods and less expensive than experiments using physical models.

### 8.2.2 Summary

#### Assumptions

1. The structure can be modeled in acceptable detail with an analog circuit.
2. The excitation can be modeled and simulated with signal generators.

#### Information Required

1. Normal mode shapes, frequencies, and damping ratios for the structure (or, alternatively, mass and stiffness distributions).
2. The spatial cross-spectral density function for the excitation.

#### Advantages

1. The procedure yields accurate results if all required information is available.
2. The procedure permits parametric studies of the structure to be performed.
3. The required models are cheap and easy to construct if a passive analog computer is available.

#### Limitations

1. The required information is difficult to obtain in practice.
2. Very few large passive analog computer facilities are available.
3. The computer facility capacity limits the detail which can be included in the model.

REFERENCES


1. W. T. Thomson, Mechanical Vibration, Second Edition, Prentice-Hall, Englewood Cliffs, N. J., 1950.

2. W. Hurty and M. Rubenstein, Dynamics of Structures, Prentice-Hall, Englewood Cliffs, N. J., 1964.

3. J. D. Robson, An Introduction to Random Vibration, Elsevier Publishing Co., New York, 1964.

4. S. H. Crandall and W. D. Mark, Random Vibration in Mechanical Systems, Academic Press, New York, 1963.

5. J. S. Bendat and A. G. Piersol, Measurement and Analysis of Random Data, John Wiley and Sons, New York, 1966.

6. P. T. Mahaffey and K. W. Smith, "A Method for Predicting Environmental Vibration Levels in Jet-Powered Vehicles," Shock and Vibration Bulletin No. 28, Part IV, pp 1-14, August 1960.

7. J. M. Brust and H. Himelblau, "Comparison of Predicted and Measured Vibration Environments for Skybolt Guidance Equipment," Shock and Vibration Bulletin No. 33, Part III, pp 231-280, March 1964.

8. L. C. Sutherland and W. V. Morgan, "Use of Model Jets for Studying Acoustic Fields near Jet and Rocket Engines," Noise Control, Vol. 6, No. 3, pp 6-12, May 1960.

9. D. A. Bies and P. A. Franken, "Notes on Scaling Jet and Rocket Noise," Journal of the Acoustical Society of America, Vol. 33, No. 9, pp 1171-1173, September 1961.

10. K. M. Eldred, W. H. Roberts, and R. White, "Structural Vibration in Space Vehicles," WADD TR 61-62, December 1961.

11. P. A. Franken, E. M. Kerwin, et al., "Methods of Flight Vehicle Noise Prediction," WADC TR 58-343, Vol. I, November 1958 and Vol. II, September 1960 (DDC No. AD 205776 and 260955).

12. I. Dyer, "Estimation of Sound-Induced Missile Vibration," Random Vibration (Ed. by S. H. Crandall), Chap. 9, John Wiley and Sons, New York, 1958.

13. J. E. Ffowcs Williams, "The Noise of High-Speed Missiles," Random Vibration, Vol. 2 (Ed. by S. H. Crandall), Chap. 6, MIT Press, Cambridge, Mass., 1963.

39. E. Ungar, "Fundamentals of Statistical Energy Analysis of Vibrating Systems," AFFDL-TR-66-52, May 1966.

40. D. E. Newland, "Calculation of Power Flow Between Coupled Oscillators," Journal of Sound and Vibration, Vol. 3, No. 3, pp 262-276, 1966.

41. T. Scharton, "Random Vibration of Coupled Oscillators and Coupled Structures," Sc. D. Thesis, Massachusetts Institute of Technology, October 1965.

42. H. L. Langhaar, Dimensional Analysis and Theory of Models, John Wiley and Sons, Inc., New York, 1951.

43. D. E. Hudson, "Scale-Model Principles," Shock and Vibration Handbook, (Ed. C. M. Harris and C. E. Crede), Vol. 2, McGraw-Hill Book Co., New York, 1961.

44. P. E. Sandorff, "Principles of Design of Dynamically Similar Models for Large Propellant Tanks," NASA TN-D-99, January 1960.

45. R. V. Doggett Jr., "Comparison of Full-Scale and Model Buffer Response of Apollo Boilerplate Service Module," NASA TMX-1202, January 1966.

46. H. L. Runyan, "Simulation of Structural Dynamics of Space Vehicles During Launch," Presented at the Conference on the Role of Simulation in Space Technology, Blacksburg, Va., August 1964.

47. S. J. Kline, Similitude and Approximation Theory, McGraw-Hill Book Co., New York, 1965.

48. R. L. Barnoski, "Electrical Analogies and the Vibration of Linear Mechanical Systems," NASA CR-510, June 1966.

49. R. L. Barnoski, "Basic Analog Circuits for Two-Dimensional Distributed Elastic Structures," NASA CR-667, January 1967.

# APPENDIX

## REFERENCES AND ABSTRACTS FOR SELECTED ARTICLES DEALING WITH THE PREDICTION OF ACOUSTIC LOADS

1. Gruner, W. J., and Johnston, G. D., "An Engineering Approach to Prediction of Space Vehicle Acoustic Environments," presented to the 67th Meeting of the Acoustical Society of America, May 6-9, 1964, New York, New York.

Precise estimation of the acoustic environment of space vehicles during the static firing, liftoff, and transonic-maximum dynamic pressure domains of the vehicle lifetime is made mandatory in order to optimize dynamic qualification of the structure and operational systems. Engineering methods of estimating the acoustic environment during these critical areas of the vehicle lifetime are presented and comparison is made for the predicted and measured data of the SATURN I, Block I, and the SATURN I, Block II vehicles. Specific direction is indicated for future analyses and research projects.

2. George, B. W., "Launch Vehicle Inflight Acoustic Environment Predictions," presented to the 72nd Meeting of the Acoustical Society of America, November 2-5, 1966, Los Angeles, California.

A state-of-the-art prediction of the inflight external acoustic environment of a current launch vehicle was made for NASA/Marshall Space

Flight Center. Representative predicted environment parameters are presented in this paper in the form of Sound Pressure Level time histories and 1/3-ovtave band spectra for each major stage or module on the vehicle. Methods used in the prediction are based on (1) wind tunnel acoustic data on scaled models; and (2) normalized empirical curves available in the literature. Aerodynamic noise sources on the vehicle and local areas with severe environments (near protuberances) are discussed. Highest noise environment over the launch flight period occurs on the nose cone. The predictions are compared with subsequent flight measurement and the results interpreted. The validity of scaling from model to flight data is demonstrated. Oscillating shock wave effects are found to contribute significantly to the acoustic signals recorded in flight in the transonic speed range. Comparisons are included of these data with recent published data on other types of flight vehicles.

3. Potter, R. C., and Crocker, M. J., "Acoustic Prediction Methods for Rocket Engines, Including the Effects of Clustered Engines and Deflected Exhaust Flow," NASA CR-566, dated October 1966.

In this report, existing methods to predict the noise generated by rocket motors are examined and calculated values compared with measured results. A method of allocating a spectrum of acoustic sources with distance downstream from the nozzle exit is produced. The final result is shown as a single normalized curve, which fits well all the reported results. It is based on measurements of acoustic sound power level on a boundary just outside and at 10 degrees to the rocket exhaust flow.

Methods to predict the noise fields generated by clustered rocket engines and deflected rocket exhaust flows are given, based on an analysis of the flow pattern produced. The flow patterns are solved in terms of the rocket flow parameters, nozzle, missile and deflector geometry, and the atmospheric conditions. The prediction method developed in the first part of this report is applied to the various segments of the flows to obtain the resultant noise fields. Comparison of predicted results with experimentally measured values indicates the usefulness of this method, which appears to cover well the whole range of rocket measurements reported.

4. Bies, D. A., "A Review of Flight and Wind Tunnel Measurements of Boundary Layer Pressure Fluctuations and Induced Structural Response," NASA CR-626, dated October 1966.

A review is presented of available data on boundary layer pressure fluctuations and induced structural response, from flight and wind tunnel investigations. The wind tunnel data include flat plate pressure fluctuation spectra and space-time correlations, displacement and acceleration spectra of flat flexible panels, and sound power spectra radiated by flat flexible panels. The flight data include pressure fluctuation spectra and "equivalent acoustic spectra," the acoustic fields that would produce the same response as the aerodynamic fields.

In order to use the same normalization procedure with all the data, engineering curves have been derived for estimating boundary layer parameters. These curves extend the estimates to Mach numbers up to 4 and Reynolds numbers based on a characteristic length up to $2 \times 10^9$.

The pressure fluctuation data show considerable scatter, especially in the wind tunnel investigations. The experimental results suggest that the scatter may be due to highly localized flow perturbations. It is argued that these perturbations may not be significant in determining structural response. General recommendations are given to guide experimental studies. A simplified procedure for estimating boundary layer pressure spectra is given in an appendix.

5. Bies, D. A., "A Wind Tunnel Investigation of Panel Response to Boundary Layer Pressure Fluctuations at Mach 1.4 and Mach 3.5," Bolt, Beranek and Newman Inc., Report No. 1264, dated October 1965.

This report describes a series of experiments investigating the structural response to boundary layer turbulence of a well-damped panel of high modal density. Investigations were conducted in the Douglas Aircraft Company 1' x 1' blowdown wind tunnel located in El Segundo, California.

Two test panels were designed, constructed and tested. The panels were designed with two purposes in mind: (1) to obtain information about response which might be scaled to full-scale, and (2) to verify or reject the possible existence of surface Mach waves predicted by theory. The design of the experimental apparatus was also strongly influenced by the practical limitations of available materials and by special problems involved in the use of a blowdown wind tunnel. As a result of the above considerations, the test apparatus is unique, and it is discussed first in Section II below in some detail. Section III also contains further detailed description of the test apparatus. In Sections

III and IV the results of wind tunnel testing and acoustic testing of the panels are reported. In Section V a comparison and synthesis of some of the results of wind tunnel and acoustic tests are made. Some estimates of full-scale panel response are also made, and the results of experiments are compared with theoretical predictions based on material given in the appendices. The summary and conclusions are given in Section VI.

The experiments discussed in this report represent an effort to develop a new approach to the problem of the interaction of boundary layer pressure fluctuations and structural response. They are exploratory in nature rather than final. The emphasis has been placed on the experimental aspects of the problem and not on the analytical approach, which has been carried out extensively elsewhere.

(6.) Cole, J. N., et al., "Noise Reduction from Fourteen Types of Rockets in the 1000 to 130,000 Pounds Thrust Range," WADC TR 57-354, dated December 1957.

Detailed noise characteristics were measured on fourteen types of rockets, with both solid and liquid propellants, in the thrust range from 1000 to 130,000 pounds. Near field and far field levels on static fired and vertical launched rockets were measured under essentially free field conditions. Measurement and data reduction methods are described. Final results are given as near field sound pressure spectra, far field directivities, acoustic power spectra and pressure-time histories. This noise environment is studied as a function of several nozzle configurations and as a function of flame front action in the jet stream.

Generalization and correlation of the data results in a formula for the overall acoustic power level output of rockets, OA PWL = 78 + 13.5 $\log_{10} W_m$ dB re $10^{-13}$ watts, where $W_m$ is the rocket jet stream mechanical power in watts. Also given is an approximate generalized power spectrum dependent upon nozzle diameter and jet flow characteristics. These correlations result in procedures for predicting far field noise environments produced by static fired or launched rockets.

7. Ailman, C. M., "On Predicting Fluctuating Pressures at a Wall Beneath a Turbulent Boundary Layer," Presented to the Acoustical Society of America, 19-21 April 1967, New York, N. Y., Douglas Aircraft Company, Paper No. 4331.

The purpose of this paper is to present graphs, nomographs and simple equations to aid in predicting the characteristics of the fluctuating pressures which cause steady-state dynamic environments during transonic and supersonic atmospheric flight. The source of these pressures is the turbulent boundary layer over the external surface of the vehicle. Such a boundary layer may be well-behaved (undisturbed and slowly growing) or disturbed by local static pressure gradients or external profile variations. The basis for the engineering prediction techniques contained herein is entirely empirical (approximately twenty documented references) since the limited theoretical treatments available today are too restrictive in their applications. Data are presented for many conditions and situations in the Mach number range from 0.6 to 5.0. Extrapolation of axissymmetric or two-dimensional results to three-dimensional prob lems by meane of static pressure studies is discussed.

8. Wiley, D. R., and Seidl, M. G., "Aerodynamic Noise Tests on X-20 Scale Models," AFFDL TR-65-192, Vol. II, dated November 1965.

Summaries of fluctuating pressure data presented in Volume I for the 1/15th-scale X-20 models are made and discussed. Particular emphasis is given to the high overall rms pressures measured aft of convex corners during transonic test conditions. Additional information relating to these pressures is presented in the form of pressure histories, peak-amplitude distributions, and power spectral densities. Fluctuating pressure data and space correlation measurements for three closely spaced microphones are presented, illustrating the local nature of the high-level pressures. Analyses of trends for the maximum overall rms pressure levels for the X-20 tests and other wind tunnel tests are made. Design charts are developed for predicting maximum levels aft of cone-cylinder transition sections as functions of transition angle and distance downstream of the transition shoulder. Recommendations are made regarding future aerodynamic noise experimental programs.

9. Rainey, A. G., "Progress on the Launch Vehicle Buffeting Problem," Journal of Spacecraft and Rockets, Vol. 2, No. 3, pp 289-299, May 1965.

Progress achieved by the large number of investigators who have studied the launch-vehicle buffeting problem in the 4 years of its recognized existence is reviewed. It is pointed out that buffeting pressures are

dimensionally well behaved in that results obtained on wind tunnel models, in most cases, can be scaled by reduced frequency concepts to full-scale conditions. A few measurements of space-time correlation characteristics for separated flows have become available which indicate a picture of convected, decaying patterns of pressure somewhat similar to that which has been found for attached boundary layers and jet noise. The state-of-the-art in techniques for predicting structural response to this aerodynamic environment is indicated to be only fair. High frequency response of structural components, such as interstage adapters, involves the effects of multiple random inputs on structures with complicated dynamic characteristics. Several active research programs aimed at developing techniques for handling this problem are discussed. Methods for treating the low frequency gross bending response problem are discussed and it is indicated that they appear to be adequately developed for design purposes.

10. Franken, P. A., "Generation of Sound in Cavities by Flow Rate Changes," Journal of the Acoustic Society of America, Vol. 33, No. 9, pp 1193-1195, September 1961.

Sound generated by mass or heat flow changes in a cylindrical cavity is considered. The special case of a high-pressure ratio orifice is studied. Experimental results show good agreement with values predicted from a scaling equation.

11. Wiener, F. M., "Rocket Noise of Large Space Vehicles," 4th International Congress on Acoustics, Copenhagen, August 1962.

The scaling of rocket noise and model experiments is discussed. Consideration is given to the far field and the geometric field (near field). Procedures are given for estimating the octave band sound pressure spectrum at a vehicle surface.

12. Franken, P. A., and Wiener, F. M., "Estimation of Noise Levels at the Surface of a Rocket Powered Vehicle," Shock and Vibration, Bulletin No. 31, Part III, pp 27-31, April 1963.

The general properti of rocket noise fields are discussed, and a procedure is presented for estimating the octave band sound pressure spectrum at a vehicle surface.

13. Bies, D. A., and Franken, P. A., "Notes on Scaling Jet and Rocket Noise," Journal of the Acoustical Society of America, Vol. 33, No. 9, pp 1171-1173, September 1961.

For dynamically similar systems it is shown that pressure fluctuation amplitudes at similar positions are the same when measured in constant-percentage frequency bands and when frequency is scaled inversely proportional to a characteristic length. This scaling relationship can be extended to systems containing acoustic liners if the linear flow resistance is held constant. Corrections for small errors in scaling are suggested for the case of rocket engines.